

HEALTH SCIENCES

JOANNA HUTTUNEN

*A Study of Rodent Brain Function
with Functional and Pharmacological
Magnetic Resonance Imaging*

PUBLICATIONS OF THE UNIVERSITY OF EASTERN FINLAND
Dissertations in Health Sciences



UNIVERSITY OF
EASTERN FINLAND

JOANNA HUTTUNEN

*A Study of Rodent Brain Function
with Functional and Pharmacological
Magnetic Resonance Imaging*

To be presented by permission of the Faculty of Health Sciences, University of Eastern Finland
for public examination in Medistudia 1, Kuopio, on Friday, August 23th 2013, at 16

Publications of the University of Eastern Finland
Dissertations in Health Sciences
Number 179

Department of Neurobiology, A. I. Virtanen Institute for Molecular Sciences,
Faculty of Health Sciences, University of Eastern Finland
Kuopio
2013

Kopijyvä Oy
Kuopio, 2013

Series Editors:

Professor Veli-Matti Kosma, M.D., Ph.D.
Institute of Clinical Medicine, Pathology
Faculty of Health Sciences

Professor Hannele Turunen, Ph.D.
Department of Nursing Science
Faculty of Health Sciences

Professor Olli Gröhn, Ph.D.
A. I. Virtanen Institute for Molecular Sciences
Faculty of Health Sciences

Professor Kai Kaarniranta, M.D., Ph.D.
Institute of Clinical Medicine, Ophthalmology
Faculty of Health Sciences

Lecturer Veli-Pekka Ranta, Ph.D. (pharmacy)
School of Pharmacy
Faculty of Health Sciences

Distributor:

University of Eastern Finland
Kuopio Campus Library
P.O.Box 1627
FI-70211 Kuopio, Finland
<http://www.uef.fi/kirjasto>

ISBN (print): 978-952-61-1177-3
ISBN (pdf): 978-952-61-1178-0
ISSN (print): 1798-5706
ISSN (pdf): 1798-5714
ISSN-L: 1798-5706

Author's address: A. I. Virtanen Institute for Molecular Sciences
University of Eastern Finland
P. O. Box 1627
FI-70211 KUOPIO
FINLAND
E-mail: Joanna.Huttunen@uef.fi

Supervisors: Professor Olli Gröhn, Ph.D.
A. I. Virtanen Institute for Molecular Sciences
University of Eastern Finland
KUOPIO
FINLAND

Docent Markku Penttonen, Ph.D.
Department of Psychology
University of Jyväskylä
JYVÄSKYLÄ
FINLAND

Reviewers: Professor Timothy Duong, Ph.D.
Research Imaging Institute
The University of Texas Health Science Center
SAN ANTONIO
UNITED STATES OF AMERICA

Professor Markus Rudin, Ph.D.
Institute for Biomedical Engineering
ETH Zürich
ZÜRICH
SWITZERLAND

Opponent: Professor Steven C. R. Williams, Ph.D.
Department of Neuroimaging
King's College London
LONDON
UNITED KINGDOM

Huttunen Joanna

A study of rodent brain function with functional and pharmacological magnetic resonance imaging

University of Eastern Finland, Faculty of Health Sciences

Publications of the University of Eastern Finland. Dissertations in Health Sciences Number 179. 2013. 76 p.

ISBN (print): 978-952-61-1177-3

ISBN (pdf): 978-952-61-1178-0

ISSN (print): 1798-5706

ISSN (pdf): 1798-5714

ISSN-L: 1798-5706

ABSTRACT

It has been known for more than a century that stimulus induced neuronal activation evokes changes in the vascular system. During neuronal activation, the blood flow increase exceeds blood demand, and the amount of deoxygenated hemoglobin becomes reduced. Since deoxyhemoglobin is paramagnetic, this leads to an increased signal detectable with blood oxygenation level dependent (BOLD) functional magnetic resonance imaging (fMRI).

The aim of this study was to measure frequency modulated neural responses in the rat somatosensory cortex under the influence of two different anesthetic agents. Simultaneously recorded neural and BOLD responses differed under urethane and alpha-chloralose anesthesia but a linear relationship between neural response and BOLD was detected that was not dependent of the anesthetic used. Based on this study, the electrical stimulus parameters need to be optimized for each anesthetic to achieve optimal neural and hemodynamic responses.

During a relatively long electrical stimulation, spontaneous fluctuations can occur in neuronal excitability. Temporal variations in BOLD responses were evaluated by a model based on the simultaneously measured neuronal local field potential (LFP) data and compared with the stimulus paradigm-based block model. Both LFP and block models alone had sufficient explanatory power to localize the activation to the somatosensory cortex of the rat. However, in comparison of these models, it was found that the LFP model was able to explain additional variation in the somatosensory BOLD signal over the block model. This indicates that there are temporal variations in the time-dependent changes in both neuronal and BOLD activation and the neurovascular coupling is preserved.

Pharmacological magnetic resonance imaging (phMRI) is a novel fMRI application where the activation in the brain is evoked by a pharmacological agent. The possible fluctuations (e.g. room temperature, hardware drifts) in the BOLD time series that occurred in the time scale of the pharmacological activation may be difficult to filter, but could be eliminated by calculating T_2 maps. The potent brain stimulant, nicotine and a weaker stimulant, apomorphine, were used in this study as test compounds to demonstrate the feasibility of using T_2 map based approach to study quantitatively pharmacological activation.

Functional and pharmacological magnetic resonance imaging in the preclinical setting offers an extensive array of possibilities with which to measure brain activity and when combined with direct invasive neuronal activity recordings, it represents an ideal way to deepen our understanding of the mechanisms of the physiological basis of the fMRI signals. The studies presented here have implications for both understanding brain function and for designing functional imaging paradigms in anesthetized animals.

National Library of Medical Classification: QV 137, QV 771, QY 58, QY 60.R6, WB 330, WL 102, WL 141.5.M2

Medical Subject Headings: Anesthetics, General; Apomorphine; Electrical Stimulation; Electrodes, Implanted; Electroencephalography; Evoked Potentials, Somatosensory; Magnetic Resonance Imaging; Nicotine; Rats; Somatosensory cortex

Huttunen Joanna

Rotan aivojen tutkiminen toiminnallisen ja farmakologisen magneettikuvauksen avulla

Itä-Suomen yliopisto, terveystieteiden tiedekunta

Publications of the University of Eastern Finland. Dissertations in Health Sciences 179. 2013. 76 s.

ISBN (print): 978-952-61-1177-3

ISBN (pdf): 978-952-61-1178-0

ISSN (print): 1798-5706

ISSN (pdf): 1798-5714

ISSN-L: 1798-5706

TIIVISTELMÄ

Aivojen sähköisen aktiivisuuden liittyminen verenkierron muutoksiin on tunnettu jo yli vuosisadan ajan. Hermoston aktivoituessa veren virtauksen määrä kasvaa suhteessa hapen kulutukseen ja sen vuoksi hapettumattoman hemoglobiinin määrä pienenee paikallisesti. Koska hapettumaton hemoglobiini on paramagneettinen, sen väheneminen näkyy veren hapettuneisuuteen perustuvan (engl. *Blood oxygenation level dependent, BOLD*) toiminnallisen magneettikuvauksen signaalin voimakkuuden muutoksena.

Tässä tutkimuksessa mitattiin rotan tuntoaivokuorelta herätevasteita eri ärsytystaajuuksilla kahden eri nukutusaineen vaikutuksessa. Samanaikaisesti mitatut sähköiset ja verenkierron vasteet poikkesivat toisistaan uretaani- ja alphakloraloosinukutuksessa, mutta näiden vasteiden välillä havaittiin lineaarinen yhteys nukutusaineesta riippumatta. Tämän tutkimuksen perusteella havaittiin lisäksi, että sähköiset tuntoaivokuvauksen parametrit tulee optimoida jokaiselle nukutusaineelle erikseen optimaalisten hermoston ja verenkierron vasteiden saavuttamiseksi.

Suhteellisen pitkän sähköisen tuntoaivokuvauksen aikana hermosolujen eksitoituvuudessa voi tapahtua spontaaneja muutoksia. Sen vuoksi BOLD signaalissa havaittuja vaihteluja pyrittiin mallintamaan sekä samanaikaisesti aivoista mitatulla sähköisellä kenttäpotentiaalisignaalilla että ärsytysjaksoihin perustuvalla blokkimallilla. Molemmat mallit erikseen pystyivät tilastollisesti osoittamaan aktivaation tuntoaivokuorella, mutta kenttäpotentiaalimalli pystyi selittämään enemmän BOLD signaalissa tapahtunutta vaihtelua kuin blokkimalli. Tämä viittaa siihen, että ajan suhteen riippuvia muutoksia on havaittavissa sekä hermoston että verenkierron aktiivisuusmittauksissa.

Farmakologinen magneettikuvaus on uusi toiminnallisen magneettikuvauksen sovellus, jossa aivojen aktivoimiseen käytetään lääkkeitä. BOLD signaalissa mahdollisesti havaittavien intensiteettivaihtelujen, jotka voivat johtua esim. huoneen lämpötilan tai laitteiston lämpenemisestä johtuvista muutoksista, taajuuksia voi olla hankalaa suodattaa pois, mutta niitä voidaan vähentää laskemalla peräkkäisistä magneettikuvista T₂ karttoja. Vahvasti aivoja stimuloivaa nikotiinia ja heikommin aivoja stimuloivaa apomorfiinia käytettiin merkkiaineina osoitettaessa, että kvantitatiivista T₂ karttoihin perustuvaa menetelmää voidaan hyödyntää farmakologisessa aktivaatiossa.

Toiminnallinen ja farmakologinen magneettikuvaus tarjoaa runsaasti erilaisia mahdollisuuksia mitata aivojen toimintaa. Yhdistämällä toiminnallinen magneettikuvaus hermoston toimintaa suoraa mittaaviin sähköisiin menetelmiin voidaan paremmin tutkia mm. toiminnallisen magneettikuvauksen fysiologisia perusteita. Tässä väitöskirjatyössä tehdyillä tutkimuksilla on vaikutusta sekä aivojen toiminnan ymmärtämiseen että nukutetuilla eläimillä tehtävien toiminnallisten tutkimusten suunnitteluun.

Luokitus: QV 137, QV 771, QY 58, QY 60.R6, WB 330, WL 102, WL 141.5.M2

Yleinen Suomalainen asiasanasto: aivotutkimus; elektrofysiologia; nikotiini; nukutusaineet; koe-eläimet – rotat; stimulointi; toiminnallinen magneettikuvaus

Äidilleni

Acknowledgements

This research was conducted in the Biomedical NMR Group at the A. I. Virtanen Institute for Molecular Sciences, University of Eastern Finland.

I am sincerely thankful to my principal supervisor, Professor Olli Gröhn for his tireless guidance and also for his patience with me. I really appreciate his down-to-earth attitude whether it is teaching the basics of NMR or solving numerous practical problems at the scanners.

This work would not have existed without my second supervisor, Adjunct Professor Markku Penttonen. He gave me the chance to start the PhD work and gave me a playground in science where I had the freedom of to do not just what was in the research plan but also what I found interesting.

I thank the reviewers of this thesis Professors Timothy Duong and Markus Rudin for their comments.

I also wish to acknowledge Dr. Ewen MacDonald, for revising the language of this thesis.

I warmly thank all co-authors of the original publications for their significant contribution. Particularly, I thank Dr. Juha Yrjänheikki and Kimmo Lehtimäki at Charles River Finland for the collaboration in the pHMRI study.

I am grateful to the current and previous Bio-NMR group members for creating such a warm and relaxed atmosphere. Specifically, I thank Johanna for the scientific (and nonscientific) discussion and also comments about this thesis; Teemu, Antti and Heikki for the laughter and joy during the workdays.

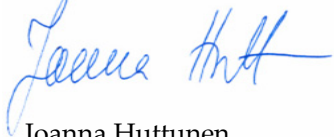
I wish to thank my parents, Eila and Urpo, for their love and support through my whole life. I dedicate this thesis to my mother, who passed away while I was conducting this research. She always had faith in me and believed that I could do anything in the world.

My dearest thanks go to my sister and brother, relatives and friends. Especially, I wish to thank Reetta for peer mentoring, encouragement and above all for friendship.

Finally, my appreciation goes to my husband Tomi for his love and support throughout this research project and to Akseli and Liina, my prides and joys.

This research has been funded by the Academy of Finland, Finnish Cultural Foundation, Finnish Cultural Foundation of Northern Savo, Instrumentarium Science Foundation, Orion-Farmos Research Foundation, The Emil Aaltonen Foundation, Vilho, Yrjö and Kalle Väisälä Foundation, Kuopio University Foundation and Finnish Concordia Fund.

Kuopio, July 2013



Joanna Huttunen

List of the original publications

This dissertation is based on the following original publications:

- I Huttunen J K, Gröhn O, and Penttonen M. Coupling between simultaneously recorded BOLD response and neuronal activity in the rat somatosensory cortex. *NeuroImage* 39: 775-785, 2008.
- II Huttunen J K, Niskanen J-P, Lehto L J, Airaksinen A M, Niskanen E I, Penttonen M, and Gröhn O. Evoked local field potentials can explain temporal variation in blood oxygenation level-dependent responses in rat somatosensory cortex. *NMR in Biomedicine* 24: 209-215, 2011.
- III Huttunen J K, Airaksinen A M, Lehtimäki K, Niskanen J-P, Shatillo A, Yrjänheikki J, and Gröhn O. Evaluation of pharmacological responses by quantitative T₂ fMRI. *Submitted*.

The publications were adapted with the permission of the copyright owners.

Contents

1 INTRODUCTION.....	1
2 REVIEW OF THE LITERATURE	3
2.1 Functional Anatomy of the Brain.....	3
2.1.1 Somatosensory Cortex	3
2.1.2 Neuronal and Glial Activity.....	4
2.1.3 Brain Energetics and Metabolism.....	5
2.1.1 Neurovascular and Neurometabolic Coupling.....	5
2.2 Electrophysiological Methods	6
2.2.1 Local Field Potentials	7
2.3 Functional Magnetic Resonance Imaging.....	8
2.3.1 Principles of Nuclear Magnetic Resonance.....	8
2.3.2 Blood Oxygenation Level Dependent Contrast	10
2.3.3 Functional Imaging with BOLD Contrast.....	11
2.3.4 fMRI in Animal Studies	14
2.3.5 Simultaneous Electrophysiological and fMRI Measurement.....	24
2.3.6 Pharmacological MRI.....	29
3 AIMS OF THE STUDY	35
4 MATERIALS AND METHODS.....	37
4.1 Animal Preparation.....	37
4.2 Electrophysiology.....	38
4.3 MRI Methods	38
4.3.1 Anatomical Imaging.....	38
4.3.1 Functional Imaging	38
4.4 Electrical Stimulation.....	40
4.5 Pharmacological Stimulation.....	40
4.6 Data Analysis	41
4.6.1 Electrophysiological Analysis.....	41
4.6.2 Generation of the LFP Based fMRI Models (II)	41
4.6.3 Calculation of T ₂ Maps (III)	42
4.6.4 fMRI Analysis.....	42
5 RESULTS	45
5.1 Somatosensory Activation	45
5.2 Pharmacological Activation.....	46
6 DISCUSSION AND CONCLUSIONS	47
6.1 Anesthesia	47
6.2 Neurovascular Coupling.....	48
6.3 Pharmacological MRI.....	50
6.4 Future Directions.....	51
7 REFERENCES	53

Abbreviations

3D	Three dimensional
ANLS	Astrocyte-neuron lactate shuttle
AMPA	α -amino-3-hydroxy-5-methyl-4-isoxazolepropionic acid
BIR pulse	B ₁ -insensitive rotation pulse
BOLD	Blood oxygenation level dependent
CBF	Cerebral blood flow
CBV	Cerebral blood volume
CMR _{gluc}	Cerebral metabolic rate of glucose, glucose consumption
CMRO ₂	Cerebral metabolic rate of oxygen, oxygen consumption
CT	Computed tomography
dHb	Deoxygenated hemoglobin
ECoG	Electrocorticography
EEG	Electroencephalography
effTE	Effective time to echo
EFP	Extracellular field potentials
EPI	Echo planar imaging
FAST(EST)MAP	Fast, automatic shim technique using echo-planar signal readout for mapping along projections
FDR	False discovery rate
FEAT	fMRI expert analysis tool
FILM	FMRIB's improved linear modeling
FLASH	Fast low angle shot
fMRI	Functional magnetic resonance imaging
FMRIB	Functional MRI of Brain (research group)
FSE	Fast spin echo
FSL	FMRIB's software library
FWE	Family wise error
GABA	Gamma-aminobutyric acid
GE	Gradient echo

GE-EPI	Gradient echo echo planar imaging
GLM	General linear model
HRF	Hemodynamic response function
ICBM	International Consortium for Brain Mapping
i.p.	Intraperitoneally
i.v.	Intravenously
LDF	Laser Doppler flowmetry
LFP	Local field potential
MEG	Magnetoencephalography
MI	Primary motor cortex
MNI	Montreal Neurological Institute
MR	Magnetic resonance
MRI	Magnetic resonance imaging
MS	Multi slice
MUA	Multi-unit activity
nAChR	Nicotinic acetylcholine receptor
NMDA	N-Methyl-D-aspartate
NMR	Nuclear magnetic resonance
pCO ₂	Partial pressure of carbon dioxide
PET	Positron emission tomography
phMRI	Pharmacological magnetic resonance imaging
RF	Radio-frequency
ROI	Region of interest
s.c.	Subcutaneously
SD	Standard deviation
SE	Spin echo
SE- EPI	Spin echo echo planar imaging
SI	Primary somatosensory cortex
SII	Secondary somatosensory cortex
SPM	Statistical parametric mapping
SPM5/8	Statistical parametric mapping, version 5/8

SS	Single slice
SUA	Single-unit activity
TE	Time to echo, "Echo time"
TR	Time to repeat, "Repetition time"

1 Introduction

The brain has intrigued scientists for many centuries. The quest to widen our knowledge about the structure and function of the most complex organ of all has triggered many technological inventions and scientific breakthroughs in the field of neuroscience. Over the course of time these technical innovations have given scientists in the course of time more advanced tools with which to explore the brain and thus have made possible a deeper understanding of the structure and function of the brain.

History has also shown that misinterpretations or even false discoveries can be made if the techniques are incorrect or performed inaccurately. One of the best examples of incorrect interpretation was done by the early 19th century scientist, Joseph Gall, who associated the shape of the skull (and thence the shape of the brain) to different behavioral traits. This discipline was named phrenology and it had a significant number of followers.

Some of the techniques such as electrophysiology have a long history in the field of neuroscience but are still used today although with modern, state-of-the-art equipment. Even with the equipment of the 19th century, it was discovered that the electrical currents in the brain were related to the function of the brain.

Subsequently new techniques to study the function of the brain have been developed. Positron emission tomography (PET) and functional magnetic resonance imaging (fMRI) have been used in studying brain function both in humans and animals. The current state of fMRI has depended on advances made in pulse sequences, imaging methods, and hardware; studies on magnetic properties of hemoglobin; and research on blood circulation related changes during functional activity.

Magnetic resonance imaging (MRI) has become increasingly popular tool to study anatomy and function of brain. The main advantages of MRI are the spatial resolution, the superior soft-tissue contrast, the noninvasiveness of the modality and the use of non-ionizing radiation. In addition, the versatility of the functional MRI methods means that there are many possibilities to study stimulus or task related changes in the brain or even resting state networks. Despite the increasing number of clinical scanners and research conducted with fMRI, the clinical use of fMRI is still somewhat limited to the surgical planning and mapping of functional areas.

Preclinical studies in animal models provide a good setting to examine normal and pathological brain function, even though more elaborate cognitive processes cannot be investigated as well as in humans. Most of the animal work still employs basic somatosensory stimulation, thus limiting the translational aspect of the research. Nonetheless, the experimental setup in animal studies can be better controlled with regard to the physiological state, immobility of the animal, and timing and conditions of the elicited responses which can lead to a reduction in the variation in the results.

The use of pharmacological agents as the stimuli has established a new branch of functional MRI research, even with its own acronym, phMRI (pharmacological magnetic resonance imaging). Despite the huge potential of this technique, the research into phMRI is relatively limited in both clinical and preclinical settings. The responses to the pharmacological stimuli can be small with poorly-defined temporal profiles and these limitations can hinder the detection of activation sites with conventional data analysis methods. Furthermore, the use of anesthetics and muscle paralyzing agents in animal studies can interact with the pharmacological stimuli complicating the detectable response. Nevertheless, preclinical phMRI is good platform in the drug discovery process and it has enormous translational potential when applied to clinically relevant disease models.

Although the use of fMRI is widespread, there is insufficient knowledge on the physiological basis of the fMRI signal to allow a confident interpretation of the data with

respect to neural activity. In animal models, the combination of functional imaging with more direct invasive neuronal activity recordings represents an ideal way to increase understanding of the mechanisms of the physiological basis of the fMRI signal.

2 Review of the Literature

2.1 FUNCTIONAL ANATOMY OF THE BRAIN

The size of the adult rat brain is small, approximately 16 mm in width, 11 mm in height and 20 mm in length (Paxinos and Watson, 1998), and it weighs about 2 g. The adult human brain weighs approximately 1.5 kg making it 750 times larger than the rat brain. Even though the number of neurons in the human brain has been generally claimed to be 100 billion, a recent study estimated the number of neurons to be 86 billion with 85 billion of glial cells (Azevedo et al., 2009). Using the same technique, it was also calculated that the rat brain has about 200 million neurons and 131 million glial cells (Herculano-Houzel et al., 2006). Therefore the number of neurons in the human brain is 430 times larger than that of the rat brain.

The relative size of the cerebral cortex amounts to 82 % of the brain mass in humans and 43 % in rats. However the relative number of neurons in the cerebral cortex is rather similar: 19 % in humans and 15.5 % in rats.

Blood vessels of the cortex can be divided into pial and intracortical vessels. Pial vessels – arteries and veins - run along the surface of the brain while intracortical vessels penetrate into the different layers of the cortex. Blood flows from the pial arteries to the intracortical arteriolar branches, then into the dense capillary network, draining back through the intracortical venules and pial veins.

The vascular network of cortex can be divided into four vascular layers (Duvernoy et al., 1981) that are correlated with the cellular layers of the cortex. The superficial cortical layer (layer I) has the lowest vascularization, layer IV displays the highest vascularization. Vascular density in the brain correlates with the number of synapses, rather than the number of neurons (Duvernoy et al., 1981). The general aspects of the cortical vasculature are also valid for many of the most widely used experimental animals, such as nonhuman primates (Weber et al., 2008) and rodents (Tsai et al., 2009).

2.1.1 Somatosensory Cortex

The rat somatosensory cortex receives information from the somatosensory receptors that detect mechanical, thermal or noxious stimuli. In the primary somatosensory cortex (SI) of the rat, there is one representation of the body surface and it is dominated by facial and whisker related areas (Paxinos, 2004). The barrel cortex receives input from whiskers and is located caudolaterally in the SI (-0.26 mm - -4.16 mm from bregma (Paxinos and Watson, 1998)). The barrel cortex contains aggregations of granule cells (barrels) and each barrel corresponds to a single vibrissa.

The digits of the forepaw are represented in an orderly sequence in the forepaw region of the cortex. Stimulation of the forepaw excites afferent nerves and travel through the spinal cord. The information crosses the midline in the medulla and is relayed through ventral posterolateral thalamic nucleus to layer IV of the primary somatosensory cortex. The forepaw region is situated caudal to the barrel cortex (1.2 - -2.12 mm from bregma (Paxinos and Watson, 1998)). The hindpaw area is situated closest to the midline (-0.26 - -2.12 mm from bregma (Paxinos and Watson, 1998)).

Neurons from the ventral posterolateral thalamic nucleus and posterior thalamic nuclear group project also to the secondary somatosensory cortex (SII) which is located laterally to the SI. Thalamocortical axons from ventrolateral thalamic nucleus terminate not only in motor cortex, but also in forepaw and hindpaw areas. This region is a partial overlap between sensory and motor cortex.

Furthermore, the cortex sends information to the pons, which is then relayed to the cerebellum. The cerebellum also receives an input directly from the spinal cord. In addition, there are reciprocal connections between the primary somatosensory cortex and the primary motor area and intracortical connections between the left and right sides of the primary somatosensory cortex.

2.1.2 Neuronal and Glial Activity

In the central nervous system, there are two types of cells: neurons and glia. The glia subsidiary cells were originally thought to outnumber the neurons by tenfold, however, based on a recent study, the number of neurons and glia in humans is almost the same (Azevedo et al., 2009).

The neurons are translational cells receiving input from receptors or other neurons and transmitting the information over distances. The neuron consists of several parts: the soma, the dendrites and the axon. The dendrites of the neuron are connected to multiple neurons and information is collected from a large area. The axon is only found in neurons and it is specialized for the transfer of information.

The information is carried through action potentials that sweep along the axons like a wave. The depolarization of the cell is caused by the influx of sodium ions across the membrane and the repolarization is attributable to the efflux of potassium ions. The axon ends in an axon terminal which is connected to other neurons via the synapse. The electrical signal in the axon has to cross the synaptic gap and evoke a postsynaptic potential in the second neuron. Most synaptic transmission is chemical where the presynaptic signal is converted into a chemical signal that crosses the synaptic cleft and is then converted back to an electrical signal in the post-synaptic dendrite.

Different neurons in the brain release different neurotransmitters. More than 90% of synapses release glutamate (Abeles, 1991; Braitenberg and Schuz, 1998), which is the main neurotransmitter in the brain. Acetylcholine is another neurotransmitter that mediates fast synaptic transmission at all neuromuscular junctions. The opening of glutamate- or acetylcholine-gated ion channels leads to the formation of excitatory postsynaptic potential in the postsynaptic dendrite. The synaptic activation of glycine- or gamma-aminobutyric acid (GABA)-gated ion channels cause inhibitory postsynaptic potential. In addition to this fast acting chemical synaptic transmission, there are G-protein coupled receptors that mediate a metabotropic postsynaptic action that is slower, longer-lasting and more diverse.

Astrocytes are the most numerous glial cells in the brain and they have important functions on their own. They provide physical support and nutrients to neurons, digest parts of dead neurons and can release transmitters (e.g. glutamate) (Haydon and Carmignoto, July 2006) and communicate with each other via the propagation of calcium elevation (Araque et al., 2001).

Astrocytes are ideally located in close proximity to the neurons and blood vessels. Their end feet are connected to blood vessels in the brain. Astrocytes, neurons and vascular cells compose a neurovascular unit which controls the cerebral blood flow and which is termed the blood brain barrier.

Astrocytes are electrically inexcitable and therefore relatively difficult to measure with traditional electrophysiological methods. Both spontaneous and stimulus induced calcium waves in astrocytes have been measured using multiphoton microscopy and calcium selective dyes. Astrocytic calcium elevations induce vasodilation in the penetrating cortical arterioles (Takano et al., 2006). Even though the calcium waves appear later than the functional hyperemia (Petzold and Murthy, 2011) indicating that calcium represents only one of many different vasoactive messengers, the astrocytes are key mediators of functional hyperemia.

2.1.3 Brain Energetics and Metabolism

Neural processing in the brain is extremely energy demanding. Even though the weight of the human brain is about 2 % of the body weight, it consumes about 20 % of the energy in rest (Kety, 1957; Sokoloff, 1960). The brain has very little energy reserve, therefore a continuous vascular supply of glucose and oxygen is mandatory in order that it can sustain neuronal activity.

In rodents, the major fraction of the energy used by the brain's grey matter is expended on signaling-related processes, i.e. in propagating action potentials (47 %) and in mediating the postsynaptic effects of glutamate (34 %) (Attwell and Laughlin, 2001). The maintenance of the resting potential in neurons and glia consumes about 15 % of the total energy. In glial cells, 60 % of their total 5 % energy budget is used for maintaining resting potentials and 40 % for glutamate recycling (Attwell and Iadecola, 2002).

During the oxidative process, glucose is converted into carbon dioxide and water, resulting in the production of large amounts of energy in the form of adenosine triphosphate. This oxygen demanding process is very efficient in producing a large quantity of energy. In the situation where there is not enough oxygen available, then anaerobic glycolysis takes place.

2.1.1 Neurovascular and Neurometabolic Coupling

The quest to understand the relationship between brain function and energy metabolism has intrigued scientists for more than a century. The early pioneers at the end of 19th century carried out experiments to measure temperature changes in the brain, trying to relate them to the functional activity (Zago et al., 2012). The results were, however, confronted by methodological problems. Italian physiologist, Angelo Mosso, measured brain activity related changes in the brain volume from patients with skull defects and postulated that the pulsation of the brain reflected the blood flow to the brain in response to an auditory stimulus or while performing an arithmetic task (Mosso, 1881).

In 1890, Roy and Sherrington implemented this method in animal studies including a craniotomy and simultaneous blood pressure measurements and recorded movement of brain surface (Roy and Sherrington, 1890). They concluded that "vascular supply can be varied locally in correspondence with local variations of functional activity" (Roy and Sherrington, 1890). The vasodilatation of the vessels was caused by an intrinsic mechanism due to "chemical products of cerebral metabolism" which has been later described in a statement that the local blood flow is driven by local metabolic demand.

In the mid-20th century, technical developments made it possible to measure the whole brain blood flow and metabolism in humans using nitrous oxide as a freely diffusible tracer (Kety and Schmidt, 1945; Schmidt and Kety, 1947; Kety and Schmidt, 1948; Kety, 1948). The whole brain measurement with a replication of Mosso's arithmetic task induced no changes in the blood flow or oxidative metabolism (Sokoloff et al., 1955) suggesting that only regional changes could be observed even with this relatively simple experimental setup.

The introduction of autoradiographic studies with radioactive tracers provided the first glimpse into in vivo quantitative changes in blood flow in response to changes in local functional activity (Landau et al., 1955; Freygang and Sokoloff, 1958). The utilization of the deoxyglucose autoradiographic technique made possible regional measurements of glucose metabolism in both conscious and anesthetized animals (Sokoloff et al., 1977). This method provided quantitative information about the energy metabolism in the brain and was the first approach that, in conjunction with electrophysiological measurements had the potential to expand the knowledge of functional brain organization. As a result of the development of deoxyglucose autoradiography, a large number of experiments have been focused on the relationship between local cerebral activation and glucose consumption in animals.

The human experiments of regional changes in brain circulation and metabolism were introduced in the 1960s when David Ingvar and Niels Lassen developed a method using

radioactive isotopes of gas with gamma ray camera used to detect regional changes in cerebral blood flow (CBF) in humans (Ingvar and Lassen, 1961; Ingvar and Lassen, 1962; Lassen et al., 1963).

It took almost 100 year before the observation of coupling between metabolism and cerebral blood flow made by Roy and Sherrington was challenged. In 1986, Fox and Raiche demonstrated the uncoupling of CBF and cerebral metabolic rate of oxygen (CMRO₂) during brain activation. At rest, the blood flow is well correlated with the oxygen consumption, but during somatosensory stimulation, the CBF increase overcompensated for the CMRO₂ increase to such an extent that a highly significant decrease in the extracted fraction of available oxygen was observed (Fox and Raichle, 1986). A similar uncoupling during activation was observed between the cerebral metabolic rate of glucose (CMRgluc) and CMRO₂ to an even higher extent (Fox et al., 1988). This uncoupling of blood flow and consumption of oxygen in the activated brain region provides the physiological basis for blood oxygenation level dependent (BOLD) contrast.

The prevalent model of CBF regulation upon neuronal activation is the astrocyte-neuron lactate shuttle (ANLS) model proposed by Pellerin and Magistretti (Pellerin and Magistretti, 1994). Neurons predominantly consume glucose in oxidative metabolism but during activation they also use glucose to release the excitatory neurotransmitter glutamate. Glutamate is taken up by astrocytes via a Na⁺-dependent transport system. In the astrocyte, glutamate stimulates glycolysis, i.e. glucose utilization and lactate production. This is a kind of signaling pathway where glutamate is acting via its transporter not its receptor. Lactate can then be oxidized by neurons to produce sufficient adenosine triphosphate. In the ANLS model, task-induced increases in neuronal activity exert minimal energy demands. CBF up-regulation is chiefly driven by the lactate generated by in the course of glutamate shuttling.

2.2 ELECTROPHYSIOLOGICAL METHODS

Electrophysiology is the study of the electrical potential difference between two locations in relation to the function of the central nervous system. In the case of recording electrical activity from the scalp the method has been referred to as electroencephalography (EEG) and when measured with subdural grid electrodes on the exposed cortical surface of the (human) brain, it has been referred to as electrocorticography (ECoG). Direct measurement using a small size electrode inside the brain is known as local field potential (LFP) or intracranial EEG measurements (also known as deep-EEG or micro-EEG).

The first electrophysiological measurement was conducted in 1875, when Richard Caton measured voltage changes using a galvanometer on rabbit and monkey brain (Caton, 1875). In his short description of the study, he reports "The electric currents of the grey matter appear to have a relationship to its function." (Caton, 1875). This initiated the practice of studying electrical brain activity through electrophysiological measurements.

The next breakthrough in electrophysiological measurements came in 1929 when Hans Berger used an amplifier to increase the signal intensity and measured the electrical activity of the human brain on the scalp (Berger, 1929). He named the technique "Elektrenkephalogramm" since the "Elektrocerebrogramm" that was based on the name of the electrocardiogram was too "barbaric".

The electroencephalography denotes the recording, *graphy*, of the electrical signals, *electro*, from the brain, *encephalo*. On other words, measuring the potential changes on the surface of skull, not directly inside the brain. The scalp EEG is a spatiotemporally smoothed version of the LFP, integrated over an area of 10 cm² or more due to the distorting and attenuating effects of the soft and hard tissues between the current source and the recording electrode.

The EEG signal is typically picked up with chloridized silver electrodes using a conductive paste to ensure low-resistance connection. In an EEG setting, the signal amplitude is usually in the range of microvolts.

Brain activity can also be measured using magnetoencephalography (MEG). When neurons generate electrical currents, they also produce very weak magnetic field. This field strength is about one billionth (10^{-9}) of the Earth's magnetic field. Compared to EEG, the magnetic field penetrates the skull without distortions but MEG is most sensitive to the activation in the fissural cortex that is tangential to the skull (Hämäläinen et al., 1993).

The electrophysiological measurements have excellent temporal resolution, usually from the submillisecond range to a few milliseconds. This leads to exceptional sensitivity to the changes in neuronal activity even though the spatial resolution is limited by the number of measuring electrodes. Therefore, topographical mapping of the electrical activity suffers from physical limitations of localizing the sources of brain signals from the multiple electrodes in the scalp EEG recordings.

2.2.1 Local Field Potentials

Neuronal activity in the brain gives rise to transmembrane currents and generates a potential that can be measured in the extracellular medium. Neurons are surrounded by the extracellular medium that is a volume conductor with resistivity. The flow of positive ions (e.g. Na^+) into the active sites of a neuron appears as a current sink. The current flows along the dendrites or axons. Since the currents flow in closed loops, a distant inactive membrane appears as the source. The finite resistance of the extracellular medium creates extracellular field potentials (EFP) that are being measured by electrodes.

The spatial and temporal sum of the sinks and sources from multiple cells is called the mean EFP. If the size of the electrode is much larger than the size of the neurons, the mean EFP is dominated by the summed synaptic and action potentials. The low frequency ranges (< 200 Hz) of mean EFP are called local field potentials. They primarily reflect the average of synchronized dendro-somatic components of the synaptic voltages, most likely from within a few millimeters of the electrode tip (Logothetis and Wandell, 2004).

Single unit activity (SUA) refers to the measurement with a microelectrode that detects the action potential of one single neuron. Multiunit activity (MUA) measures multiple unit spiking activity that is high-pass filtered from the mean EFP with cut-off at 300 - 400 Hz. Depending on the recording site and the electrode properties, the MUA is likely to represent a weighted sum of the extracellular action potentials of neurons within a sphere of 200 - 300 μm radius, with the electrode at its center (Logothetis, 2002).

The LFP measures slow waveforms, including synaptic potentials, afterpotentials of somatodendritic spikes, and voltage-gated membrane oscillations but not the action potentials carried by principal output neurons. The amplitude and frequency of the LFP waveform depends on the proportional contribution of the multiple sources and various properties of the brain tissue. The larger the distance to the source, the less it contributes to the measured LFP. The generated potential is then inversely related to the distance of the source.

All neuron types contribute to the LFPs, even though pyramidal cells contribute more due to substantial separation of the active sink from the return current in the long dendrites than for example spherically symmetric neurons that have dendrites of relatively equal size in all directions (Buzsaki et al., 2012). In addition, the strength of the LFP is determined by the spatial alignment of neurons and temporal synchrony of the generated fields of the neurons. Since the alignment of the pyramidal dendrites is parallel in the cortex, this gives rise to large LFPs in the cortex. Another important factor in determining the magnitude of LFPs is the temporally synchronous activity.

Synchronous oscillatory activity is typical for neurons and neuronal networks. The neuronal rhythms are employed to coordinate activity between different brain regions (Freeman, 1975). The slow rhythms involve a large number of cells and they can convey

information over long distances, furthermore fast rhythms are more localized and engage a small number of neurons (Buzsáki, 2006).

The magnitude of the LFP power can be quantified as a square of amplitude and it is inversely related to the frequency, i.e. $1/f$. There are multiple mechanisms that contribute to the power law of the LFP but it is primarily due to the low pass frequency filtering property of the dendrites due to signal attenuation between the input location in the distal dendrite and soma (Buzsaki et al., 2012).

Different frequency bands can be attributed to the electrophysiological signals. The frequency bands are delta (0.5 – 4 Hz), theta (4 – 8 Hz), alpha (8 – 13 Hz), beta (14 – 30 Hz) and gamma (30 – 80 Hz) (International Federation of Societies for Electroencephalography and Clinical Neurophysiology, 1974; Steriade et al., 1990). High frequencies have short time windows for information processing and are therefore used in local computation. The lower frequencies with long time windows are used for long distance interactions. Low-frequency oscillations can also modulate high-frequency activity and these kinds of cross-frequency coupling may integrate functions across multiple spatiotemporal scales (Wang et al., 2012). In addition to these established frequency bands, very slow (0.02 – 0.5 Hz) and very high (80 – 600 Hz) frequency bands have been characterized (Penttonen and Buzsáki, 2003).

Evoked potentials are electrical response of the brain to a specific stimulus. They were discovered already in 1893 by Fleischl von Marxow (Fleischl von Marxow, 1893). Since evoked potentials have explicit timing in relation to the stimulus, the identification of the latency, amplitude and duration of the response offers a unique window from which to view the neuronal pathways, e.g. the somatosensory pathway, in the brain. In LFP measurements, individual evoked responses can easily be identified, but in the EEG due to the relatively high background noise and low amplitude response, averaging is usually necessary to detect and analyze these responses.

2.3 FUNCTIONAL MAGNETIC RESONANCE IMAGING

Nuclear magnetic resonance (NMR) was discovered in 1946 when Bloch (Bloch, 1946) and Purcell with colleagues (Purcell et al., 1946) independently detected a resonance phenomenon in samples placed in the magnetic field. Imaging using NMR was introduced in 1970s when Lauterbur pioneered the idea of using additional gradients and back-projection method known from computed tomography (CT) to create an image (Lauterbur, 1973). He named the image formation technique as zeugmatography which came from Greek “that which is used for joining”, however that name never became widely accepted.

The functional magnetic resonance imaging began in the 1990s. However the enabling breakthroughs in understanding the magnetic properties of red blood cells, neuronal activation related changes in hemodynamics and development of fast imaging sequences were made much earlier. The rapid increase in functional imaging is due to the prevalence of MRI scanners and noninvasiveness and nonradioactiveness of the method and the enormous versatility of sensory and cognitive processes that it can be used to study.

2.3.1 Principles of Nuclear Magnetic Resonance

Most tissue types, especially the brain, consist mainly of water. The hydrogen atoms, ^1H , are present in each water molecule and are therefore the most abundant, biologically relevant nucleus for NMR. A proton possesses a physical property, spin, which can be considered as a small magnet. Hydrogen has a spin number of $\frac{1}{2}$, and when placed in the external magnetic field B_0 , there are two possible energy states for the nucleus. The lower energy state is aligned in parallel and the higher energy state is aligned as anti-parallel to the external magnetic field B_0 . Slightly more spins are in the parallel state due to thermodynamic balance. The Boltzmann distribution determines the relative numbers of

nuclei within each energy state, and this difference provides the basis for the NMR experiments.

Transition between these two energy states either emits or absorbs energy in the radiofrequency (RF) range. An oscillating magnetic field B_1 is applied through a radiofrequency wave pulse to excite the spins that matches the energy difference of the two states. The radio frequency pulse is matched with the Larmor frequency (ω_0) and it is determined by the external magnetic field B_0 and the gyromagnetic ratio γ of the nucleus

$$\omega_0 = \gamma B_0. \quad (1)$$

The gyromagnetic ratio for hydrogen is 42.577 MHz/Tesla meaning that hydrogen atom will resonate at 200 MHz in a 4.7 T magnet and at 298 MHz in a 7.0 T magnet.

Since slightly more spins will align in parallel to the magnetic field, a net magnetization is created. By applying radio frequency energy, spins can be lifted from a low energy state to a high energy state and combined with phase coherence, the net magnetization is tilted, forming the xy-plane that can be measured. After the RF pulse is switched off, the absorbed energy in the nuclei is used by the interactions between other nuclei and the surrounding lattice. Thus the spins return to the thermal equilibrium and the net magnetization recovers to its equilibrium position. The rotating xy-component of net magnetization induces a voltage which varies at the Larmor frequency and can be detected via the induction of current to an RF coil tuned to the frequency of the oscillation.

The thermal equilibrium in the spin system is recovered and this process is called T_1 relaxation. The recovery of the longitudinal component of the net magnetization depends on the spins' interaction with their surrounding environment ('lattice'). The recovery is an exponential process. If a new excitation RF pulse is applied more rapidly than the full relaxation, only a proportion of the spins can be lifted to the high energy state and the detectable signal decreases.

The loss of the transverse component of net magnetization is called T_2^* relaxation. It occurs when the phase coherence of the spins decreases after excitation. This is due to the transfer of energy between the spins but it does not change the net energy of the whole system. The degree of the spin-spin interaction is defined by the physical and chemical environment of the nuclei and thus is varied between tissues. Rapid dephasing of the phase coherence leads to fast T_2^* relaxation and therefore short T_2^* times.

The net transverse magnetization disappears at the rate of $1/T_2^*$ as the phases of the individual spins diverge. By applying a refocusing RF pulse, the phase distribution is inverted. If the environment of each spin remains similar during the refocusing time, then the net transverse magnetization can be restored. T_2^* depends on both static and varying field fluctuations and is described as the apparent transverse relaxation time. For T_2 , the static and slowly varying effects are cancelled and this term is called the intrinsic transverse relaxation time. The T_2^* relaxation time is always shorter than the T_2 . The components contributing to the loss of the transverse component can be expressed as:

$$\frac{1}{T_2^*} = \frac{1}{T_2} + \frac{1}{T_2'} \quad (2)$$

where T_2' is the contribution from static field inhomogeneities that can be cancelled by the refocusing pulse. T_2 processes cannot be refocused due to the randomness of the processes occurring at the molecular level.

The static magnetic field over the sample is not homogenous and the nuclei will experience a slightly different field according to their position. In addition, different magnetic susceptibility properties in the sample will cause local inhomogeneities in the magnetic field. Since T_2^* relaxation is affected by differences in the magnetic field, this has

great importance in fMRI because it is sensitive also to the field distortions caused by the paramagnetic deoxyhemoglobin (Ogawa et al., 1990b).

2.3.2 Blood Oxygenation Level Dependent Contrast

Hemoglobin is a large protein that consists of two pairs of polypeptide chains (globin). Each chain is attached to a complex of porphyrin and iron (heme group). One oxygen molecule can bind to each heme. In deoxygenated hemoglobin (dHb), the iron (Fe^{2+}) is in a paramagnetic high-spin state, as four of its six outer electrons are unpaired (Pauling and Coryell, 1936). The electronic structure of hemoglobin will undergo a change in the presence of an oxygen molecule. When hemoglobin becomes oxygenated, the heme iron changes to a diamagnetic low-spin state and will thus have zero magnetic moment. This change in the spin-state is the basis of the oxygenation dependence of the transverse relaxation time of water protons in blood. The blood oxygenation has a quadratic dependence for the rate of transverse relaxation, $1/T_2$ (Thulborn et al., 1982), meaning that the more deoxygenated hemoglobin that is present, the shorter will be the T_2 .

The paramagnetic dHb is restrained in red blood cells which are in turn restricted to blood vessels. The paramagnetic dHb enhances T_2 relaxation of the blood and surrounding tissue. Ogawa et al. observed that the appearance of the dark lines in the cortices of rodents in the gradient echo images was dependent on the blood oxygenation level, since the lines disappeared when the blood was completely oxygenated (Ogawa et al., 1990b). The dark lines were caused by the paramagnetic deoxygenated hemoglobin in blood while the diamagnetic oxygenated or carbon monoxide hemoglobin did not give the contrast. The presence of deoxygenated hemoglobin in blood produced BOLD contrast (Ogawa et al., 1990a).

The emergence of the BOLD contrast from the deoxygenated hemoglobin can be divided into intravascular and extravascular components. Depending on the magnetic field strength, pulse sequence and imaging parameters, the contribution of the effect of these components can vary.

The intravascular component arises from the loss of phase coherence resulting from exchange and diffusion processes. Water rapidly exchanges between plasma and red blood cells that contain paramagnetic deoxyhemoglobin. Inside the vessels, water also diffuses in and around erythrocytes under the magnetic field gradients that are generated by deoxyhemoglobin. Since all the water molecules inside the vessel experience these processes similarly, this leads to a reduction of T_2 of blood water in the veins.

The magnetic field gradients generated by deoxyhemoglobin decline as a function of $(r/a)^2$, where r is the distance from vessel and a is the vessel radius (Kim and Ogawa, 2012). Therefore the magnetic susceptibility effect also extends to the extravascular tissue. The dephasing effect around a larger vessel expands more widely because of a smaller susceptibility gradient, therefore contributing BOLD signal significantly, regardless of the magnetic field strength (Lee et al., 1999).

During rest, blood in capillaries and veins contains a relatively high concentration of deoxyhemoglobin whereas the brain tissue itself is diamagnetic, creating a magnetic susceptibility difference between blood and tissue. During neuronal activation, the CBF increases bringing oxygenated hemoglobin into the brain and this leads to a washout of deoxygenated hemoglobin (Figure 1). Therefore the magnetic susceptibility difference between blood and tissue decreases, leading to a reduction in the local extravascular field gradients and to an increase in the T_2 values and thus an elevation in the BOLD signal.

An additional component giving rise to the positive BOLD contrast is the increase in cerebral blood volume (CBV). An increase in blood volume leads to an increase in the BOLD signal, even when the blood oxygenation remains constant (van Zijl et al., 1998). The influence of the CBV change is highest at low magnetic field strengths due to long T_2 values of the blood as compared to tissue T_2 values.

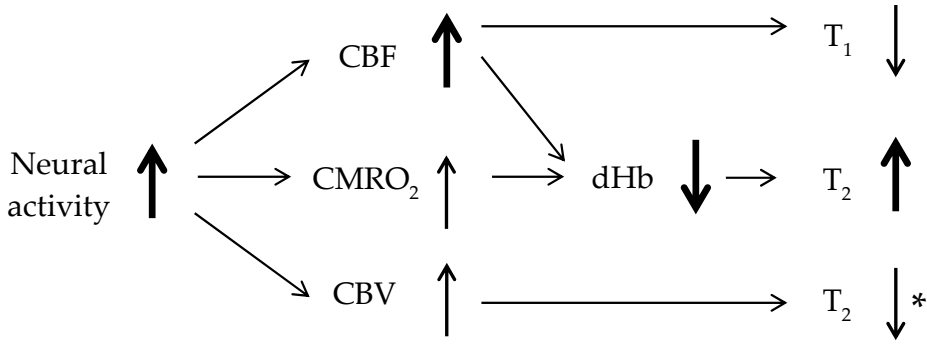


Figure 1. Schematic illustration of the fMRI related signal changes. After a task or a stimulus, neural activity is increased and this causes an increase in vascular and metabolic responses. The CBF increase exceeds the CMRO₂ increase, therefore the venous dHb concentration declines leading to an increase in T₂. An increase in CBF decreases T₁. * An increase in CBV decreases T₂, when the blood water T₂ exceeds the grey matter T₂. At low magnetic field strength, an increase in CBV increases T₂. Modified from (Kim and Bandettini, 2010).

In addition to positive BOLD responses, also stimulus evoked negative BOLD responses have been observed in both humans and animals (e.g. (Harel et al., 2002; Shmuel et al., 2006; Schridde et al., 2008; Goense et al., 2012; Schäfer et al., 2012)). Since a positive BOLD response is due to a decrease in the amount of deoxygenated hemoglobin, negative BOLD signal should reflect an increase in deoxygenated hemoglobin.

The negative BOLD response may be explained by a decrease in blood flow that is associated with decreased oxygen consumption or in a situation where the oxygen metabolism outnumbers the blood flow increase. In other words, a decrease in CBF is associated with a comparable decrease in CMRO₂ (Shmuel et al., 2002; Stefanovic et al., 2004) with a smaller decrease in CMRO₂ (Nair, 2005) or when a larger fractional increase in CMRO₂ is found compared to CBF (Vafaei and Gjedde, 2004). A decrease in the CBF has also been attributed to “vascular stealing” (Harel et al., 2002), where blood flow from the less demanding areas may be reallocated to those regions demanding the greatest blood flow.

By measuring both electrophysiological and BOLD signals, it has been possible to link the stimulus evoked negative BOLD response with decreased CBF and neuronal activity (Shmuel et al., 2002; Shmuel et al., 2006; Devor et al., 2007; Boorman et al., 2010). Nevertheless in a recent study, negative BOLD signals were associated together with increased neuronal, hemodynamic, and metabolic activity during epileptic seizure in hippocampus (Schridde et al., 2008). Consequently in this condition, the negative BOLD response may arise from changes in oxygen consumption that far exceeds the oxygen supply. Altogether the mechanisms behind the negative BOLD response is far from completely understood.

2.3.3 Functional Imaging with BOLD Contrast

In order to create an image, the spatial localization of the protons throughout the sample must be resolved. Spatial localization of the nuclei relies on the principle that the precession frequency of a nucleus linearly depends on magnetic field strength. Localization is performed using three orthogonal magnetic field gradients.

Slice selective RF pulses with specific frequency and bandwidth transfer energy to the nuclei with matching resonance frequency. Therefore using the selective RF pulse simultaneously with a linear gradient, excites only the nuclei within a selected slice. Spatial encoding within the selected slice is then achieved with two additional orthogonal gradients. The frequency gradient is applied when the signal is acquired. When the

frequency (readout) gradient is applied, the spinning nuclei within the selected slice will oscillate with different frequencies depending on their experienced magnetic field strength. The phase gradient is applied before the signal collection so that the magnetic field gradient should induce a phase shift between the nuclei within the selected slice. The phase shift is dependent on the applied field gradient strength and duration. Therefore, the nuclei from each position within the selected slice carry a distinct frequency and a distinct phase that allows for encoding of the coordinates within the imaged slice. The magnetic resonance (MR) image is created by using a Fourier transformation on the collected phase and frequency information within each slice.

The RF pulses and the magnetic field gradients are controlled by a pulse sequence. In principle, there are three main parameters in the pulse sequences that are varied to create an image with selected contrast: flip angle, repetition time and echo time. The flip angle is dependent on the energy of the radiofrequency pulse and it describes how much the net magnetization is tilted towards the transversal plane. The more energy that is used, the more time is needed for full relaxation. The time to repeat the applied RF pulses is called the repetition time (TR). The shorter the TR, the less time there is for net magnetization to recover. After excitation, the waiting time before the signal is detected is called echo time (TE). The longer the TE, the less those nuclei with short T_2 times will contribute to the image.

Echo Planar Imaging Sequence

The echo planar imaging (EPI) sequence for the first time provided the opportunity to collect entire image after one excitation pulse (Mansfield, 1977). This enabled fast imaging which is necessary for detecting changes in hemodynamic activation occurring within a range of seconds.

After slice selection by RF excitation, a series of gradient echoes are acquired by inverting the readout gradient. A short gradient pulse, a blip, between the alternating acquisition is applied by the phase gradient in the orthogonal direction. The typical acquisition time is less than 100 ms per slice. The gradient echo EPI (GE-EPI) is a heavily T_2^* weighted sequence and it is the most commonly used pulse sequence in fMRI studies due its high sensitivity for the magnetic susceptibility effects attributable to paramagnetic deoxygenated hemoglobin.

Spin echo EPI (SE-EPI) was used as an alternative in functional imaging to GE-EPI in 1.5 T for the first time in 1994 (Bandettini et al., 1994). After tilting the magnetization with 90° excitation pulse, a strong signal, that decays with a time constant T_2^* , can be detected. After a short time, a 180° refocusing pulse is applied and part of the signal builds up again. This effect is known as spin echo (SE) (Hahn, 1950). In the EPI sequence, T_2 (spin echo) weighting results when a 180° refocusing pulse is applied prior to the gradient echo train and the center of the echo train coincides with the center of the spin echo.

By varying the echo time, the maximum BOLD signal was achieved using $TE \sim T_2^*$ of grey matter for GE-EPI and $TE \sim T_2$ of grey matter for SE-EPI (Bandettini et al., 1994). This is still used as a general rule of thumb when selecting the optimal imaging parameters for BOLD fMRI studies. The same relationship between optimal TE and T_2^* was also shown with the multi-echo imaging sequence (Posse et al., 1999).

The contributions of the intravascular and extravascular component to the BOLD contrast depend on the magnetic field strength, pulse sequence and imaging parameters. The gradient echo BOLD signal consists of both extravascular and intravascular components regardless of the vessel size (Bandettini, 1999). As the magnetic field strength increases and as TE increases, the intravascular component decreases as well. T_2 values for blood water and grey matter decrease as a function of magnetic field strength (Table 1). By selecting the echo time to be much longer than the T_2 of blood water in veins, the intravascular component can be minimized. Therefore at high magnetic fields, the intravascular component can be eliminated and the signal originates from the extravascular component.

Table 1. T_2 values for blood water and grey matter at different magnetic field strengths.

Magnetic field strength	T_2 (ms) blood water	Reference	T_2 (ms) grey matter	Reference
1.5 T	~ 127 122	Wright et al., 1991 Silvennoinen et al., 2003	91 ± 6	Breger et al., 1989
3.0 T	31.1	Zhao et al., 2007	70.7 ± 10.4	Gelman et al., 1999
4.0 T			67.1 ± 6.0 63.0 ± 6.2	Yacoub et al., 2003 Jezzard et al., 1996
4.7 T			67.5	Pfeuffer et al., 2004
7.0 T	$\sim 12 - 15$ ~ 7	Ogawa et al. 1993 Yacoub et al., 2001	55.0 ± 4.1 59.1	Yacoub et al., 2003 Pfeuffer et al., 2004
9.4 T	9.2 ± 2.3	Lee et al., 1999	38.6 ± 2.1	Lee et al., 1999

By using spin-echo techniques, the extravascular contribution of large vessels can be reduced by applying the 180° RF pulse which refocuses the dephasing effect around the large vessels. This is due to the long echo time when tissue water around the large vessels can be locally averaged. Therefore the spin echo BOLD image contains mainly the extravascular effect of small vessels which is supra-linearly dependent on the magnetic field. In the gradient echo BOLD signal, the extravascular effect of large vessels is linearly dependent upon the magnetic field strength and the effect of the small vessels is supra-linearly dependent. Therefore the spin-echo BOLD contrast is more specific for the parenchyma than the gradient echo BOLD contrast. However, because the dephasing effect of the large vessels is refocused, the spin echo BOLD signal is smaller than the gradient echo BOLD signal.

Experimental Design and Data Analysis

The experimental design or the stimulus paradigm for functional studies can be planned in many different ways. The choice is governed by the methodological limitations of fMRI and the properties of the measured physiological parameters. The stimulus paradigm can be designed in three ways with the main difference being the time scale of the stimulus or task. In an event related design, the stimulus is presented with a very short duration. This allows imaging of transient neuronal changes. In addition, by varying the inter-stimulus interval, the habituation to the same stimulus can be minimized.

The most commonly used type of stimulus paradigm is called the block design; in this the stimulus is presented for a longer time period. The advantage of the block design is that during the longer stimulus period, the BOLD response is temporally integrated and it improves the detection power of the statistical analysis. In addition, a mixed combination of events and blocks can be used.

The main goal of the fMRI analysis is to detect and localize robust changes that result from the applied stimulus or from the physical or cognitive task. Since BOLD fMRI is sensitive to deoxygenated hemoglobin, images taken during the stimulus or the task period should show increased intensity compared to images taken at baseline or rest. fMRI data analysis typically involves some preprocessing steps before the analysis of stimulus induced responses. Some preprocessing is needed to remove unfavorable artifacts and to prepare the data for statistical analysis.

Movement of the subject evokes artifacts to the MR images. In the time series of functional images, this causes the voxels to shift from their original position, and thus to induce unwanted signal changes. In animal studies, movement related artifacts can be

minimized by restraining the anesthetized animal with ear plugs and a bite bar. In addition, the use of a muscle relaxant in ventilated animals reduces motion during scanning. Even though the head might be tightly secured, breathing and beating of the heart can cause the brain to move inside the skull. This is usually more problematic in human studies. Motion correction can be performed in several different ways. Typically, a rigid-body registration is performed with three translation and three rotation parameters.

The whole brain can be covered with multiple functional slices that are acquired within the TR. Therefore depending on the length of the TR, there may be a time difference between the first and the last slice. This can be adjusted by interpolating the data so that it seems that all slices have been acquired simultaneously or by adding temporal derivatives to the hemodynamic response function.

In order to compare results from individual subjects, normalization to a standard template needs to be performed since all brains are not equal in size and shape. The most commonly used coordinate systems for humans are the Talairach system (Talairach and Tournoux, 1988) and the Montreal Neurological Institute (MNI) template that is currently known as the International Consortium for Brain Mapping (ICBM) template (Mazziotta et al., 2001). For rats, anatomical MRI templates have been created for the Sprague-Dawley strain (Schweinhardt et al., 2003; Schwarz et al., 2006; Nie et al., 2013) and for the Wistar strain (Valdes Hernandez et al., 2011).

Spatial smoothing is conducted to improve signal-to-noise ratio and to impose a normal distribution on the data, so that the Gaussian random field theory can be utilized in the statistical testing (Worsley and Friston, 1995).

After preprocessing, the statistical analysis is carried out to determine which voxels are activated by the stimulation. In the most simplest way, subtraction of the baseline images from the activation images should yield an image where the signal increase due to the stimulus can be observed (e.g. (Hyder et al., 1994)). More sophisticated methods for functional MRI data analysis have been developed in recent years. The most commonly used method is the general linear model (GLM) where a model based on the expected response is fitted to the measured time series of each voxel.

Since the statistical testing is performed for each voxel separately, a multiple comparison correction is conducted to account for the simultaneous statistical tests to determine proper threshold for the statistical parametric map. A threshold is needed to determine the activated voxels and in addition to limit the number of false positive voxels. If multiple comparison correction is not used, this will lead to false positive voxels, meaning that too many voxels are considered active even in the case when they are not truly active. This can be overcome by using different methods to correct for the numerous statistical tests. The family wise error (FWE) rate is the likelihood that the family of voxel values could have arisen by chance. The false discovery rate (FDR) is the proportion of false discoveries among total rejections (Benjamini and Hochberg, 1995). The FDR threshold is determined from the observed p-value distribution in the data. Therefore it adapts to the amount of signal in the data and is more sensitive when the signal is small.

2.3.4 fMRI in Animal Studies

As the BOLD contrast is based on paramagnetic deoxygenated hemoglobin, it inherently can be thought of using blood as the endogenous contrast agent. This also makes the imaging method noninvasive and very desirable in many human and animal studies. In contrast, the first functional MRI studies in humans were invasive using the exogenous paramagnetic contrast agent, gadolinium for cerebral blood volume based imaging (Belliveau et al., 1991; Rosen et al., 1991). Only one year later, the first human BOLD fMRI studies using visual and sensory stimulation were published (Ogawa et al., 1992; Kwong et al., 1992; Bandettini et al., 1992).

Despite the obvious need to understand the human brain, there is also a demand for animal studies. Animal fMRI studies can be used to study different disease models to

further increase the knowledge of the human condition and to improve the predictive and diagnostic value. In drug development, animal models provide a useful tool with which to study the effect of unknown compounds in the brain and in addition, test their treatment value in disease models. Furthermore, combining fMRI with more invasive techniques can improve the understanding of the physiological basis of the fMRI signals. One major goal in animal fMRI studies is to build the homology between brain activity in humans and laboratory animals.

The very first study that described the BOLD phenomenon was conducted in rats (Ogawa et al., 1990b). Due to the well characterized nervous system (Paxinos, 2004), rats are well suited for studying functional and anatomical organization of the brain. Many of the rodent studies have utilized somatosensory stimulation, although other networks including visual (Van Camp et al., 2006a), auditory (Cheung et al., 2012) and odor (Yang et al., 1998) have also been studied.

Even though fMRI in rats has been commonly conducted, functional imaging in other rodent species, mice, has not gained similar widespread popularity. This may be due to the difficulty of imaging the small size of the mouse brain in combination with difficulty of shimming and of producing stable anesthesia. The first fMRI study in the mouse showed a transient fMRI response related to photic stimulation (Huang et al., 1996), however there are some criticisms about the quality of the study. Therefore it is generally considered that the first study to demonstrate the feasibility of somatosensory BOLD fMRI studies in mice was published as late as 2001 (Ahrens and Dubowitz, 2001). Recently, experimental protocols for longitudinal studies (Adamczak et al., 2010) and for pharmacological studies (Ferrari et al., 2012) have been developed in mice.

Cats have a well characterized visual system (Payne and Peters, 2002) which was studied in one of the first in vivo BOLD experiments (Jezzard et al., 1997) and these have been extended to more elaborate measurements where CBF responses have been localized to individual submillimeter cortical columns (Duong et al., 2001).

The extensive and groundbreaking work providing insights into the physiological events underlying the BOLD fMRI contrast has been carried out in both anesthetized and alert monkeys (Logothetis et al., 1999; Logothetis et al., 2001; Leopold and Logothetis, 2003; Oeltermann et al., 2007). However, the first fMRI studies in the monkey brain (Stefanacci et al., 1998; Dubowitz et al., 1998) did not show “clear, focal, stimulus-induced activations, probably due to suboptimal signal-to-noise ratio and motion artifacts” (Logothetis, 2012).

Functional MRI studies have been conducted in other species, including rabbits (Wyrwicz et al., 2000), pigs (Mäkiranta et al., 2005), sheep (Opdam et al., 2002), dogs (Willis et al., 2001; Rioja et al., 2010), bats (Kamada et al., 1999), songbirds (Van der Linden et al., 2007; Poirier et al., 2010), and even fish (van den Burg et al., 2005; Bando et al., 2011).

BOLD fMRI during Electrical Forepaw Stimulation

The rodent forepaw somatosensory system is a commonly used robust model for examining cortical activity. Many BOLD fMRI studies in rats have been conducted with electrical forepaw stimulation (Table 2). The first experiment was carried out by Hyder et al. in 1994 using the GE sequence with a single axial slice positioned separately at 4 different locations. They reported a relative signal intensity change of 17 % in somatosensory cortex and 6 % in the motor cortex (Hyder et al., 1994).

Despite to the huge response in the first forepaw stimulation study, the BOLD response in the primary somatosensory cortex of a rat during electrical forepaw stimulation is typically 2 – 5 %. The magnitude of the response depends on the anesthesia, magnetic field strength, imaging sequence, stimulation protocol, data analysis method and the quantification of the BOLD response.

During forepaw stimulation, the BOLD response can be detected mainly in the primary somatosensory cortex but activity in the secondary somatosensory cortex and thalamus and cerebellum has been reported (Hyder et al., 1994; Peeters et al., 1999; Peeters et al., 2001; Keilholz et al., 2004; Liu et al., 2004; Weber et al., 2006; Keilholz et al., 2006; Zhao et al.,

2008). In thalamus, the BOLD response was detected in 29-45 % of rats and in SII in 54-73 % of rats under alpha-chloralose anesthesia (Keilholz et al., 2004; Keilholz et al., 2006). Interestingly, by using the CBV method (30 mg Fe/kg), the activation in SII and thalamus was detected more often than in BOLD measurements using the same animals in consecutive imaging sessions (Keilholz et al., 2006). Under medetomidine sedation, however, activity in thalamus and SII was detected in all animals (Zhao et al., 2008).

In the case of single slice data acquisition, the one (usually axial) slice has usually been positioned to the SI of forepaw which hinders the visibility of the SII and thalamus. Despite multi-slice acquisition, the secondary and subcortical forepaw pathway areas have not always been detectable. This may indicate that the responses that are below the statistical threshold due to either the effects of anesthesia, to partial volume effects or to differences in the hemodynamic response function in SII and subcortical regions.

The typical electrical forepaw stimulation protocol in BOLD fMRI studies consists of alternating baseline and stimulus periods that can vary from a few seconds up to minutes. Nevertheless, even a single electrical stimulus pulse of 333 μ s duration to the forepaw has elicited detectable signal intensity change in the BOLD, CBF and CBV measurements under alpha-chloralose anesthesia (Silva et al., 2007; Hirano et al., 2011).

The most commonly used pulse sequence in functional imaging is EPI which makes it possible to conduct fast imaging with temporal resolution of seconds and whole brain coverage with submillimeter resolution. GE-EPI is also more commonly used in rodent fMRI studies than SE-EPI. However, when combined with invasive electrophysiological measurements, SE-EPI is the best choice due to reduced magnetic susceptibility effects caused by invasive electrodes.

In addition to the EPI sequence, the “fast low angle shot” (FLASH) sequence (Haase et al., 1986) has been used in some forepaw stimulation studies (Gyngell et al., 1996; Brinker et al., 1999; Sommers et al., 2009). The temporal resolution of FLASH compared to EPI is slower but the signal intensity change has been high, 4-11 %, during activation in these studies. In the FLASH sequence, the image contrast is influenced by an inflow (T_1) effect since the transverse magnetization is spoiled between two RF excitations.

The BOLD response is a semi quantitative index of brain activity, first of all because it measures neural activity indirectly. Secondly, it is not an absolute value since it is calculated in relative terms to a baseline. In different studies many different ways have been used to define and report the amplitude of the BOLD response. The BOLD response can be defined as a maximum response, temporal average (with varying length) obtained either from a single activated pixel or from the region of interest (ROI) with anatomically fixed size or from ROI selected from the statistical analysis.

Taking into account all the differences in animal models, experimental setups, data analysis, and reporting the results, it is clear that direct comparison of fMRI results between studies is not straightforward and interpreting the results requires considerable caution.

Table 2. Forepaw stimulation parameters used in BOLD fMRI studies in rats.

Anesthetic (dosage)	Pulse width (ms)	Stimulus current (mA)	Frequency range (Hz)	Duration (s)	Optimal stimulus protocol	Magnetic field strength (T)	Sequence	TE (ms)	BOLD response in SI	Activated areas	Reference
α -chloralose (40 mg/kg, i.p., 30 mg/kg at 2 h)	0.5	0.2	2.5	115.2	0.5 ms, 0.2 mA, 2.5 Hz	7	GE (MS)	16	n/a	SI, Cerebellum	Peeters et al., 1999
α -chloralose (40 mg/kg/h, i.p.)	0.3	2	0.5-12	30	0.3 ms, 2 mA, 1.5 Hz	11.7	GE-EPI (SS)	13	~ 12 %	SI	Sanganahalli et al., 2008
α -chloralose (40 mg/kg/h, i.p.)	0.3	2	1-10	4 / 32	0.3 ms, 2 mA, 3 Hz	7	SE-EPI (SS)	40	~ 4 - 5 %	SI	Kida et al., 2008
α -chloralose (50 mg/kg, i.v., 40 mg/kg/hr)	0.3	5 V	3	6	0.3 ms, 5 V, 3 Hz	2 / 4.7	GE (SS)	25	1 - 1.5 %	SI	Marota et al., 1999
α -chloralose (60 mg/kg, i.p.)	10	1	1-12	40	10 ms, 1 mA, 8 Hz	7	GE-EPI (SS)	26	~ 3 %	SI	van Camp et al., 2006
α -chloralose (60 mg/kg, i.v.)	0.5	0.6	2.5	307.2	0.5 ms, 0.6 mA, 2.5 Hz	7	GE (MS)	14		SI	Peeters et al., 2001
α -chloralose (60 mg/kg, i.v., 30 mg/kg at 1 h)	0.3	0.5	1-15	30	0.3 ms, 1 mA, 1-3 Hz	4.7	SE-EPI (SS)	60	~ 2 - 4 %	SI	Study I
α -chloralose (80 mg/kg, i.p., 20 mg/kg at 30 min)	0.3	5 V	3	198	0.3 ms, 5 V, 3 Hz	7	GE (SS)	16	~ 17 %	SI, MI	Hyder et al., 1994

Table 2 (cont.). Forepaw stimulation parameters used in BOLD fMRI studies in rats.

Anesthetic (dosage)	Pulse width (ms)	Stimulus current (mA)	Frequency range (Hz)	Duration (s)	Optimal stimulus protocol	Magnetic field strength (T)	Sequence	TE (ms)	BOLD response in SI	Activated areas	Reference
α -chloralose (80 mg/kg, i.v., 26.7 mg/kg/h)	0.3	3	3	30	0.3 ms, 3 mA, 3 Hz	7	GE-EPI (MS)	15	~ 3 %	SI	Sumiyoshi et al., 2012
α -chloralose (80 mg/kg, i.v., 27 mg/kg/h)	0.3	2	1-8	60-90	0.3 ms, 2 mA, 3 Hz	11.7	SE-EPI (MS)	30	~ 6 - 8 %	SI, SII, Thalamus, Cerebellum	Keilholz et al., 2004
α -chloralose (80 mg/kg, i.v., 40 mg/kg at 90 min)	0.3	0.5	1.5-6	50	0.3 ms, 0.5 mA, 1.5 Hz	4.7	FLASH (SS)	60	~ 6 %	SI	Brinker et al., 1999
α -chloralose (80 mg/kg, i.v., 40 mg/kg at 90 min)	0.3	0.5	1.5-9	40	0.3 ms, 0.5 mA, 1.5-3 Hz	4.7	FLASH (SS)	60	~ 9 - 11 %	SI	Gyngell et al., 1996
α -chloralose (80 mg/kg, i.v., 40 mg/kg at 90 min)	0.3	1.5	3	18 30	0.3 ms, 1.5 mA, 3 Hz	9.4	GE-EPI (MS)	10	~ 3 %	SI	Silva et al., 1999
α -chloralose (80 mg/kg, i.v., 40 mg/kg/h)	0.5	1-2	3	16	0.5 ms, 2 mA, 3 Hz	7	FLASH (MS)	10	~ 6 - 8 %	SI	Sommers et al., 2009
Awake	0.5	0.6	2.5	307.2	0.5 ms, 0.6 mA, 2.5 Hz	7	GE (MS)	14		SI, SI ipsilateral	Peeters et al., 2001
Urethane (1.25 g/kg, i.p.)	0.3	1-1.2	1-15	30	0.3 ms, 1 mA, 7-15 Hz	4.7	SE-EPI (SS)	60	~ 4 %	SI	Study I

Table 2 (cont.). Forepaw stimulation parameters used in BOLD fMRI studies in rats.

Anesthetic (dosage)	Pulse width (ms)	Stimulus current (mA)	Frequency range (Hz)	Duration (s)	Optimal stimulus protocol	Magnetic field strength		Sequence	TE (ms)	BOLD response in SI	Activated areas	Reference
						(T)	(T)					
Halothane (1 %)	0.3	2	3	30-300	0.3 ms, 2 mA, 3 Hz	7 11.7	GE-EPI / SE-EPI (MS)	40	~ 2 %	SI		Maandag et al., 2007
Isoflurane (1.2 %)	0.5	1-2	3	16	0.5 ms, 2 mA, 3 Hz	7	FLASH (MS)	10	~ 4 - 6 %	SI		Sommers et al., 2009
Isoflurane (1.3 %)	0.1 - 5	0.2 - 2	2-20	10 pulses	1 ms, 1.4 mA, 12 Hz	9.4	GE-EPI (SS)	20	~ 2 - 3 %	SI		Masamoto et al., 2007
Isoflurane (1.3-1.5 %)	1	1.5	1.5-12	30	1 ms, 1.5 mA, 12 Hz	9.4	GE-EPI (SS)	20	~ 3 %	SI		Kim et al., 2010
Isoflurane (1-1.2 %)	0.3	4-8	3	120	0.3 ms, 6 mA, 3 Hz	4.7	GE-EPI (MS)	15	~ 1.4 %	SI, SII		Liu et al., 2004
Medetomidine (0.05 mg/kg, i.p., 0.1-0.3 mg/kg/hr)	0.3	1-4	3-12	20	0.3 ms, 4 mA, 9 Hz	9.4	SE-EPI (MS)	38	~ 2 - 3 %	SI		Nashrallah et al., 2012
Medetomidine (0.05 mg/kg, s.c., 0.1 mg/kg/hr)	0.3	2	3	15	0.3 ms, 2 mA, 3 Hz	7	SE-EPI (MS)	30	~ 2 %	SI, SII		Weber et al., 2006
Medetomidine (0.05 mg/kg, s.c., 0.1 mg/kg/hr)	0.3	1-8	1-18	20	0.3 ms, 2 mA, 9 Hz	9.4	GE-EPI (MS)	15	~ 2 %	SI, SII, Thalamus		Zhao et al., 2008

Abbreviations: BOLD, blood oxygenation level dependent; FLASH, Fast low angle shot; GE, gradient echo; GE-EPI, gradient echo planar imaging; i.p., intraperitoneally; i.v., intravenously; MI, Primary motor cortex; MS, multi slice; s.c., subcutaneously; SE-EPI, spin echo echo planar imaging; SI, Primary somatosensory cortex, SII, Secondary somatosensory cortex; SS, single slice; TE, time to echo

Studies on Awake Animals

Anesthetics may have profound influences on the basal brain activity and the brain activation during stimulation (Ueki et al., 1992; Lindauer et al., 1993; Rojas et al., 2006). Therefore fMRI studies without anesthesia provide valuable information about brain activity that has not been altered with an anesthetic agent.

Only a few rodent BOLD fMRI studies have been conducted in the awake state. One major practical issue in the awake animal fMRI is how to prevent the movement of the animal. The MRI environment is extremely noisy and requires restrictions of the movement for a long time. Animals can be trained and acclimatized to physical restraint and noise of the scanner (Sachdev et al., 2003) or paralyzed and mechanically ventilated (Peeters et al., 2001) or restrained after an initial anesthesia (Lahti et al., 1999). The awake restrained condition inside the scanner is not a synonym to a awake freely moving condition due the stress levels of the animal which are difficult to monitor. A recent study has however revealed that blood gases, heart rate, respiration rate, and mean arterial blood pressure in the awake animals were within normal physiological ranges, and the struggling movements had markedly reduced after the first hour of being held in the restrainer (Duong, 2007).

Despite the technical difficulty of restraining the animals, there have been some fMRI studies performed in awake rats using somatosensory stimulation. Somatosensory stimulus to the hindpaw elicited changes in both CBF (Lahti et al., 1998) and BOLD (Lahti et al., 1999) but the BOLD response was significantly reduced with propofol anesthesia. Similarly, during forepaw stimulation, the BOLD response was higher, but more non-specific areas were activated in the awake condition compared to the situation with alpha-chloralose anesthesia (Peeters et al., 2001). The whisker stimulus elicited BOLD responses in both barrel cortices while the response in the contralateral cortex was more pronounced (Sachdev et al., 2003). In addition, both hypercapnic (Sicard et al., 2003) and hypoxic (Duong, 2007) conditions have been implemented.

In pharmacological MRI, the role of anesthesia is critical, therefore experiments performed in awake animals provide information about the drug related responses without the confounding factor of the anesthetic agent. Nicotinic receptor agonists (Skoubis et al., 2006), glutamate receptors agonist (Simon et al., 2011), apomorphine (Chin et al., 2006), subanesthetic dose of ketamine (Chin et al., 2011), xanomeline modulation of ketamine (Baker et al., 2012) and amphetamine sensitization (Febo and Pira, 2011) have been studied in awake animals.

Resting state functional connectivity analysis in awake animals revealed 7 different components (Becerra et al., 2011) that displayed some similarities with human networks. In addition, the anticorrelated circuitry between infralimbic cortex and amygdala was reported a factor that was absent in anesthetized animals (Liang et al., 2012).

Simultaneous electrophysiological and fMRI measurements (Khubchandani et al., 2003) during epileptiform activity (Van Camp et al., 2003; Airaksinen et al., 2012) has also been performed.

Despite the difficulty of performing functional MRI studies in awake animals, a rather extensive selection of experiments has been carried out even though the total number of studies is not high. The anesthesia has an effect on the magnitude of the elicited functional and pharmacological responses and the resting state connectivity, nevertheless the awake restrained condition of the animal inside the scanner does not truly represent the condition of a freely moving animal.

Anesthesia in Animal fMRI Studies

The selection of the anesthesia in functional imaging studies should be made carefully. Anesthesia affects many mechanisms and biochemical pathways at the molecular level. It can change neuronal excitability, vascular reactivity, baseline CBF, and baseline cerebral energy metabolism (Masamoto and Kanno, 2012) and have profound and differential

effects on both neuronal and hemodynamic responses (Lindauer et al., 1993; Rojas et al., 2006; Franceschini et al., 2010). Consequently, this may cause interpretation errors when comparing the results of experiments conducted with different anesthetics.

In addition, the level of anesthesia is important in fMRI studies. If the anesthesia level is too deep, it can suppress both neural activity and the hemodynamic response. There are ways to determine the depth of anesthesia by e.g. measuring breathing, blood pressure, heart rate or electrical activity in the brain.

The most commonly used anesthetic in functional MRI studies is alpha-chloralose. It is favored due to its minor effects on cardiovascular and reflex functions and the belief that it minimally suppresses central nervous system activation (Lees, 1972). Metabolic activation under alpha-chloralose anesthesia is said to be similar to that encountered in awake animals, although the resting metabolic level is lower (Ueki et al., 1992). However, alpha-chloralose induces high-amplitude transient peaks and occasional burst suppression episodes in an otherwise normal appearing electroencephalograph (Balis and Monroe, 1964; Ueki et al., 1992; Peeters et al., 2001; Austin et al., 2005). Increases in activity, such as an increase in median EEG frequency, are observed with an increase in the BOLD response amplitude under alpha-chloralose anesthesia, although there are substantial variations in both the extent and magnitude of the response (Austin et al., 2005).

The use of alpha-chloralose as an anesthetic agent might result in unexpected and uncontrolled changes in the responses of neurons under study (Collins et al., 1983) and it markedly influences behavior (Balis and Monroe, 1964). The use of alpha-chloralose is limited to experiments with nonsurvival protocols (Silverman and Muir, 1993), however, a recent study has reported that a new commercial alpha-chloralose with a careful application scheme as being suitable for longitudinal fMRI studies (de Celis Alonso et al., 2011).

The advantages of inhaled anesthetics such as isoflurane are the rapid induction of anesthesia, easy maintenance and controllability of the depth of the anesthesia and fast recovery which makes them suitable for longitudinal studies. However isoflurane is a potent vasodilator which can lead to high baseline CBF levels (Eger, 1984; Maekawa et al., 1986) and has a dose-dependent effect on the CBF response varied with the stimulus frequency (Masamoto et al., 2009). It also affects the field potential signal in a burst-suppression manner, i.e. depressed background activity alternating with high voltage activity (Masamoto et al., 2007). In addition, isoflurane has increased the latencies and decreased the amplitudes of the evoked somatosensory responses (Hayton et al., 1999). Isoflurane inhibited neurotransmitter release without altering postsynaptic function (Sandstrom, 2004), therefore resulting in a decrease in the degree of cortical activation obtained by the primary afferent input.

Medetomidine is a potent and highly selective α_2 -adenoreceptor agonist that has been used for sedation of rats (Weber et al., 2006) and mice (Adamczak et al., 2010) in functional MRI studies. The sedative effects are mediated by binding to α_2 -adenoreceptors primarily located in the locus coeruleus preventing further release of the neurotransmitter, norepinephrine (Sinclair, 2003). The sedative effects of medetomidine can be reversed by administering the antagonist atipamezole, which makes medetomidine ideal for longitudinal fMRI studies. This was confirmed in a study, where two fMRI sessions five days apart revealed no significant difference in the BOLD response or the area of activation during forepaw stimulation (Weber et al., 2006).

Medetomidine sedation can be maintained for as long as 6 h (Pawela et al., 2009), if the dosage is increased after 90 min of infusion. However, prolonged (> 2 h) sedation with dexmedetomidine, the active dextro-isomer of the medetomidine formulation, caused epileptic activity triggered by the forepaw stimulation (Fukuda et al., 2013) and this could be detected in LFP and CBF measurements. Increasing the dose did not prevent the development of epileptic responses, but they were suppressed by an additional low dose (~ 0.3 %) of isoflurane. Spontaneous depolarization waves have been observed in BOLD fMRI

measurements although these waves were not detected in LFP measurements under medetomidine sedation (Shatillo et al., 2012). During one hour follow up, 2.1 ± 1.4 spreading depolarizations per animal were observed, some even crossing the hemispherical border, which is not typical for the commonly reported spreading depression (Leo, 1944; Lauritzen, 2001; Dreier et al., 2012).

Local field potential and intracellular membrane potential measurements are often performed in urethane (ethyl carbamate) -anesthetized rats. Urethane induces surgical anesthesia without affecting neurotransmission or spontaneous firing in subcortical areas and induces only a slight depression in cortical areas (Maggi and Meli, 1986a; Hara and Harris, 2002). Electrophysiology conducted under urethane anesthesia is similar to that in awake animals, despite the burst suppression pattern observed by Rojas et al. (2006) with a high urethane dose (1.5–2 g/kg), indicating that there is a deeper anesthetic state (Rojas et al., 2006). It is also assumed that animals anesthetized with urethane display similar physiologic and pharmacologic behavioral states to those observed in awake animals (Hara and Harris, 2002). Barrel cortex neuron LFPs due to whisker stimulation are similar in the awake and urethane anesthetized conditions, despite a larger late component being detected during urethane anesthesia (Simons et al., 1992).

Optical imaging spectroscopy and laser Doppler flowmetry have been conducted together with electrophysiological measurements in order to study the whisker-barrel pathway (Martin et al., 2002; Jones et al., 2002; Jones et al., 2004; Martin et al., 2006) under urethane anesthesia. In their series of studies, these researchers have altered both frequency and intensity of the stimulation and observed a nonlinear relationship between neural activity and hemodynamic response.

Urethane appears to modulate all neurotransmitter-gated ion channels (Hara and Harris, 2002). It produces a long-lasting anesthesia (Lincoln, 1969; Field et al., 1993) and preserves cardiorespiratory function and also induces profound skeletal muscle relaxation (Maggi and Meli, 1986b), which is very desirable in fMRI experiments. Urethane, however, is a potent mutagen and carcinogen (Field and Lang, 1988), therefore handling, especially in the powder form, requires special caution.

Urethane has also been used in functional imaging studies. Baseline cerebral blood flow values under urethane anesthesia [70 ml/100 g/min, hydrogen clearance method, (Gröhn et al., 2000)] are similar to that of alpha-chloralose anesthesia [60–70 ml/100 g/min, arterial spin labeling method, (Duong et al., 2000; Kim and Lee, 2004)] but they are remarkably lower than the values seen under isoflurane anesthesia [100–120 ml/100 g/min, autoradiography (Young et al., 1991), intravenous bolus injection of [^{14}C]iodoantipyrine (Lauritzen, 1984)]. Therefore with urethane anesthesia, it should be possible to achieve BOLD responses that match the amplitude of those elicited under alpha-chloralose anesthesia.

One of the earliest fMRI studies conducted under urethane anesthesia was a study where odor-elicited olfactory responses were detected with BOLD fMRI at the laminar level in the rat olfactory bulb (Yang et al., 1998).

Urethane has been used as an anesthetic in a few pharmacological MRI studies. The earliest report revealed that morphine withdrawal BOLD activation patterns correlated with behavioral observations and the known biochemical measures of opioid withdrawal (Lowe et al., 2002). A recent study compared the effects of different anesthetics on pharmacological activation. Acute levo-tetrahydropalmatine administration caused the smallest BOLD activation areas under isoflurane anesthesia, mixed positive and negative activations under medetomidine sedation and the largest but only negative activations when animals were anesthetized with urethane (Liu et al., 2012).

Pentobarbital influences the GABAergic mechanisms involved in the control of cardiovascular functions (Yamada et al., 1983) and in this respect is unlike urethane (Maggi and Meli, 1986a). Therefore the effects on the mean arterial pressure dynamics induced by apnea should differ with these anesthetics. Although the apnea-induced decrease in BOLD signal intensity was similar in rats anesthetized with either pentobarbital or urethane, CBF

and mean arterial pressure varied considerably between them indicating that CMRO₂ was relatively higher with urethane anesthesia than that detected with pentobarbital anesthesia (Kannurpatti and Biswal, 2004).

In addition to isoflurane, alpha-chloralose, urethane and medetomidine, other anesthetics used in functional MRI studies have included halothane (Detre et al., 1992; Austin et al., 2005), barbiturates such as pentobarbital (Ogawa et al., 1990b; Kannurpatti et al., 2003) and thiobutabarbital (Paasonen et al., 2013), ketamine (Shih et al., 2008), ketamine-xylazine (Hutchison et al., 2010), fentanyl-haloperidol (Nersesyan et al., 2004), fentanyl-medetomidine (Choy et al., 2010), dexmedetomidine-isoflurane (Fukuda et al., 2013), propofol (Lahti et al., 1999; Kalisch et al., 2001; Griffin et al., 2010), the hypnotic agent, etomidate (Leithner et al., 2008) and equithesin (Dashti et al., 2005).

BOLD Response Dependence on Stimulus Parameters

The stimuli used in an animal experiment are usually specific to the question or designed to elicit intense neural responses. Electrical stimuli are delivered with a selected frequency, amplitude, pulse duration and stimulus duration to forepaws, hindpaws or whisker area to produce robust and well defined neural responses.

The optimal forepaw stimulus parameters are different for each anesthetic. Under alpha-chloralose anesthesia, a 0.3 ms pulse width and 1.2 mA current are used as standard stimulus parameters, while the optimal frequency range is between 1 and 3 Hz (Table 2). This indicates that under alpha-chloralose anesthesia both neuronal and hemodynamic systems are tuned to low frequency stimulation, which may be related to the fact that also spontaneous neuronal activation consists of low-frequency bursts. The thalamic relay nuclei do not respond to stimuli in the presence of alpha-chloralose anesthesia (Ueki et al., 1992). The reticular nucleus of the thalamus might have a role in mediating stimuli at different frequencies to the cortical areas because the diminishing responses for repetitive stimulation are suggested to be due to active inhibition, probably reticular in origin (Chalmers and Erickson, 1964). This might indicate a lack of activity in response to high-frequency stimuli and the low optimal frequency range while under alpha-chloralose anesthesia.

In a recent study both whisker and forepaw stimulations were performed on the same animal under alpha-chloralose anesthesia (Sanganahalli et al., 2008). There was no significant spatial overlap between the activated regions. Although the magnitude of the BOLD response was largest for forepaw stimulus frequencies of 1.5 and 3 Hz, there was hardly any activity after 10 Hz while the whisker stimulus elicited BOLD responses up to the maximum frequency (30 Hz) tested. In contrast, increasing the stimulus strength by changing the pulse width to 10 ms caused the frequency dependence of both summated field potentials and BOLD responses under alpha-chloralose anesthesia to reach a plateau between 5 Hz and 12 Hz (Van Camp et al., 2006b). This suggests that the increased pulse duration of an electrical stimulus may alter the nature of the excitation and subsequently of the activated neuronal pathways and therefore cause a shift in the optimal response frequencies. In an earlier study, the activation intensity decreased with increasing stimulus frequency of the forepaw under alpha-chloralose anesthesia being negligible at 9 Hz (Gyngell et al., 1996).

Even though there are not that many forepaw stimulation studies conducted under alpha-chloralose anesthesia that have extended the stimulus frequency beyond 5 Hz, it is clear that with 0.3 - 0.5 ms pulse duration and 0.5 - 3 mA stimulus intensity, the optimal frequency is between 1-3 Hz.

Since alpha-chloralose anesthesia has been traditionally used in early fMRI studies, only recently has the need to study optimal stimulus parameters for different anesthetics become evident. In the only forepaw BOLD study conducted in the awake condition, the stimulus parameters were kept the same as in the alpha-chloralose anesthesia protocol (Peeters et al., 2001), therefore there is not enough knowledge to estimate the optimal parameters for the BOLD response in awake rats. Under isoflurane anesthesia, however robust BOLD

responses were detected after increasing pulse width, current and frequency (Masamoto et al., 2007; Kim et al., 2007) or increasing dramatically the current to 6 mA (Liu et al., 2004). The increase in stimulus parameters might be explained by a reduction in excitatory synaptic transmission (Berg-Johnsen and Langmoen, 1992) and high baseline blood flow under isoflurane anesthesia.

During medetomidine sedation, stimulus current and frequency have been varied for forepaw stimulation. There was a nearly linear increase in the BOLD signal change with the increased stimulus current from 1 to 4 mA, however the frequency dependence of the BOLD response was not detailed in the publication, although it was concluded that 9 Hz stimulus frequency produced maximal response (Nasrallah et al., 2012). In another study, the stimulus frequency was extended from 1 Hz up to 18 Hz under medetomidine sedation (Zhao et al., 2008). The tuning curve at the SI peaked at 9 Hz, after which the BOLD response gradually decreased. However in thalamus, there was no statistical difference in the responses at 6 Hz or above. Based on these two studies under medetomidine sedation, the optimal forepaw stimulus protocol is 0.3 ms pulse width and 2 mA current and 9 Hz stimulus frequency (Zhao et al., 2008; Nasrallah et al., 2012).

In the only forepaw stimulus study performed under urethane anesthesia, the optimal stimulus parameters were 0.3 ms, 1 mA and 7-15 Hz (Huttunen et al., 2008), however the pulse width and the current were not optimized.

The whole brain coverage, however, shows that the frequency dependence of the neural and hemodynamic responses varies between brain regions. In brainstem, the BOLD responses increased monotonically with increasing stimulation frequencies (up to 20 Hz) while only thalamus exhibited strong responses at or above 10 Hz, whereas BOLD responses in the cortex were greatest in mid-range stimulation frequencies (maximally at 5 Hz) under urethane-chloral hydrate anesthesia for a whisker stimulus (Devonshire et al., 2012). The magnitude of the blood flow response due to whisker stimulation under urethane anesthesia increased linearly with increasing frequency while the temporal parameters of time to half maximal value and time to return halfway to baseline after stimulus termination did not vary (Gerrits et al., 1998).

In summary, the stimulus parameters to elicit optimal neural and hemodynamic responses vary with the different anesthetics. Therefore it is especially important when establishing fMRI protocols with new anesthetics, that at least the stimulus frequency and amplitude should be varied to obtain tuning curves and hence the optimal stimulus parameters.

2.3.5 Simultaneous Electrophysiological and fMRI Measurement

The brain activity is never constant nor stable, and applying identical stimuli may not always produce identical responses due to underlying neural processes. Correlations between responses across modalities have been performed by different investigators (e.g. (Ureshi et al., 2004; Van Camp et al., 2006b; Devonshire et al., 2012)) or in separate measurement sessions on the same subjects (e.g. (Singh et al., 2003)). These, however, only provide indirect information about the correlation, and are based on the assumption that the measurements have been acquired in the same brain state. Combining different modalities simultaneously offers significant advantages when compared to separate imaging sessions especially when measuring individual events or in studying spontaneous brain activity in the baseline condition or for example during epileptic activity.

The simultaneous EEG and fMRI measurements have been driven by epileptologists to localize electrical sources of epileptic discharges (Laufs, 2012). The first measurement in humans was conducted in 1993 to study interictal epileptic spikes (Ives et al., 1993). In addition to combining with EEG, MRI has been combined simultaneously with MEG (Zotef et al., 2008), PET (Catana et al., 2008) and optical imaging (Kida et al., 1996; Kleinschmidt et al., 1996).

In animal models, simultaneous electrophysiological and fMRI measurements have been performed with different stimuli, disease models, and species. Most commonly, simultaneous measurements have been performed in rats and monkeys (e.g. (Logothetis et al., 2001; Shmuel et al., 2006; Rauch et al., 2008; Lippert et al., 2010)) but also pigs (Mäkiranta et al., 2005) and sheep (Opdam et al., 2002) have been utilized.

An electrical stimulus to the perforant path evokes a field potential in the soma layer of the dentate gyrus in hippocampus. The input-output relationship can be used to characterize the functional state of the neuronal networks in the dentate gyrus (Angenstein et al., 2010). Simultaneous electrophysiological and BOLD fMRI measurement have shown that the generation of a BOLD response within the hippocampus requires a certain amount of neuronal stimulation (Angenstein et al., 2007; Canals et al., 2008) and the BOLD response is dependent on the processing of the neuronal signals rather than either the input or output of the signals (Angenstein et al., 2009).

Electrical stimulus to the forepaw of the rat has been quite extensively used as a model in simultaneous electrophysiological and fMRI measurements (Brinker et al., 1999; Gsell et al., 2006; Masamoto et al., 2007; Huttunen et al., 2008; Huttunen et al., 2011; Sumiyoshi et al., 2012). In addition to correlating evoked neural responses to the hemodynamic response, other variables have been used. From different frequency bands, gamma band power correlated best with simultaneous BOLD responses (Sumiyoshi et al., 2012) during forepaw stimulation under alpha-chloralose anesthesia. In addition, temporal variations in the BOLD response were better explained by a model based on measured LFP responses than on a model based on stimulus blocks (Huttunen et al., 2011). In addition, the role of different glutamate receptors on simultaneously measured evoked somatosensory response has been evaluated (Gsell et al., 2006). N-methyl-D-aspartate (NMDA) receptor antagonist significantly decreased BOLD and CBF responses but reduced the somatosensory evoked potentials only marginally, while an antagonist of α -amino-3-hydroxy-5-methyl-4-isoxazolepropionic acid (AMPA) receptors significantly decreased both the hemodynamic responses and the evoked neural responses evidence of a differential role of these receptors on the signaling chain from increased neuronal activity up to the hemodynamic response observed in the somatosensory cortex.

Since epileptic activity is by nature spontaneous, time varying activity, simultaneous electrophysiological and hemodynamic measurements can capture the different elements of epileptic seizures (e.g. (Van Audekerke et al., 2000; Van Camp et al., 2003; Nersesyan et al., 2004; Mirsattari et al., 2006; Schridde et al., 2008; Airaksinen et al., 2010; Mishra et al., 2011; Airaksinen et al., 2012)).

Limitations of Simultaneous Measurements

Simultaneous electrophysiological and functional MR imaging measurements provide complimentary information about the brain activity. The good temporal resolution of the electrophysiological measurement is combined with good spatial resolution of the functional MRI, therefore providing more information than these methods alone.

There are disadvantages in combining different modalities as they may interfere with each other. The implantation of the LFP electrode into the brain tissue requires scalp removal, craniotomy, and incision of dura. All of these procedures may introduce bleeding and thus add confounding effects to the EPI images that are sensitive to local field inhomogeneities.

The LFP electrode should be biocompatible and MRI-compatible. In addition, there should not be a significant mismatch between magnetic susceptibility of the electrode and the brain tissue because it introduces significant susceptibility artifacts in MR images and this could compromise the quality of the MR images. The most commonly used LFP electrodes are made of tungsten (Angenstein et al., 2007; Huttunen et al., 2008; Huttunen et al., 2011) and carbon fiber (Opdam et al., 2002; Van Camp et al., 2003; Dunn et al., 2009).

Typical EEG electrodes used in animal studies are made of silver (Ag/AgCl) (Gsell et al., 2006) and calomel (Hg/HgCl) (Brinker et al., 1999). The EEG electrodes cause less artifacts

to the MR images, since they are positioned either on top of the skull or on top of the scalp. In addition to using just a few electrodes on the skull of the rat brain, a 32 electrode EEG mini-cap has been developed for rat EEG–fMRI recording without significant signal loss (Sumiyoshi et al., 2011).

Electrodes made of carbon fiber have also been used for direct cortical (Austin et al., 2003), or thalamic (Shyu et al., 2004) stimulation in rats and those made of tungsten for perforant pathway stimulation (Angenstein et al., 2007) or electrodes made of tungsten, stainless steel or gold have been used in a technique called amygdala kindling induced epileptogenesis (Jupp et al., 2006).

During simultaneous electrophysiological and MRI measurements, image acquisition can cause artifacts in the electrophysiological signal. The gradient coil induced magnetic field variations and radiofrequency pulses can be responsible for the high voltages in the electrophysiological recordings concealing the neuronal activity. The simplest way to avoid this is to analyze the clean electrophysiological signal between the artifacts (e.g. (Huttunen et al., 2008; Huttunen et al., 2011)). This is possible with a relatively short image acquisition time of the EPI sequence combined with a long repetition time and a suitable amount of slices. More sophisticated methods for revealing the electrophysiological signal are available. They include subtraction of a template of the MRI-induced artifact (Allen et al., 2000), temporal principal component analysis (Negishi et al., 2004) or independent component analysis (Mantini et al., 2007) based methods, or filtering in the frequency domain (Hoffmann et al., 2000). In addition to these post-hoc artifact removal methods, the gradient switching artifact can be significantly attenuated by utilizing synchronous electrophysiological and fMRI data acquisition (Anami et al., 2003).

Correlation between LFP and BOLD Signals

Much research is being conducted into the understanding how the neural activity is related to the BOLD signal change. Due to the complex nature of neural processing, the correlation is often context-sensitive, i.e. a correlation cannot be generalized for every condition or brain region (Lauritzen, 2005). The determination of the relationship between neural hemodynamic activity is preferably conducted with simultaneous measurements of these entities or at least parallel measurements with a similar experimental setup. However, interspecies comparison of single-neuron activity and BOLD responses have been conducted (Rees et al., 2000; Heeger et al., 2000).

If one wishes to correlate these fundamentally different properties, one needs to quantify both items. Since the changes in the electrical activity occur in the range of milliseconds, integrated neural activity has been defined as a sum of evoked responses over a fixed time. Therefore it includes information about changes in field potential amplitudes throughout the stimulus period. In addition, the amplitudes of the neural or hemodynamic responses can be normalized to better accommodate the correlation calculation.

The linearity of neural and hemodynamic responses has been analyzed in relation to different stimulus related parameters in both humans and animals (Table 3). The correlation analysis can be made by using a statistical method (e.g. Pearson's correlation) between the measured parameter or by fitting different linear or nonlinear (e.g. power law) models to the data.

A linear correlation between neural and hemodynamic responses has been reported in many studies. Interestingly, in most of the studies depicting a linear relationship, neural and hemodynamic activity have been modulated by changing the stimulus frequency. In contrast, changing the stimulus intensity has resulted more often in a nonlinear relationship. Therefore, when reporting either a linear or nonlinear relationship between measured entities, the varied stimulus parameter needs to be clearly defined.

Table 3. Relationship between neural and hemodynamic responses in rat.

Anesthesia	Stimulus	Variation	Neural	Hemodynamic	Simultaneously measured	Results	Reference
Urethane / α -chloralose	Forepaw	Frequency	LFP (integrated)	BOLD (mean)	Yes	Linear	Study I
α -chloralose	Forepaw	Frequency	EEG (integrated)	BOLD (maximum)	No	Linear	van Camp et al., 2006
α -chloralose	Sciatic nerve	Frequency	LFP (integrated)	CBF (mean)	Yes	Linear	Ngai et al., 1999
α -chloralose	Hindpaw	Frequency	LFP (integrated)	CBF (integrated)	No	Linear	Ureshi et al., 2004
Urethane	Whisker	Frequency	LFP (integrated)	CBF (integrated)	Yes	Linear	Martindale et al., 2003
α -chloralose	Forepaw	Frequency	EEG (peak-to-peak)	BOLD (n/a)	Yes	Linear	Brinker et al., 1999
Halothane / α -chloralose	Climbing and parallel fibers	Frequency	LFP & SUA (integrated)	CBF (maximum)	Yes	Linear	Mathiesen et al., 1998
Chloral hydrate - urethane	Whisker	Frequency	MUA (integrated)	BOLD (integrated)	No	Linear in cortex, thalamus and brainstem	Devonshire et al., 2012
Isoflurane	Forepaw	Frequency Amplitude Pulse width	LFP (integrated)	CBF (integrated)	Yes	Linear (pulse width 0.5 - 5.0 ms, current 1.4 - 2.0 mA, frequency of 2 - 4 Hz)	Masamoto et al., 2007

Table 3 (cont.). Relationship between neural and hemodynamic responses in rat.

Anesthesia	Stimulus	Variation	Neural	Hemodynamic	Simultaneously measured	Results	Reference
Chloral hydrate - urethane	Whisker	Frequency	LFP (integrated)	BOLD (integrated)	No	Linear in cortex and thalamus Nonlinear (power law) in brainstem	Devonshire et al., 2012
Isoflurane	Forepaw	Frequency	LFP (integrated)	CBF (maximum)	Yes	No clear correlation at different anesthesia levels	Masamoto et al., 2009
α -chloralose	Infraorbital nerve	Frequency	LFP (integrated or mean)	CBF (mean)	Yes	Nonlinear	Norup Nielsen et al., 2001
Awake / Urethane	Whisker	Frequency	LFP (integrated)	CBF (maximum)	No	Nonlinear	Martin et al., 2006
α -chloralose	Hindpaw	Intensity	LFP (integrated)	CBF (integrated)	No	Nonlinear	Ureshi et al., 2005
α -chloralose	Infraorbital nerve	Intensity	LFP (mean)	CBF (mean)	Yes	Nonlinear (sigmoidal)	Norup Nielsen et al., 2001
Urethane	Whisker	Intensity	LFP & MUA (integrated)	CBF (maximum)	Yes	Nonlinear (sigmoidal)	Jones et al., 2004
Urethane	Whisker	Intensity Frequency	LFP (integrated)	CBF (maximum)	Yes	Nonlinear (sigmoidal), frequency and intensity data pooled together	Hewson-Stoate et al., 2005

Abbreviations: BOLD, blood oxygenation level dependent; CBF, cerebral blood flow; CBV, cerebral blood volume; EEG, electroencephalography; LFP, local field potential; MUA, multi-unit activity; SUA, single-unit activity

To conclude, it is still not clear what aspects of the neural activity are responsible for the changes in BOLD and whether the neurovascular coupling is linear or nonlinear or whether the range of measured response are too narrow to make it possible to draw firm conclusions. One of the fundamental questions would also be to distinguish between simple correlation and actual causation between these signals.

2.3.6 Pharmacological MRI

Most of the fMRI studies use stimulus or task activation to elicit changes in neuronal and hemodynamic activity, however, also pharmacological agents can be used as stimuli to elicit detectable signal intensity changes in the brain. This branch of functional imaging has been named as pharmacological MRI (Chen et al., 1997; Leslie and James, 2000), since drug related responses differ somewhat from functional tasks. In task related fMRI, the time course of the stimuli can be controlled but in phMRI the time course of activation is determined by the pharmacokinetic or pharmacodynamic profile of the drug. For many drugs, the time courses may be long (or even unknown) as compared to task related stimuli and the amplitude of the response may be very small. Therefore there are needs to have stable scanning conditions if one wishes to conduct phMRI experiments.

The very first pharmacokinetic observation of the brain was appeared in the early BOLD fMRI article (Ogawa et al., 1990a) describing how the BOLD contrast was reduced by a reduction of the blood glucose levels by insulin. The first human pharmacological study was done in 1997 (Breiter et al., 1997). They demonstrated that functional MRI can be used to map dynamic patterns of brain activity following cocaine infusion. In addition, they were able to correlate differences in a temporal pattern of activation to more cognitive processes of cocaine rush and craving.

There are several ways to utilize the pharmacological agents in the context of functional imaging. The acute drug administration can stimulate or inhibit activity in neuronal circuits and hence can be measured with functional MRI methods. This has been the main approach in phMRI and it is often called “drug challenge” study. There are several ways to perform these measurements, such as combining the use of antagonists of the drug or by combining chronic and acute effects of the drugs. In addition, drugs can be used to study the modulatory effects to a task related stimulus (Rauch et al., 2008) or to drug induced stimulus (Chin et al., 2011).

Monitoring the drug related hemodynamic responses can lead to a number of different outcomes. In the case where there is no detectable response or correlation with other measured parameters, the conclusion of no activity may not hold. For example, the drug can have both vasoconstrictive and vasodilative effects that cancel each other. One consideration is the direct vascular effect of the drug. In that case, the measured hemodynamic change reflects the vascular and not purely the neural effects of the drug. In many phMRI studies both positive and negative responses have been simultaneously observed (e.g. (Easton et al., 2007; Easton et al., 2009; Liu et al., 2012)).

In general, the data analysis in pharmacological MRI can be performed in a similar way as in task induced fMRI. However, the drug response may differ dramatically from the response of the electrically precisely timed sensory stimuli, therefore more suitable models for estimating the BOLD response have been sought. The first attempt was done by Bloom and colleagues (Bloom et al., 1999) when they applied a model based on the plasma pharmacokinetics of nicotine. With this model they were able to show that nicotine activated several key cortical and subcortical brain regions consistent with the known neuroanatomy, pharmacology, and behavioral effects of nicotine in humans. Nicotine, however, may be an exception in allowing pharmacokinetics to be used as an activation model, since its pharmacokinetics and pharmacodynamics coincide so well. In general, phMRI reflects the pharmacodynamics rather than the pharmacokinetics of the drug as shown with studies on dopaminergic system (Jenkins, 2012).

The advantage of pHMRI is the ability to produce drug related specific and predictable brain activation patterns even under anesthesia. In other words, this technique provides a means to study neurochemical basis of the fMRI signals by enabling selective stimulation of different receptors or neurotransmitter systems. The translational aspect of pHMRI may provide a significant opportunity to utilize preclinical results in designing treatments for humans.

Nicotine

Nicotine is a widely used compound in pHMRI. It is also one of the most addictive substances known. Nicotine binds to the nicotinic acetylcholine receptors (nAChRs) in the brain. nAChRs are ligand-gated ion channels with multiple subunit combinations and the endogenous agonist is acetylcholine. Hexamethonium, a nicotinic receptor antagonist, does not readily enter the brain (Goodman Gilman et al., 1980), and therefore it can be used to reduce the peripheral effects of nicotine on autonomic and neuromuscular acetylcholine receptors (McNamara et al., 1990). In addition pretreatment with the nAChR antagonist, mecamylamine, has attenuated the CBV responses to nicotine antagonist ABT-594 (Skoubis et al., 2006).

Nicotine is known to improve cognitive functions in both human and animals (Levin et al., 2006). In the rat pHMRI studies with a nicotine challenge, a variety of responses have been observed (Table 4). This may be due to differences in dose, administration routes, rat strain, anesthesia and imaging modalities.

Little is known about the mechanisms to explain how nAChR activation leads to a modification of electrical oscillation frequencies in EEG signal (Mansvelder et al., 2006). In rat EEG studies, nicotine (0.4 mg/kg, s.c.) produced a desynchronization in the EEG and a decrease in the power (Ferber and Kuschinsky, 1997). In addition, nicotine has reduced the magnitude of the cortical slow wave potential in EEG signal measured under urethane anesthesia (Ebenezer, 1986).

A functional connectivity analysis was conducted after an acute challenge with nicotine. Two networks were activated, one consisting of sensorimotor regions and the other network included voxels in cingulate, prefrontal and orbitofrontal cortices, extending back to the striatum, amygdala, piriform cortex, entorhinal cortex and visual/parietal cortices (Schwarz et al., 2009). Nicotine increased the relative CBV in the same cortical regions, such as medial prefrontal, cingulate orbitofrontal, insular cortices, and in addition in amygdala and dorsomedial hippocampus (Gozzi et al., 2006). In addition, they noted that although a systemic infusion of norepinephrine caused a similar blood pressure response as nicotine, no detectable CBV changes were observed and a compound that possessed similar high affinity towards specific nAChR subtypes as nicotine produced the same kind of region-specific CBV changes as nicotine. Thus, one can conclude that the CBV changes are due to the nicotine-induced regional increase in neuronal activity and not due to unspecific peripheral effects of nicotine or to any global effect on the cerebral vasculature.

The nicotine antagonist, ABT-594, induced dose-dependent and region-specific cerebral hemodynamic changes in awake rats (Skoubis et al., 2006) that were “dampened” under alpha-chloralose anesthesia (Chin et al., 2008). This indicates that the anesthesia is a confounding factor in pHMRI studies and emphasizes that the selection of anesthetic should be made with care.

Apomorphine

Apomorphine is a substance that causes smaller responses in pHMRI. Apomorphine is a nonspecific dopamine receptor agonist which produces stereotypical behavior in rats characterized by continuous and compulsive sniffing, licking and gnawing (Finch and Haeusler, 1973) and locomotor activity (Maj et al., 1972).

An apomorphine challenge has been used in several pHMRI studies with rats (Table 5). In awake rats, autoradiographic technique have revealed that both CBF (McCulloch et al., 1982) and local cerebral glucose utilization (Beck et al., 1987) increased in the somatomotor

cortex. Decreases in blood flow were observed in anterior cingulate cortex and lateral habenula nucleus (McCulloch et al., 1982), areas which also exhibited reductions in local cerebral glucose utilization, in addition declines were detected in parietal and occipital cortex and lateral thalamus (Beck et al., 1987).

In a recent study, no CBV changes were detected in response to a low (0.05 mg/kg, i.v.) dose of apomorphine (Schwarz et al., 2006). Nevertheless with a higher dose (0.2 mg/kg), an increases in the orbitofrontal and prefrontal cortices, in the insular cortex extending back to the ectorhinal/perirhinal cortices and also elevation were also detected in the thalamus.

The anesthetic can also influence the changes evoked by apomorphine administration. In awake monkeys, a 9 % increase in putamen, 4 % in caudate nucleus and 10 % in substantia nigra were observed in the BOLD responses (Zhang et al., 2000) which were abolished in putamen and caudate nucleus and reduced to 2 % increase in substantia nigra under isoflurane anesthesia.

Table 4. Nicotine challenge in rats.

Anesthesia	Drug	Dose	Dose (tartrate salt)	Method	Magnetic field strength (T)	Results	Reference
Awake	Nicotine (s.c., 5 days)		0.4 mg/kg	BOLD	4.7	~ 4 % in prefrontal and visual cortex and anterior cingulate gyrus after acute exposure. Longer activation time in sensitized animals.	Li et al., 2008
Urethane (1.1 g/kg, i.p.)	Nicotine (i.v.)	0.03 mg/kg		CBF (LDF)		160 % (from baseline)	Uchida et al., 2002
Urethane (1.1 g/kg, i.p.)	Nicotine (i.v.)	0.0003 mg/kg 0.003 mg/kg 0.03 mg/kg		CBF (LDF)		Frontal cortex: No response (0.0003 mg/kg), 10 % (0.003 mg/kg), 171 ± 16 % (0.03 mg/kg)	Uchida et al., 1997
Urethane (1.5 g/kg, i.p.)	Nicotine (microinjection)	0.25 nmol		CBF (LDF)		188 ± 26 % in basal forebrain, No response in cerebral cortex	Linville et al., 1993
Morphine sulfate (50 mg/kg, i.p, 30 mg/kg at 30 mins)	Nicotine (i.v. infusion 16.7 µL/min)		4 mg/kg	CBF CMRO ₂	7	CBF increased 41 % ± 5%, CMRO ₂ increased 30% ± 3%	Hyder et al., 2000
Halothane (1.5 %)	Nicotine	0.1 mg/kg 0.35 mg/kg	1 mg/kg	CBV	4.7	14 - 19 % in cingulate and prefrontal cortex	Gozzi et al., 2006
Halothane (1 - 1.5 %)	Nicotine (i.v.)	0.07 mg/kg	0.2 mg/kg	CBV	4.7 9.4	10 - 36 % in cortical areas	Choi et al., 2006
Isoflurane (1-2 %)	Nicotine (s.c., 4 days)	0.4 mg/kg/day		CBV	4.7	T2 increase in cingulate cortex. CBV increase in mediodorsal thalamus, lateral posterior thalamus, cingulate cortex, prefrontal cortex	Calderan et al., 2005
Urethane (1.2 - 1.5 g/kg, i.p.)	Nicotine (s.c.)		0.4 mg/kg	EEG		Decrease in slow wave potential	Ebenezer et al., 1986

Table 4 (cont.). Nicotine challenge in rats.

Anesthesia	Drug	Dose	Dose (tartrate salt)	Method	Magnetic field strength (T)	Results	Reference
α -chloralose (80 mg/kg, 40 mg/kg/h, i.v.)	Nicotine agonist (ATB-594, i.v.)	0.1 μ mol/kg 0.3 μ mol/kg		CBV	4.7	"Dampened" response in cortical areas under anesthesia compared to awake condition	Chin et al., 2008
α -chloralose (80 mg/kg, 40 mg/kg/h, i.v.)	Nicotine agonist (ATB-594, i.v.)	0.1 μ mol/kg		CBV	4.7	Decrease in all areas	Skoubis et al., 2006
Awake	Nicotine agonist (ATB-594, i.v.)	0.1 μ mol/kg 0.3 μ mol/kg		CBV	4.7	5-30 % in cortical areas (0.1 μ mol/kg) 15-45 % in cortical areas (0.3 μ mol/kg)	Chin et al., 2008
Awake	Nicotine agonist (ATB-594, i.v.)	0.03 μ mol/kg 0.1 μ mol/kg 0.3 μ mol/kg		CBV	4.7	Decrease (0.03 μ mol/kg) 20 - 40 % in cortical areas (0.1 μ mol/kg) 30 - 60 % in cortical areas (0.3 μ mol/kg)	Skoubis et al., 2006
Awake	Nicotine (s.c.)		0.4 mg/kg ?	CMRgluc (autoradiography)		In freely-moving, drug-naïve animals, nicotine increased local glucose consumption in several brain regions (30-38 %), but the predominant effect of nicotine was inhibitory.	Marenco et al., 2000
Halothane (1 %)	Nicotine (i.v.)		0.1 mg/kg 1 mg/kg 10 mg/kg	CMRgluc (autoradiography)		No response (0.1 mg/kg) Mean increase 20 % in 21/71 areas (1 mg/kg) Mean increase 50 % in 56/71 areas (10 mg/kg)	McNamara et al., 1990

Abbreviations: BOLD, blood oxygenation level dependent; CBF, cerebral blood flow; CBV, cerebral blood volume; CMRgluc, cerebral metabolic rate of glucose; CMRO₂, cerebral metabolic rate of oxygen; EEG, electroencephalography; ; i.p., intraperitoneally; i.v., intravenously; LDF, Laser Doppler flowmetry; s.c., subcutaneously

Table 5. Apomorphine challenge in rats.

Anesthesia	Dose	Method	Magnetic field strength (T)	Results	Reference
Awake	0.1 µmol/kg	CBV	4.7	20 % increase within area postrema and nucleus tractus solitarius (0.1 µmol/kg).	Chin et al., 2006
	0.3 µmol/kg (i.v.)			20% increase in the activated area (0.3 µmol/kg).	
				65 % increase within area postrema and nucleus tractus solitarius (0.3 µmol/kg).	
Halothane (0.8 %)	0.05 mg/kg	CBV	4.7	No change (0.05 mg/kg).	Schwarz et al., 2006
	0.2 mg/kg (i.v.)			Increase in the orbitofrontal, prefrontal and insular cortices, and in the superior colliculi and thalamus (0.2 mg/kg).	
Awake	0.5 mg/kg (i.v.)	CMRgluc CBF (autoradiography)		Increase in frontal and sensory-motor cortices, ventral thalamus, caudate nucleus, globus pallidus, subthalamic nucleus, substantia nigra, and cerebellar cortex.	McCulloch et al., 1982
				Decrease in anterior cingulate cortex and lateral habenular nucleus.	
Isoflurane (1.5 %)	1 mg/kg (i.p.)	BOLD	7	Decrease in BOLD signal in caudate putamen was changed to increase in BOLD signal after the control of changes in blood pressure	Kalisch et al., 2005
Isoflurane (1.5 %)	1.25 mg/kg (i.p.)	BOLD	7	No significant BOLD signal changes in non-sensitized animals. "Moderate" intensity increase in striatum	Delfino et al., 2007
Halothane (1.0 %)	2 mg/kg (i.p.)	CBV	4.7	20 % increase in striatum	Nguyen et al., 2000

Abbreviations: BOLD, blood oxygenation level dependent; CBF, cerebral blood flow; CBV, cerebral blood volume; CMRgluc, cerebral metabolic rate of glucose; i.p., intraperitoneally; i.v., intravenously

3 Aims of the Study

The research in this thesis is based on functional and pharmacological magnetic resonance imaging of the rat brain. By implementing simultaneous electrophysiological and functional magnetic resonance imaging protocol, it is possible to associate direct neural activity with the elicited hemodynamic changes.

The aims of this study were

1. to investigate neurovascular coupling in the somatosensory cortex of the rat brain under urethane anesthesia
2. to develop a protocol for pharmacological activation that would account for baseline fluctuations

4 Materials and Methods

In this chapter, the animals, MRI and electrophysiological methods, and analyses used in the original articles are presented. In all of the studies, all animal procedures were approved by the State Provincial Office of Eastern Finland (99–61/2002) or the Animal Ethics Committee of the Provincial Government of Southern Finland (ESLH-2007-00440/Ym-23), and conducted in accordance with the guidelines set by the European Community Council Directives 86/609/EEC. These guidelines are set to ensure the welfare of the laboratory animals in research. The use of laboratory animals is justified when the experiments have been designed to assess, detect, regulate or modify the physiological conditions in man or animals (European Union, Council Directives, 86/609/EEC).

4.1 ANIMAL PREPARATION

Adult male Wistar ($n=22$, Laboratory Animal Center, University of Eastern Finland) (**I** and **II**) or Sprague-Dawley rats ($n=13$, Charles River Laboratory) (**III**) were used in the studies. Before the experiments, the rats were housed under controlled conditions (12 h light/dark cycle, temperature 22 ± 1 °C, humidity 50 - 60 %, ad libitum access to food and water).

Animals were anesthetized with an inhalation anesthetic during the surgery. The surgical level anesthesia with inhalation anesthetics is straightforward and controllable. After surgery, the chosen anesthetic for functional imaging was administered. This ensured that the anesthesia level during functional imaging was not too deep to hinder the detection of activation. Urethane (1.25 g/kg, i.p.) was used in all studies except for three animals in the study **I** that were anesthetized with alpha-chloralose (60 mg/kg, i.v.), with an additional dose (30 mg/kg, i.v.) given after 1 h.

Prior to surgery, animals were anesthetized with halothane (**I**) or isoflurane (**II**, **III**) (4% for induction and 1.5% for maintenance during surgery) in a 70% N₂O – 30% O₂ mixture. After the first study, halothane was changed to isoflurane on the recommendation from the Laboratory Animal Center of University of Eastern Finland.

The femoral artery was cannulated to allow monitoring the blood gases and pH. The femoral vein was cannulated for administration of alpha-chloralose in study **I**. In study **III**, depending on the pharmacological stimulation, either the left femoral vein was cannulated for nicotine administration or an intraperitoneal line was implanted for apomorphine administration.

In the local field potential measurements (**I**, **II**), an electrode was implanted into the right primary somatosensory cortex. The scalp was removed and a small craniotomy was drilled in the right hemisphere above the somatosensory cortex, 4 mm from the midline and 0.5 – 1 mm posterior to the bregma (Paxinos and Watson, 1998). A small incision was made in the dura. An insulated tungsten wire (diameter 50 µm) electrode was targeted to layer IV, at a depth of approximately 1 mm from the surface of the cortex. The electrode was guided with a stereotaxic electrode holder. Gelfoam gelatin sponge was used to fill the hole in the skull to prevent the dental acrylic from irritating the brain and to minimize differences in the magnetic susceptibilities. The electrode was bent towards the neck of the animal and glued to the skull with dental acrylic to prevent its movement. An in-house made chloridized silver wire (diameter 0.25 mm) reference and ground electrodes were implanted subcutaneously in the neck.

In studies **I** and **II**, animals were allowed to breathe normally a mixture of 70% N₂–30% O₂. The spontaneously breathing animals under urethane anesthesia exhibit slightly elevated pCO₂ values although the BOLD response to forepaw stimulation has been shown

to be close to normal with moderate hypercapnic condition (Sicard and Duong, 2005). In addition, a similar hypercapnic condition did not alter the EEG signal nor the hemodynamic response to whisker stimulation under urethane anesthesia (Jones et al., 2005).

In study **III**, animals were tracheotomized and artificially ventilated using a mechanical ventilator. The ventilator was set to provide 55 - 65 breaths per min depending on the underlying physiology. The animals that were ventilated had also the right femoral vein cannulated to allow the administration of the muscle relaxant, pancuronium bromide (2 mg/kg/h).

After surgery, rats were fixed in nonmagnetic stereotaxic frame with a bite bar and earplugs for the MRI experiments. Temperature was maintained at approximately 37 °C with either water circulation or electrical heating pad.

4.2 ELECTROPHYSIOLOGY

The signal from the tungsten wire electrode was amplified 1000 times and band-pass filtered between 0.1 Hz and 5 kHz using an in-house made amplifier. The signal was then digitized, anti-alias filtered with MiniDigi, resampled at 1 kHz, and read on a computer with the Axoscope 9.0 program for further offline analysis.

4.3 MRI METHODS

Magnetic resonance images were acquired using 4.7 T horizontal MRI scanner (Magnex Scientific) interfaced with a Varian UnityInova console at the A. I. Virtanen Institute for Molecular Science, University of Eastern Finland (**I**, **II**) and 7.0 T horizontal MRI scanner interfaced with a Varian DirectDrive console at Charles River Finland, Kuopio (**III**).

A quadrature surface coil (Highfield Imaging) with two 1.8 cm loops was used for signal transmission and reception (**I**). Actively decoupled volume radiofrequency coil and quadrature surface coil pairs (RAPID Biomedical) were used for signal transmission and reception (**II**, **III**).

4.3.1 Anatomical Imaging

Anatomical images were acquired using different spin-eco based pulse sequences with T₂ weighting (Table 6). The pulse sequence and imaging parameters were optimized for the hardware configuration available at the time of these experiments. The resolution of the images were 97.7 $\mu\text{m} \times 97.7 \mu\text{m} \times 1.5 \text{ mm}$ (**I**), 195.3 $\mu\text{m} \times 195.3 \mu\text{m} \times 1.5 \text{ mm}$ (**II**) and 97.7 $\mu\text{m} \times 97.7 \mu\text{m} \times 0.75 \text{ mm}$ (**III**). In studies **II** and **III** the whole brain was covered with multiple slices.

4.3.1 Functional Imaging

Functional magnetic resonance data were acquired with single-shot spin-echo echo-planar-imaging sequence (Table 6). Spin echo EPI was selected instead of gradient echo EPI because the tungsten wire electrode induced an artifact in the images during the simultaneous LFP measurement. The signal void area in a GE-EPI image was approximately one half of the brain.

The temporal resolution of the functional images, 2 - 4 s, was kept as short as possible without compromising the image quality and stability and LFP data quality. A decrease in the temporal resolution is a way to decrease the signal to noise ratio of the images. In study **III**, the collection of 15 slices required an even longer imaging time (4 s) to ensure stability over the long scan time.

Table 6. Magnetic resonance imaging and data analysis parameters.

Study	Magnetic field strength	Coils	Anatomical data	Functional data	Functional data analysis
I	4.7 T	quadrature surface coil for transmitting and receiving	double SE (adiabatic pulses) (TR 2.5 s, TE 60 ms, 256 × 256, 2.5 cm × 2.5 cm, 1 slice, 1.5 mm)	SE-EPI (adiabatic 180° pulse) (TR 2 s, TE 60 ms, 90 × 64, 1.5 cm × 2.0 cm, 1 slice, 1.5 mm)	FSL no smoothing Z (Gaussianized T/F) statistics, $Z > 2.3$ and (corrected) cluster significance threshold of $p = 0.01$
II	4.7 T	volume transmitter, quadrature surface receiver	multislice SE (TR 2.5 s, TE 60 ms, 256 × 256, 5 cm × 5 cm, 9 slices, 1.5 mm)	SE-EPI (TR 2 s, TE 60 ms, 64 × 64, 2.5 cm × 2.5 cm, 1 slice, 1.5 mm)	SPM5 3 × 3 smoothing voxel, one-sample t-test thresholded at $p \leq 0.05$ (FWE corrected)
III	7.0 T	volume transmitter, quadrature surface receiver	FSE (TR 3 s, effTE 48 ms, 512 × 512, 5 cm × 5 cm, 40 slices, 0.75 mm)	SE-EPI (TR 4 s, TE 32 and 50 ms, 64 × 56, 2.5 cm × 2.5 cm, 15 slices, 1.5 mm)	SPM8 2 × 2 smoothing voxel, one-sample t-test thresholded at $p \leq 0.05$ (FDR corrected)

Abbreviations: effTE, effective time to echo; FDR, False discovery rate; FSE, fast spin echo; FSL, FMRIB's software library; FWE, family wise error; SE, spin echo; SE-EPI, spin echo echo planar imaging; SPM5/8, statistical parametric mapping, version 5/8; TE, time to echo; TR, time to repeat

The echo time in studies **I** and **II** was 60 ms. This is longer than the T_2 values in the gray matter at 4.7 T, but it was the shortest possible echo time to allow collecting of the data in a single shot manner with full k-space coverage. In study **III**, two different the echo times, 32 ms and 50 ms, were used for consecutive EPI images, keeping the data collection part identical.

Since the data in study **I** was acquired using a quadrature surface transceiver coil, the EPI image quality was improved by implementing an adiabatic B_1 -insensitive rotation pulse, BIR-4 pulse (Staewen et al., 1990), as the refocusing 180° pulse. As BIR-4 is not a slice selective RF pulse, the number of functional slices was limited to a single slice. Due to imaging of one functional slice, the MRI scanner artifact was only 130 ms long and therefore a sufficient amount of clean evoked LFP data could be collected simultaneously and used without gradient artifact correction.

In study **I**, the acquisition matrix was not zero-padded. Thus, the in-plane resolution was $167 \mu\text{m} \times 312 \mu\text{m}$ with a slice thickness of 1.5 mm. In study **II**, the in-plane resolution of $390 \mu\text{m} \times 390 \mu\text{m}$ and the slice thickness was 1.5 mm. In study **III**, the collection of entire k-space was not possible due to the shorter echo time of 32 ms, therefore only partial k-space of 64×56 data points was collected. The k-space was filled to 64×64 points with a complex conjugate from the other half of the k-space resulting in an in-plane resolution of $390 \mu\text{m} \times 390 \mu\text{m}$.

At high fields, it is crucial for the quality of the echo-planar images that the magnetic field is spatially homogenous. In the presence of a heterogeneous subject, the magnetic field is distorted mainly due to susceptibility differences between air and tissue. Shimming is a method where the static magnetic field inhomogeneities are adjusted by changing the currents in separate shim coils. "Fast, automatic shim technique using echo-planar signal readout for mapping along projections" (FAST(EST)MAP) sequence is based on measuring

B_0 field plots along projections instead of mapping whole imaging planes (Gruetter, 1993; Gruetter and Tkác, 2000). This method uses all first- and second-order shim coils. After FAST(EST)MAP shimming, the proton line width at half-maximum was between 10 and 15 Hz in an approximately 7 mm \times 10 mm \times 5 mm size voxel (**I**, **II**) at 4.7 T. A three-dimensional (3D) field map was measured and the shim currents needed to minimize this field were determined in study **III**. After 3D gradient shimming protocol, proton line width at half of maximum was between 30 and 39 Hz in the shimmed volume of 13 mm \times 18 mm \times 17 mm at 7.0 T.

In studies **I** and **II**, the electrical stimulus was applied for 30 s, i.e. for 15 EPI images. In study **I**, the baseline was the same length as the stimulus period, but the baseline was doubled to that in study **II** to ensure that the signal had returned to the baseline level before the next stimulus period. Four dummy scans were acquired before collecting the functional data to reach steady state. In study **I**, there was a total of 60 images with a total collecting time of 2 minutes per run. An additional stimulus period was also added in study **II** to increase the number of time points for statistical analysis. Therefore, the total number of images was 165 and the total imaging time was 5 min 40 s per each run.

4.4 ELECTRICAL STIMULATION

Bipolar rectangular electrical pulses of 0.3 ms duration and 1.0 to 1.2 mA intensity were applied to a forepaw with a constant current stimulator.

In study **I**, the stimulus frequencies were selected to include the commonly used 1, 3, and 5 Hz frequencies in the alpha-chloralose studies (Silva et al., 1999; Brinker et al., 1999; Matsuura and Kanno, 2001; Keilholz et al., 2004) and extended to higher frequencies. The order of stimulation frequencies of 1, 3, 5, 7, 9, 11, 13, and 15 Hz was randomized to avoid any habituation effects. All the frequencies were applied to the left forepaw but the 11 Hz frequency was applied also to the right forepaw in four urethane anesthetized animals to compare the results with the intact left somatosensory cortex in order to rule out possible effects caused by the surgery or the magnetic susceptibility of the electrode. Based on the results from study **I**, the stimulus frequency was selected to be 10 Hz for study **II** in order to produce robust BOLD and neural activation under urethane anesthesia.

4.5 PHARMACOLOGICAL STIMULATION

Two compounds, nicotine and apomorphine, were used as pharmacological stimuli to elicit hemodynamic activity in the brain. Nicotine was chosen because it is widely used in pharmacological studies and it is known to produce large cortical responses (Gozzi et al., 2006).

A dose of 0.25 mg/kg nicotine tartrate salt (0.081 mg/kg free base), i.v. was used. This corresponds in a 70 kg human to 5.67 mg of nicotine and thus is equivalent to the amount of nicotine present in 3-7 regular cigarettes (Matta et al., 2007).

To test the pharmacological protocol after optimization with nicotine, apomorphine was used since it produces weaker positive and negative activations (Schwarz et al., 2006). Apomorphine is a nonselective dopamine receptor agonist and it was administered at a dose of 0.25 mg/kg subcutaneously.

Both drugs were administered as boluses after 500 baseline echo planar images and the scan was continued for a further 1000 images.

4.6 DATA ANALYSIS

4.6.1 Electrophysiological Analysis

The electrophysiological data were analyzed offline in Matlab. The fast switching gradients of the EPI sequence caused large artifacts in the LFP signal. The artifact also caused the signal to overshoot which made it impossible to correct so that the underlying LFP signal could be restored. Since there was enough clean data which could be used between the artifacts, the gradient switching artifact was simply cut off from the LFP signal and the analysis was conducted at times between the artifacts.

To quantify the evoked somatosensory responses, the lowest negative response peak was identified within 40 ms of each stimulus and the amplitude was calculated with an in-house program written with Matlab. In the case of no detectable response, this approach provides an estimate of baseline activity.

Integrated neural activity was defined as the sum of amplitudes of all evoked potentials during stimulation. To eliminate fluctuations due to asynchrony in the stimulation paradigm caused by manual starting of the stimulator, the number of evoked potentials for summation was corrected according to the stimulation frequency.

4.6.2 Generation of the LFP Based fMRI Models (II)

In the traditional fMRI analysis, a block design model is used in the block paradigm study. The block design model assumes that the BOLD response will remain the same throughout the stimulus period. However during study I, it was noted that during a relatively long stimulus period with the high frequencies required to produce a BOLD response under urethane anesthesia, the evoked LFP and BOLD responses did not remain constant. Therefore, a model was generated on the basis of the theory that the integrated neural activity, i.e. the sum of evoked responses over time, would correlate with the BOLD response (Logothetis et al., 2001; Huttunen et al., 2008).

The first model was constructed using the LFP data measured from the primary somatosensory cortex of a rat simultaneously with BOLD fMRI. The LFP model was calculated as the sum of the amplitudes for the 1.9-s uncontaminated interval between every MRI artifact. For the intervals in which the forepaw stimulation was switched off, the sum was set to zero, as the aim of this study was to utilize the temporal effects of evoked somatosensory responses, not the spontaneous LFP signal fluctuations during activation and baseline periods. Finally, the LFP model was normalized with respect to its maximum value. The length of the final LFP model was 165 points, corresponding to the number of functional images.

The second model was a standard block design model derived from the stimulus paradigm, and consisting of 30 baseline points followed by 15 activation points, repeated three times, with a 30-point baseline period at the end. Special care was taken to handle the LFP model in a similar manner to the block model in the SPM5 (Statistical parametric mapping, version 5) program. Therefore, the LFP model was linearly interpolated to the same time grid as the block model prior to convolution, and resampled at the same points as the block model after the convolution, using the same time-bin per scan and bin offset (16 and 32, respectively). Both LFP and block models were convolved with a hemodynamic response function (HRF) to account for the delay between electrical stimuli and the onset of the BOLD response. A fairly short HRF was chosen based on the results in one study (Silva et al., 2007).

These convolved models were used separately in the first BOLD fMRI analysis and together in the second analysis.

4.6.3 Calculation of T₂ Maps (III)

T₂ maps were calculated on a voxel by voxel basis from two sequential SE-EPI images by fitting the signal data to the following equation

$$S(TE) = S_0 e^{\frac{-TE}{T_2}}, \quad (3)$$

where $S(TE)$ is the signal intensity at the time of data acquisition, S_0 is the signal intensity immediately after RF excitation and TE is the echo time and T_2 are the values to be estimated. The fitting was linear, since two echo times 32 ms and 50 ms were used. In the general estimate of the baseline T₂ values, a 125 pixel ROI placed on the frontal cortex and T₂ values for each rat were calculated as the mean value.

4.6.4 fMRI Analysis

In all of the studies, an individual general linear model analysis was performed on a voxel-by-voxel basis. The choice for the fMRI data analysis methods was based on the current knowledge at the time. fMRI data were analyzed with two different analysis softwares (FEAT, the fMRI Expert Analysis Tool, which is part of FSL ("Functional MRI of Brain"'s (FMRIB's) Software Library) and Statistical Parametric Mapping, SPM) and using in-house written Matlab code including Aedes software (<http://aedes.uef.fi/>) (Table 6).

In study **I**, the model was the electrical stimulus paradigm whereas in study **II** this was further improved by using the measured neural somatosensory activity. In study **III**, a block design model was used. All the models were convolved with the hemodynamic response function to account for the delay between neural and vascular responses.

The hemodynamic response to evoked changes in neuronal activity is transient, delayed, and dispersed in time (Friston et al., 1994). There is extensive variability in the HRF across species, subjects and brain regions within subjects. The SPM analysis software use a canonical gamma function parameterized by a peak delay of 6 s, a return to baseline at around 15 s and an undershoot delay of 16 s (Friston et al., 2007) which is optimal for human HRF (Aguirre et al., 1998).

Only a few studies have addressed the issue of HRF selection in rodents. The optimal HRF for adult rats under light isoflurane anesthesia has a delay of 6 s and a dispersion of 0.8 s (Colonnese et al., 2008). Under alpha-chloralose anesthesia, the delay is 2 – 3 s and the return to baseline occurs at around 5 – 6 s (de Zwart et al., 2005; Silva et al., 2007). Since the BOLD impulse response in rodents is quite fast, a gamma function with peak delay of 2 s and a return to baseline at 5 s was used as HRF in the studies **II** and **III**.

In study **I**, time-series statistical analysis was performed using FMRIB's improved linear modeling (FILM) with a local autocorrelation correction (Woolrich et al., 2001). Z (Gaussianized T/F) statistic images were thresholded using the clusters determined by $Z > 2.3$ and a (corrected) cluster significance threshold of $p = 0.01$ (Worsley et al., 1992).

In study **II**, the statistical analysis was performed using the general linear model on a voxel-by-voxel basis (Friston et al., 2007). First, to evaluate the performance of the block and LFP models separately, two SPM5 analyses were conducted for each rat, one analysis using the block model as the regressor and one using the LFP model. The activated brain areas during forepaw stimulation in both of these designs were assessed using a one-sample t-test thresholded at $p < 0.05$ (FWE corrected).

In the second analysis set, the block and LFP models were used together in the same design matrix in SPM5 to identify these areas in which the LFP model would explain additional variation over the block model in the BOLD signal. The differences in activation for block and LFP models were inferred using an F-test thresholded at $p < 0.05$ (FWE corrected).

In study **III**, the statistical analysis was performed using the general linear model on a voxel-by-voxel basis (Friston et al., 2007) using SPM8 (Statistical parametric mapping,

version 8). The analysis was performed for the T₂ maps. The activated brain areas after drug administration were assessed using a one-sample t-test thresholded at $p \leq 0.05$ (FDR corrected).

In addition to GLM analysis, also ROI based analysis was performed in all studies. In the variable sized ROI analysis (I), the ROIs were defined by the statistical calculation in FSL for each animal separately. A fixed size ROI of 20 pixels was determined according to the response to the concatenated data from all animals under all conditions in order to allow a more objective comparison of the different conditions and their relationship to neuronal activity.

In study II, a fixed size ROI of 16 voxels was drawn on the primary somatosensory cortex area in the echo-planar imaging data of all rats. The BOLD time courses were extracted from these ROIs and averaged time courses were calculated after removing a linear trend. Raw spatially unsmoothed EPI data were used in order to prevent spatial information outside the ROI from influencing the analysis. The block and LFP models convolved with the modified gamma function were fitted into the averaged ROI time courses in a least-squares sense. Finally, a one-tailed (paired) t-test was performed for the parameter estimates to compare the two models between rats.

In studies I and II, the BOLD response was defined as the number of activated voxels. In addition in study I, the magnitude of the BOLD response was calculated as the mean for the 30 s long period, starting from 4 s after stimulation.

In study III, ROIs were created from the individual statistical parametric activation maps calculated from the T₂ maps. The average signal time series was calculated from the pixels exceeding the threshold of $t > 4.5$. The same ROI was then used to obtain BOLD time series from the EPI images acquired with the echo time of 50 ms. To quantify the maximum and mean responses, a low frequency trend of the averaged time series was estimated and this was to calculate the maximum and mean responses.

5 Results

5.1 SOMATOSENSORY ACTIVATION

Under urethane anesthesia, the evoked LFP responses at the primary somatosensory cortex were detected at each measured stimulus frequency (1 - 15 Hz). The first negative peak occurred within 12 to 16 ms after the onset of electrical stimulus and the latency increased with the stimulus frequency. The amplitude of the evoked response varied from 0.28 mV to 0.61 mV, the highest value being detected at 5 Hz frequency after which they declined.

The BOLD response in the somatosensory cortex under urethane anesthesia was detected at all stimulus frequencies except 1 Hz. The highest BOLD response was 4.8 ± 0.5 % at the 11 Hz frequency. The BOLD signal intensity was also measured in the intact left somatosensory cortex in 4 animals using same stimulus frequency. The BOLD response in the intact cortex was 4.5 ± 1.0 % and there was no statistical difference between responses in both cortices. This indicates that surgery and susceptibility effects did not have significant influence on fMRI results.

Under alpha-chloralose anesthesia, both LFP and BOLD responses were detected only with 1 and 3 Hz stimulus frequencies. The latencies were longer (17.5 ± 0.8 ms and 16.9 ± 0.6 ms for the 1 and 3 Hz stimulus frequencies, respectively) than under urethane anesthesia but consistent with other studies (Brinker et al., 1999). The amplitudes of the evoked potentials at 1 and 3 Hz were twofold greater under alpha-chloralose anesthesia than the corresponding values with urethane anesthesia. The BOLD responses were 2.1 ± 1.0 % and 3.7 ± 0.1 % at the 1 and 3 Hz stimulus frequencies, respectively.

One noticeable feature in the LFP signal under alpha-chloralose anesthesia was the high frequency transient peaks during the baseline periods. These peaks along with occasional burst suppression episodes are typical in otherwise normal looking electroencephalography under alpha-chloralose anesthesia (Balis and Monroe, 1964; Ueki et al., 1992; Peeters et al., 2001; Austin et al., 2005) and might indicate a subconvulsive state of the cortical neurons in the absence of normal cortical rhythms (Moruzzi, 1950; Lees, 1972). Under urethane anesthesia, however, these transient baseline components were missing and baseline activity matched that seen in awake animals.

Because the timescales of neural activity and the BOLD response are intrinsically different, it was necessary to undertake quantification to investigate the relationship of neural activity and BOLD. Integrated neural activity was defined as the sum of amplitudes of all the evoked potentials during stimulation. In contrast to evoked response amplitudes under urethane anesthesia which declined after 5 Hz, the summated LFP increased up to 7 Hz but thereafter plateaued. BOLD responses were correlated with the integrated neural activity with both anesthetics, however, the correlated responses as a function of frequency were different between the anesthetics.

Simultaneously recorded neural and BOLD responses differed with the two different anesthetic agents, but there was an overlap the magnitude of the range of neural responses, and thus neural-BOLD coupling could be compared. A linear relationship was observed that was independent of the anesthetic used in conjunction with a nonpainful tactile stimulus.

When relatively long stimulation and rest periods are used to detect the functional response to neuronal activation, the block model has been often used to estimate BOLD responses in both human and animal studies. A block model takes into account the 'on' and 'off' stimulus periods, but assumes that the BOLD response remains constant during the stimulation period even though with higher stimulus frequencies, there can be the occurrence of both neuronal adaptation and habituation.

The LFP model in study **II** was based on the simultaneously measured somatosensory evoked field potential data. The model was generated on the basis of the theory that the integrated neural activity, i.e. the sum of evoked responses over time, is correlated with the BOLD response (Logothetis et al., 2001).

Although the majority of the BOLD signal variation was clearly explained by the block model, there were some stimulus-related variations remained in the BOLD signal that were not accounted for by the block model. Consequently, the LFP model was able to explain these temporal variations in nine of 12 rats in the somatosensory cortex. This means that in this experimental set-up, there are variations of neuronal origin in the BOLD signal that the block model alone does not completely explain. This is a result of variations in the neuronal responses, i.e. that the neurovascular coupling remains unaffected by the variations in the neuronal responses.

5.2 PHARMACOLOGICAL ACTIVATION

T_2 values varied in the cortex between 21 and 71 ms in a 125 pixel ROI at 7.0 T. The average was 45.2 ± 5.1 ms, which is somewhat lower than has been measured from human brain (55.0 ± 4.1 ms) (Yacoub et al., 2003).

Nicotine produced robust positive activations in the cortical areas in all animals and this was detected using T_2 maps. The standard deviation (SD) of the baseline fluctuation was ~ 0.5 ms and no fluctuations or trends could be observed. The maximum T_2 increase in the cortex after nicotine activation was 3.5 ± 0.6 ms (7.5 ± 1.3 %). The duration of the nicotine response was 280 ± 48 s at full width at half maximum and the mean response during that period was 2.5 ± 0.5 ms.

In contrast, the baseline of the BOLD signal exhibited fluctuations that were in the range of a few percent. However, since the maximum BOLD signal increase (7.3 ± 2.6 %) was more than twice the baseline fluctuations, the activation peak could still be detected. The duration of the BOLD nicotine response was 243 ± 91 s at full width at half maximum and the mean response during that period was 5.4 ± 2.0 %. There was no statistical difference between the duration of the nicotine response in T_2 and BOLD signals.

Apomorphine evoked smaller and, in contrast, negative activation in the cortical areas. The maximum T_2 decrease after apomorphine activation was 1.8 ± 0.6 ms (3.5 ± 1.3 %). The duration of the nicotine response was 727 ± 185 s at full width at half maximum and the mean response during that period was 1.2 ± 0.5 ms. It was not possible to determine the mean decrease of the BOLD signal due to the substantial cyclic baseline fluctuations in relation to apomorphine activation. The baseline fluctuation was ~ 16 min of wavelength and ~ 2 % in magnitude. This systematic cycle in the baseline fluctuations was caused by changes in the room temperature and consequently due to the air-conditioning.

6 Discussion and Conclusions

In this thesis, rodent brain activity was studied with functional and pharmacological magnetic resonance imaging. Functional MRI was combined with simultaneous local field potential measurements in order to study the neurovascular coupling in anesthetized rats. Quantitative pharmacological mapping was developed to account for the baseline signal intensity fluctuations, and two pharmacological compounds, nicotine and apomorphine, were used to test the feasibility of the method.

6.1 ANESTHESIA

The selection of anesthesia is one of the most important issues in conducting research with animals that require immobilization. The need for an anesthetic protocol in animal studies is dependent on the experimental protocol. Electrophysiological measurements can be performed in awake and freely moving animals without compromising the signal quality. Neural recordings are possible in behaving animals without anesthesia by using implanted EEG or LFP electrodes that are connected with a wire to a recording system. These measurement can even be conducted without wires via telemetry methods.

In the MRI environment where the image quality relies also on the immobility of the subject, the measurement of awake animals is possible but requires either extensive training of the animals to adjust them to the environment (e.g. some restraint) or paralyzing the animal. It does not however provide matching data to awake animals, since the restrained-related stress and discomfort or enhanced arousal due to MRI noises may interfere with the results (Lahti et al., 1998; Lahti et al., 1999).

The reason for using urethane in the fMRI studies presented here came from electrophysiological measurements. Simultaneous electrophysiological and fMRI measurements required an anesthetic that would meet the requirements for “awake”-like neural activity in addition with preserved cardiovascular function. Due to the presence of high frequency bursts (Austin et al., 2005) alpha-chloralose was not optimal anesthesia for the electrophysiological part of these experiments even though it has been widely used in fMRI studies. Since urethane is a suitable and well established anesthesia in electrophysiological studies (Maggi and Meli, 1986a), the need to test its ability in functional studies became evident.

The main result emerging from study I is the frequency dependence of the somatosensory stimulation under urethane anesthesia. At the time of this research, fMRI studies performed on rodents were conducted mainly under alpha-chloralose anesthesia. The first articles using medetomidine sedation (Weber et al., 2006) and isoflurane anesthesia (Liu et al., 2004; Masamoto et al., 2007) have only been recently published. The advantage of these two anesthetics was that they provided the possibility to perform longitudinal studies whereas urethane anesthesia is always used for terminal experiments. However, with our experimental setup, this was not the most important factor when selecting the anesthetic drug.

Since urethane had not been used in electrical forepaw studies conducted using fMRI, it was necessary to determine the optimal stimulus parameters for urethane anesthesia. The frequency tuning curve revealed that one needs to optimize the electrical stimulus parameters for each anesthetic if one wishes to achieve optimal neural and hemodynamic responses. To date, there have been very few fMRI studies performed under urethane anesthesia (Wu et al., 2002; Lowe et al., 2002; Kannurpatti and Biswal, 2004; Shoaib et al., 2004; Boumans et al., 2007; Liu et al., 2012), and it seems that this was the first time when

electrical forepaw stimulus elicited changes under urethane-anesthetized rats have been measured with fMRI. Since there are no other results that could confirm those findings, the most closely resembling study is an electrical whisker stimulus study conducted under urethane anesthesia using Laser-Doppler flowmetry (LDF) in which reflected laser light is used to determine changes in blood flow (Gerrits et al., 1998). Blood flow increased linearly with stimulus frequency indicating that the optimal stimulus frequencies for urethane anesthesia lay close to 10 Hz, which was the maximum frequency tested, also during a slightly hypercapnic condition.

Urethane anesthesia can be used without mechanical ventilation as shown in studies **I** and **II**. The use of urethane in spontaneously breathing animals requires a wait period of 1-2 hours so that the influence of initial inhalation anesthesia, which is needed prior to surgery, can be considered as over. In study **I**, spontaneously breathing animals anesthetized with urethane were slightly hypercapnic. Hypercapnia causes vasodilatation which decreases the measured hemodynamic responses. However, sensory stimulation in slightly hypercapnic condition has not been shown to affect either electrophysiological or hemodynamic responses (Sicard and Duong, 2005; Jones et al., 2005). Therefore, the results in study **I** do not seem to be compromised by spontaneous breathing.

Even though urethane has been well established anesthesia in electrophysiological studies, it has not gained similar popularity in functional imaging. Urethane, as well as alpha-chloralose, can only be used in terminal experiments, therefore limiting their usage. In addition, urethane is potent mutagen and carcinogen (Field et al., 1993), thus the handling, especially in its powder form, requires special caution. Despite these limitations and based on studies presented here, urethane is well suited anesthesia for functional and pharmacological MRI studies in rats.

6.2 NEUROVASCULAR COUPLING

It is difficult to study neurovascular coupling. Since the brain activity is very complex in nature and not static, a change in one single measurable parameter cannot provide enough information about the entire process of neural and hemodynamic activity. Therefore there is a clear need to implement different types of instrumentation together, if one wishes to answer the question: How is the electrical brain activity linked to the hemodynamic changes?

Different combinations of modalities have been experimented in simultaneous measurements to investigate this connection (Mulert and Lemieux, 2010), although the most common one is EEG combined with fMRI. This combination is especially used in human studies, since it is noninvasive in nature and relatively easy to implement.

In animal studies, a preferable option is to measure neural activity directly from the brain avoiding the diffusivity effect of the skull. It is technically very challenging to combine invasive electrophysiological methods to functional imaging in animals due to difficulties in constructing the experimental setups and the coincidental artifacts in the data. Nevertheless it provides insights into the complexity of the brain activity and to the coupling of neural and hemodynamic activity.

In study **I**, the neurovascular coupling was preserved during both urethane and alpha-chloralose anesthesia despite the differences in the frequency tuning curve. The neurovascular coupling was found to be linear in the measured frequency range. Varying the stimulus frequency during electrical forepaw stimulus has led to the hypothesis that there is a linear relationship between electrophysiological and hemodynamic responses and this holds true in spite of differences in anesthesia or methodological issues (Brinker et al., 1999; Van Camp et al., 2005; Masamoto et al., 2007). This indicates that the stimuli are being presented in a non-painful, tactile fashion and that neither neural or hemodynamic components are saturated.

For electrical hindpaw or whisker stimulus, both linear (Martindale et al., 2003; Ureshi et al., 2004; Devonshire et al., 2012) and nonlinear (Sheth et al., 2004; Jones et al., 2004; Ureshi et al., 2005; Hewson-Stoate et al., 2005; Martin et al., 2006) relationships have been observed. There are several reasons for these nonlinearities. In the study of Martin and colleagues, a linear neural-hemodynamic coupling relationship was found for the awake rats but it was nonlinear in urethane anesthetized animals (Martin et al., 2006). They also showed that if one used the same neural data but now in absolute terms (i.e. neural responses were not normalized to the 1 Hz stimulus frequency) then a complex and nonlinear relationship could be revealed. This indicates that also the data analysis methods may play a role in determining the nature of the neurovascular coupling.

It is interesting that varying stimulus intensity has resulted in nonlinear (Norup Nielsen and Lauritzen, 2001; Jones et al., 2004; Ureshi et al., 2005) neurovascular coupling also in the case when stimulus frequency and intensity data have been merged (Sheth et al., 2004; Hewson-Stoate et al., 2005). Modeling analysis demonstrated that the relationship might appear linear over a narrow range of responses, but it incorporated important nonlinear properties that were better described by a threshold or power law relationship (Sheth et al., 2004). The nonlinearity indicates that at the both ends of the scale, changes in the neural activity are accompanied by disproportionate large or small changes in the hemodynamic responses.

At the lower end of the scale, there may be a threshold that needs to be reached before any hemodynamic response is elicited (Norup Nielsen and Lauritzen, 2001). This was also the case in study I, where no BOLD response was detected under urethane anesthesia even though the 1 Hz stimulus frequency elicited clear responses in the LFP signal.

In the case of designing a study for functional imaging, it may be useful to select the stimulus parameters to elicit responses which are either known to be in the linear region or to elicit responses in the mid-range of the relationship so that the neurovascular coupling is linear and thence the interpretation of the results becomes more straightforward.

In study II, the temporal variation of the neurovascular coupling was studied further. The main result was that the model created from actual simultaneously measured neuronal activity was able to explain additional BOLD variation over the block model that captures only the rest and stimulus periods. It was also shown that the integrated neural activity decreased during stimulation, however this decrease was neither linear nor constant between animals. In addition there were also random periods of increases in the integrated neural activity. The possible mechanisms are reductions in excitatory or increases in inhibitory synaptic effects or changes in neuronal excitability related to the long duration or to the rhythmic nature of the stimulation (Buzsaki et al., 2007). Furthermore, the fluctuations in spontaneous neuronal activity range from hundreds of milliseconds to tens of seconds and these have a definite effect on the synaptic responses; either diminishing or boosting them temporally (Fox et al., 2007).

At low stimulus frequencies, a block model is likely to be adequately representative for the hemodynamic response. However, under urethane anesthesia, the stimulus frequency should be higher in order to achieve optimal responses. At higher stimulus frequencies, neuronal adaptation and habituation may occur and therefore the neuronal responses are not constant throughout the relatively long stimulus period. To conclude, the stimulus paradigm-derived model examined in study II does not always provide the most optimal estimate for BOLD responses under these types of experimental conditions. However, this approach would require measuring neuronal activity simultaneously and consequently to create a model on an individual basis.

The limitation of study II is the use of a single electrode and single functional imaging slice. It would have been interesting to observe whether the neuronal and hemodynamic responses would undergo similar decay in other areas in the somatosensory pathway such as thalamus or secondary somatosensory cortex and whether the neurovascular coupling would have been similarly preserved. In the limited number of studies that have focused

on multiple brain areas in addition to the primary location, the coupling between neuronal and hemodynamic responses has been shown to be region dependent. A linear relationship was found in cortex and thalamus, however a nonlinear relationship between BOLD and LFP was detected in brainstem (Devonshire et al., 2012). Similarly, the relationship the fMRI response and LFP is not the same in different cortical and subcortical regions (Sloan et al., 2010).

6.3 PHARMACOLOGICAL MRI

During the preliminary BOLD fMRI measurement conducted for study **III**, noticeable fluctuations in the BOLD signal were observed. This baseline fluctuation was found to be approximately 16 min in wavelength and 2 % in magnitude. This systematic cycle was caused by changes in the room temperature and consequently due to the air-conditioning in the scanner room. To overcome this problem, a T_2 map based timeseries approach was implemented. The calculation of T_2 maps from sequential images should be one way to diminish these baseline variations since the signal intensity changes caused by air-conditioning were presumed to be approximately similar in both images. This approach reduced the baseline fluctuations and thus both nicotine and apomorphine activations could be detected in the T_2 map timeseries.

T_2 maps have been used to quantify the changes caused by sub-chronic administration of nicotine (Calderan et al., 2005), but this was done at a single time point. As far as is known, the T_2 map timeseries based approach has not been used before to study acute pharmacological activations.

Nicotine produces a distinctive and reproducible pattern of activation involved both cortical and subcortical structures which mediate its acute cognitive and behavioral effects (Gozzi et al., 2006). The increases in relative cerebral blood volume (rCBV) are observed in medial prefrontal, cingulate orbitofrontal and insular cortices (Gozzi et al., 2006), and furthermore the infralimbic and visual cortices have been shown to be robustly activated (Choi et al., 2006). Using CBF measurements, nicotine has been found to produce dose dependent changes in the frontal cortex under urethane anesthesia (Uchida et al., 1997). In an acute drug challenge, BOLD response was increased by ~ 4 % in prefrontal and visual cortices in conscious animals. Overall, these findings are consistent with the results obtained in the present pHMRI study using T_2 maps.

Apomorphine produced negative T_2 responses in motor cortices. Similarly, a decrease in the BOLD signal has been observed in the intact side of the rats with a unilateral nigrostriatal lesion (Delfino et al., 2007). In addition, no CBV response to apomorphine challenge was observed in the cortex of the intact side (Nguyen et al., 2000). In both of these previous studies, the apomorphine dose was higher than that used in study **III**. In contrast, clear positive rCBV effects in the orbitofrontal, prefrontal and insular cortices have been detected (Schwarz et al., 2006) with a similar (0.2 mg/kg) dose. Both local cerebral glucose utilization and CBF are increased in frontal and sensory-motor cortices and decreased in anterior cingulate cortex in conscious animals detected using autoradiographic techniques (McCulloch et al., 1982; Beck et al., 1987).

The term functional MRI covers all the experiments where magnetic resonance imaging is used to study brain function, even though in the majority of the cases, it refers to BOLD fMRI. The definition of pharmacological MRI is still somewhat vague; however every pHMRI study is an fMRI study. According to the currently established description, the pHMRI refers to all the studies that use drugs to produce acute or chronic effect in the brain or modulate some other task.

Although the first pharmacological stimulus induced activation was already published in 1997 (Breiter et al., 1997), the numbers of pHMRI studies have not increased as dramatically as the fMRI studies due to several reasons. One of the major issues is the

inaccurate timing of the drug induced responses in comparison to a task induced response. When using drugs with little or unknown responses, the statistical detection of activation may be difficult due to unpredictability of optimal timing. This may hinder the analysis of novel pharmaceutical agents even those with known pharmacokinetics.

In preclinical settings, anesthesia is a critical factor in drug challenges. The activation depends on the underlying physiological state of the animal and that is extensively and differently influenced by the various anesthetic agents. In addition, rodents are usually mechanically ventilated thus requiring the use of muscle relaxants, another confounding factor.

Despite some of the problems described above, phMRI is at present the best noninvasive mapping tool with which to study the effects of drug. phMRI will have a major impact in drug and treatment development and in understanding the brain function in the healthy and diseased brain.

6.4 FUTURE DIRECTIONS

Functional magnetic resonance imaging has proved to be a successful tool to study brain function in both humans and animals. The numbers of clinical and preclinical scanners have increased in recent years. At the same time, the selection of available pulse sequences and the general usability of the imaging systems have improved and the scanners have become more “plug-and-play” types of machines. When the use of the MRI imaging system becomes easier and the analysis methods become automated, more emphasis must be placed on conducting fMRI experiments. Valid research questions and hypothesis should be set in such a way that those could be answered with the available techniques.

It is essential to be aware of what really is being measured with the selected techniques in order to understand the results and thus to draw the correct conclusions. Unfortunately, the fundamental basis of BOLD fMRI signal is not completely understood. In recent years, the trend in fMRI studies has shifted towards more neuroscientific applications instead of investigating the tool itself. There should be some emphasis in resolving the basis of the BOLD signal since that represents the foundation of all results from studies using that principle.

In addition to resolving the basis of the BOLD signal, also research attempting to elucidate the neurovascular and neurometabolic coupling should continue. The link between neural activity and hemodynamic responses is complex but fascinating since it involves so many processes and factors. There is still incomplete knowledge about the spatial and temporal characteristics of neural versus vascular responses. Other undetermined key points are the contribution of the astrocytes to the hemodynamic responses and the contributions of excitatory versus inhibitory neurotransmission to the BOLD response.

Research conducted in animals has its own merit. The ability to elicit robust and reliable activations under anesthesia is one of the key aspects in animal functional and pharmacological MRI. Animal studies can provide information that cannot be gathered from human studies. Animal models provide a platform to study the generation and progression of different diseases and thus enable a better prediction of the outcome and in addition can help in the development of new drugs. The translational aspect of animal studies may be important if one considers ways to decrease the gap between preclinical and clinical research.

7 References

- Abeles, M., 1991. *Corticonics: Neural Circuits of the Cerebral Cortex*. New York: Cambridge University Press.
- Adamczak, J.M., Farr, T.D., Seehafer, J.U., Kalthoff, D. and Hoehn, M., 2010. High field BOLD response to forepaw stimulation in the mouse. *NeuroImage*, vol. 51, no. 2, pp. 704-712.
- Aguirre, G.K., Zarahn, E. and D'Esposito, M., 1998. The variability of human, BOLD hemodynamic responses. *NeuroImage*, vol. 8, no. 4, pp. 360-369.
- Ahrens, E.T. and Dubowitz, D.J., 2001. Peripheral somatosensory fMRI in mouse at 11.7 T. *NMR in Biomedicine*, vol. 14, no. 5, pp. 318-324.
- Airaksinen, A.M., Hekmatyar, S.K., Jerome, N., Niskanen, J.P., Huttunen, J.K., Pitkänen, A., Kauppinen, R.A. and Gröhn, O.H., 2012. Simultaneous BOLD fMRI and local field potential measurements during kainic acid-induced seizures. *Epilepsia*, vol. 53, no. 7, pp. 1245-1253.
- Airaksinen, A.M., Niskanen, J.P., Chamberlain, R., Huttunen, J.K., Nissinen, J., Garwood, M., Pitkänen, A. and Gröhn, O., 2010. Simultaneous fMRI and local field potential measurements during epileptic seizures in medetomidine-sedated rats using raster pulse sequence. *Magnetic Resonance in Medicine*, vol. 64, no. 4, pp. 1191-1199.
- Allen, P.J., Josephs, O. and Turner, R., 2000. A method for removing imaging artifact from continuous EEG recorded during functional MRI. *NeuroImage*, vol. 12, no. 2, pp. 230-239.
- Anami, K., Mori, T., Tanaka, F., Kawagoe, Y., Okamoto, J., Yarita, M., Ohnishi, T., Yumoto, M., Matsuda, H. and Saitoh, O., 2003. Stepping stone sampling for retrieving artifact-free electroencephalogram during functional magnetic resonance imaging. *NeuroImage*, vol. 19, no. 2, pp. 281-295.
- Angenstein, F., Kammerer, E. and Scheich, H., 2009. The BOLD response in the rat hippocampus depends rather on local processing of signals than on the input or output activity. A combined functional MRI and electrophysiological study. *The Journal of Neuroscience*, vol. 29, no. 8, pp. 2428-2439.
- Angenstein, F., Kammerer, E., Niessen, H.G., Frey, J.U., Scheich, H. and Frey, S., 2007. Frequency-dependent activation pattern in the rat hippocampus, a simultaneous electrophysiological and fMRI study. *NeuroImage*, vol. 38, no. 1, pp. 150-163.
- Angenstein, F., Krautwald, K. and Scheich, H., 2010. The current functional state of local neuronal circuits controls the magnitude of a BOLD response to incoming stimuli. *NeuroImage*, vol. 50, no. 4, pp. 1364-1375.
- Araque, A., Carmignoto, G. and Haydon, P.G., 2001. Dynamic signaling between astrocytes and neurons. *Annual Review of Physiology*, vol. 63, pp. 795-813.
- Attwell, D. and Iadecola, C., 2002. The neural basis of functional brain imaging signals. *Trends in Neurosciences*, vol. 25, no. 12, pp. 621-625.

- Attwell, D. and Laughlin, S.B., 2001. An energy budget for signaling in the grey matter of the brain. *Journal of Cerebral Blood Flow and Metabolism*, vol. 21, no. 10, pp. 1133-1145.
- Austin, V.C., Blamire, A.M., Allers, K.A., Sharp, T., Styles, P., Matthews, P.M. and Sibson, N.R., 2005. Confounding effects of anesthesia on functional activation in rodent brain: A study of halothane and alpha-chloralose anesthesia. *NeuroImage*, vol. 24, no. 1, pp. 92-100.
- Austin, V.C., Blamire, A.M., Grieve, S.M., O'Neill, M.J., Styles, P., Matthews, P.M. and Sibson, N.R., 2003. Differences in the BOLD fMRI response to direct and indirect cortical stimulation in the rat. *Magnetic Resonance in Medicine*, vol. 49, no. 5, pp. 838-847.
- Azevedo, F.A.C., Carvalho, L.R.B., Grinberg, L.T., Farfel, J.M., Ferretti, R.E.L., Leite, R.E.P., Filho, W.J., Lent, R. and Herculano-Houzel, S., 2009. Equal numbers of neuronal and nonneuronal cells make the human brain an isometrically scaled-up primate brain. *The Journal of Comparative Neurology*, vol. 513, no. 5, pp. 532-541.
- Baker, S., Chin, C., Basso, A.M., Fox, G.B., Marek, G.J. and Day, M., 2012. Xanomeline modulation of the blood oxygenation level-dependent signal in awake rats: Development of pharmacological magnetic resonance imaging as a translatable pharmacodynamic biomarker for central activity and dose selection. *Journal of Pharmacology and Experimental Therapeutics*, vol. 341, no. 1, pp. 263-273.
- Balis, G.U. and Monroe, R.R., 1964. The pharmacology of chloralose. *Psychopharmacologia*, vol. 6, no. 1, pp. 1-30.
- Bandettini, P., 1999. The Temporal Resolution of Functional MRI. pp. 205-220. Moonen, C. and Bandettini, P. eds., *Functional MRI*, Berlin: Springer - Verlag.
- Bandettini, P.A., Wong, E.C., Hinks, R.S., Tikofsky, R.S. and Hyde, J.S., 1992. Time course EPI of human brain function during task activation. *Magnetic Resonance in Medicine*, vol. 25, no. 2, pp. 390-397.
- Bandettini, P.A., Wong, E.C., Jesmanowicz, A., Hinks, R.S. and Hyde, J.S., 1994. Spin-echo and gradient-echo epi of human brain activation using BOLD contrast: A comparative study at 1.5 T. *NMR in Biomedicine*, vol. 7, no. 1-2, pp. 12-20.
- Bandoh, H., Kida, I. and Ueda, H., 2011. Olfactory responses to natal stream water in sockeye salmon by BOLD fMRI. *PLoS ONE*, vol. 6, no. 1, pp. e16051.
- Becerra, L., Pendse, G., Chang, P., Bishop, J. and Borsook, D., 2011. Robust reproducible resting state networks in the awake rodent brain. *PLoS ONE*, vol. 6, no. 10, pp. e25701.
- Beck, T., Möller, H., Nowak, K., Krieglstein, J. and Kuschinsky, K., 1987. Alterations in regional energy metabolism in rat brain produced by small and by large doses of apomorphine: Possible relations to autoreceptors. *European Journal of Pharmacology*, vol. 139, no. 2, pp. 139-146.
- Belliveau, J., Kennedy, D., McKinstry, R., Buchbinder, B., Weisskoff, R., Cohen, M., Vevea, J., Brady, T. and Rosen, B., 1991. Functional mapping of the human visual cortex by magnetic resonance imaging. *Science*, vol. 254, no. 5032, pp. 716-719.

- Benjamini, Y. and Hochberg, Y., 1995. Controlling the false discovery rate: A practical and powerful approach to multiple testing. *Journal of the Royal Statistical Society. Series B (Methodological)*, vol. 57, no. 1, pp. 289-300.
- Berger, H., 1929. Über das elektrenkephalogramm des menschen. *Archiv Für Psychiatrie Und Nervenkrankheiten*, vol. 87, pp. 527-570.
- Berg-Johnsen, J. and Langmoen, I.A., 1992. The effect of isoflurane on excitatory synaptic transmission in the rat hippocampus. *Acta Anaesthesiologica Scandinavica*, vol. 36, no. 4, pp. 350-355.
- Bloch, F., 1946. Nuclear induction. *Physical Review*, vol. 70, no. 7-8, pp. 460-474.
- Bloom, A.S., Hoffmann, R.G., Fuller, S.A., Pankiewicz, J., Harsch, H.H. and Stein, E.A., 1999. Determination of drug-induced changes in functional MRI signal using a pharmacokinetic model. *Human Brain Mapping*, vol. 8, no. 4, pp. 235-244.
- Boorman, L., Kennerley, A.J., Johnston, D., Jones, M., Zheng, Y., Redgrave, P. and Berwick, J., 2010. Negative blood oxygen level dependence in the rat: A model for investigating the role of suppression in neurovascular coupling. *The Journal of Neuroscience*, vol. 30, no. 12, pp. 4285-4294.
- Boumans, T., Theunissen, F.E., Poirier, C. and Van Der Linden, A., 2007. Neural representation of spectral and temporal features of song in the auditory forebrain of zebra finches as revealed by functional MRI. *The European Journal of Neuroscience*, vol. 26, no. 9, pp. 2613-2626.
- Braitenberg, V. and Schuz, A., 1998. *Cortex: Statistics and Geometry of Neuronal Connectivity*. 2nd ed., New York: Springer.
- Breger, R.K., Rimm, A.A., Fischer, M.E., Papke, R.A. and Haughton, V.M., 1989. T1 and T2 measurements on a 1.5-T commercial MR imager. *Radiology*, vol. 171, no. 1, pp. 273-276.
- Breiter, H.C., Gollub, R.L., Weisskoff, R.M., Kennedy, D.N., Makris, N., Berke, J.D., Goodman, J.M., Kantor, H.L., Gastfriend, D.R., Riorden, J.P., Mathew, R.T., Rosen, B.R. and Hyman, S.E., 1997. Acute effects of cocaine on human brain activity and emotion. *Neuron*, vol. 19, no. 3, pp. 591-611.
- Brinker, G., Bock, C., Busch, E., Krep, H., Hossmann, K.A. and Hoehn-Berlage, M., 1999. Simultaneous recording of evoked potentials and T2*-weighted MR images during somatosensory stimulation of rat. *Magnetic Resonance in Medicine*, vol. 41, no. 3, pp. 469-473.
- Buzsaki, G., Anastassiou, C.A. and Koch, C., 2012. The origin of extracellular fields and currents - EEG, ECoG, LFP and spikes. *Nature Reviews. Neuroscience*, vol. 13, no. 6, pp. 407-420.
- Buzsáki, G., 2006. *Rhythms of the Brain*. New York: Oxford University Press.
- Buzsaki, G., Kaila, K. and Raichle, M., 2007. Inhibition and brain work. *Neuron*, vol. 56, no. 5, pp. 771-783.
- Calderan, L., Chiamulera, C., Marzola, P., Fabene, P.F., Fumagalli, G.F. and Sbarbati, A., 2005. Sub-chronic nicotine-induced changes in regional cerebral blood volume and

transversal relaxation time patterns in the rat: A magnetic resonance study. *Neuroscience Letters*, vol. 377, no. 3, pp. 195-199.

- Canals, S., Beyerlein, M., Murayama, Y. and Logothetis, N.K., 2008. Electric stimulation fMRI of the perforant pathway to the rat hippocampus. *Magnetic Resonance Imaging*, vol. 26, no. 7, pp. 978-986.
- Catana, C., Procissi, D., Wu, Y., Judenhofer, M.S., Qi, J., Pichler, B.J., Jacobs, R.E. and Cherry, S.R., 2008. Simultaneous in vivo positron emission tomography and magnetic resonance imaging. *Proceedings of the National Academy of Sciences*, vol. 105, no. 10, pp. 3705-3710.
- Caton, R., 1875. The electric current of the brain. *British Medical Journal*, vol. 2, pp. 278.
- Chalmers, R.K. and Erickson, C.K., 1964. Central cholinergic blockade of the conditioned avoidance response in rats. *Psychopharmacologia*, vol. 6, no. 1, pp. 31-41.
- Chen, Y.C., Galpern, W.R., Brownell, A.L., Matthews, R.T., Bogdanov, M., Isacson, O., Keltner, J.R., Beal, M.F., Rosen, B.R. and Jenkins, B.G., 1997. Detection of dopaminergic neurotransmitter activity using pharmacologic MRI: Correlation with PET, microdialysis, and behavioral data. *Magnetic Resonance in Medicine*, vol. 38, no. 3, pp. 389-398.
- Cheung, M.M., Lau, C., Zhou, I.Y., Chan, K.C., Cheng, J.S., Zhang, J.W., Ho, L.C. and Wu, E.X., 2012. BOLD fMRI investigation of the rat auditory pathway and tonotopic organization. *NeuroImage*, vol. 60, no. 2, pp. 1205-1211.
- Chin, C.L., Pauly, J.R., Surber, B.W., Skoubis, P.D., McGaraughty, S., Hradil, V.P., Luo, Y., Cox, B.F. and Fox, G.B., 2008. Pharmacological MRI in awake rats predicts selective binding of alpha4beta2 nicotinic receptors. *Synapse*, vol. 62, no. 3, pp. 159-168.
- Chin, C., Fox, G.B., Hradil, V.P., Osinski, M.A., McGaraughty, S.P., Skoubis, P.D., Cox, B.F. and Luo, Y., 2006. Pharmacological MRI in awake rats reveals neural activity in area postrema and nucleus tractus solitarius: Relevance as a potential biomarker for detecting drug-induced emesis. *NeuroImage*, vol. 33, no. 4, pp. 1152-1160.
- Chin, C., Upadhyay, J., Marek, G.J., Baker, S.J., Zhang, M., Mezler, M., Fox, G.B. and Day, M., 2011. Awake rat pharmacological magnetic resonance imaging as a translational pharmacodynamic biomarker: Metabotropic glutamate 2/3 agonist modulation of ketamine-induced blood oxygenation level dependence signals. *Journal of Pharmacology and Experimental Therapeutics*, vol. 336, no. 3, pp. 709-715.
- Choi, J., Mandeville, J.B., Chen, Y.I., Kim, Y.R. and Jenkins, B.G., 2006. High resolution spatial mapping of nicotine action using pharmacologic magnetic resonance imaging. *Synapse*, vol. 60, no. 2, pp. 152-157.
- Choy, M., Wells, J.A., Thomas, D.L., Gadian, D.G., Scott, R.C. and Lythgoe, M.F., 2010. Cerebral blood flow changes during pilocarpine-induced status epilepticus activity in the rat hippocampus. *Experimental Neurology*, vol. 225, no. 1, pp. 196-201.
- Collins, J.G., Kawahara, M., Homma, E. and Kitahata, L.M., 1983. Alpha-chloralose suppression of neuronal activity. *Life Sciences*, vol. 32, no. 26, pp. 2995-2999.

- Colonnese, M.T., Phillips, M.A., Constantine-Paton, M., Kaila, K. and Jasanoff, A., 2008. Development of hemodynamic responses and functional connectivity in rat somatosensory cortex. *Nature Neuroscience*, vol. 11, no. 1, pp. 72-79.
- Dashti, M., Geso, M. and Williams, J., 2005. The effects of anaesthesia on cortical stimulation in rats: A functional MRI study. *Australasian Physical & Engineering Sciences in Medicine*, vol. 28, no. 1, pp. 21-25.
- de Celis Alonso, B., Makarova, T. and Hess, A., 2011. On the use of α -chloralose for repeated BOLD fMRI measurements in rats. *Journal of Neuroscience Methods*, vol. 195, no. 2, pp. 236-240.
- de Zwart, J.A., Silva, A.C., van Gelderen, P., Kellman, P., Fukunaga, M., Chu, R., Koretsky, A.P., Frank, J.A. and Duyn, J.H., 2005. Temporal dynamics of the BOLD fMRI impulse response. *NeuroImage*, vol. 24, no. 3, pp. 667-677.
- Delfino, M., Kalisch, R., Czisch, M., Larramendy, C., Ricatti, J., Taravini, I.R.E., Trenkwalder, C., Murer, M.G., Auer, D.P. and Gershanik, O.S., 2007. Mapping the effects of three dopamine agonists with different dyskinesogenic potential and receptor selectivity using pharmacological functional magnetic resonance imaging. *Neuropsychopharmacology*, vol. 32, no. 9, pp. 1911-1921.
- Detre, J.A., Leigh, J.S., Williams, D.S. and Koretsky, A.P., 1992. Perfusion imaging. *Magnetic Resonance in Medicine*, vol. 23, no. 1, pp. 37-45.
- Devonshire, I.M., Papadakis, N.G., Port, M., Berwick, J., Kennerley, A.J., Mayhew, J.E.W. and Overton, P.G., 2012. Neurovascular coupling is brain region-dependent. *NeuroImage*, vol. 59, no. 3, pp. 1997-2006.
- Devor, A., Tian, P., Nishimura, N., Teng, I.C., Hillman, E.M.C., Narayanan, S.N., Ulbert, I., Boas, D.A., Kleinfeld, D. and Dale, A.M., 2007. Suppressed neuronal activity and concurrent arteriolar vasoconstriction may explain negative blood oxygenation level-dependent signal. *The Journal of Neuroscience*, vol. 27, no. 16, pp. 4452-4459.
- Dreier, J.P., Major, S., Pannek, H., Woitzik, J., Scheel, M., Wiesenthal, D., Martus, P., Winkler, M.K.L., Hartings, J.A., Fabricius, M., Speckmann, E., Gorji, A. and for the COSBID study group, 2012. Spreading convulsions, spreading depolarization and epileptogenesis in human cerebral cortex. *Brain*, vol. 135, no. 1, pp. 259-275.
- Dubowitz, D.J., Chen, D.Y., Atkinson, D.J., Grieve, K.L., Gillikin, B., Bradley, W.G., Jr and Andersen, R.A., 1998. Functional magnetic resonance imaging in macaque cortex. *Neuroreport*, vol. 9, no. 10, pp. 2213-2218.
- Dunn, J.F., Tuor, U.I., Kmech, J., Young, N.A., Henderson, A.K., Jackson, J.C., Valentine, P.A. and Teskey, G.C., 2009. Functional brain mapping at 9.4T using a new MRI-compatible electrode chronically implanted in rats. *Magnetic Resonance in Medicine*, vol. 61, no. 1, pp. 222-228.
- Duong, T.Q., 2007. Cerebral blood flow and BOLD fMRI responses to hypoxia in awake and anesthetized rats. *Brain Research*, vol. 1135, no. 1, pp. 186-194.
- Duong, T.Q., Silva, A.C., Lee, S.P. and Kim, S.G., 2000. Functional MRI of calcium-dependent synaptic activity: Cross correlation with CBF and BOLD measurements. *Magnetic Resonance in Medicine*, vol. 43, no. 3, pp. 383-392.

- Duong, T.Q., Kim, D., Uğurbil, K. and Kim, S., 2001. Localized cerebral blood flow response at submillimeter columnar resolution. *Proceedings of the National Academy of Sciences*, vol. 98, no. 19, pp. 10904-10909.
- Duvernoy, H.M., Delon, S. and Vannson, J.L., 1981. Cortical blood vessels of the human brain. *Brain Research Bulletin*, vol. 7, no. 5, pp. 519-579.
- Easton, N., Marshall, F.H., Marsden, C.A. and Fone, K.C.F., 2009. Mapping the central effects of methylphenidate in the rat using pharmacological MRI BOLD contrast. *Neuropharmacology*, vol. 57, no. 7-8, pp. 653-664.
- Easton, N., Marshall, F., Fone, K. and Marsden, C., 2007. Atomoxetine produces changes in cortico-basal thalamic loop circuits: Assessed by phMRI BOLD contrast. *Neuropharmacology*, vol. 52, no. 3, pp. 812-826.
- Ebenezer, I.S., 1986. The generation of cortical slow potentials in the rat anaesthetised with urethane and their modification by nicotine. *Neuropharmacology*, vol. 25, no. 6, pp. 639-643.
- Eger, E., 1984. The pharmacology of isoflurane. *British Journal of Anaesthesia*, vol. 56, no. Suppl 1, pp. 71S-99S.
- Febo, M. and Pira, A.S., 2011. Increased BOLD activation to predator stressor in subiculum and midbrain of amphetamine-sensitized maternal rats. *Brain Research*, vol. 1382, pp. 118-127.
- Ferger, B. and Kuschinsky, K., 1997. Biochemical studies support the assumption that dopamine plays a minor role in the EEG effects of nicotine. *Psychopharmacology*, vol. 129, no. 2, pp. 192-196.
- Ferrari, L., Turrini, G., Crestan, V., Bertani, S., Cristofori, P., Bifone, A. and Gozzi, A., 2012. A robust experimental protocol for pharmacological fMRI in rats and mice. *Journal of Neuroscience Methods*, vol. 204, no. 1, pp. 9-18.
- Field, K.J. and Lang, C.M., 1988. Hazards of urethane (ethyl carbamate): A review of the literature. *Laboratory Animals*, vol. 22, no. 3, pp. 255-262.
- Field, K.J., White, W.J. and Lang, C.M., 1993. Anaesthetic effects of chloral hydrate, pentobarbitone and urethane in adult male rats. *Laboratory Animals*, vol. 27, no. 3, pp. 258-269.
- Finch, L. and Haeusler, G., 1973. The cardiovascular effects of apomorphine in the anaesthetized rat. *European Journal of Pharmacology*, vol. 21, no. 3, pp. 264-270.
- Fleischl von Marxow, Ernst., 1893. *Gesammelte Abhandlungen*. Leipzig: J. A. Barth.
- Fox, M.D., Snyder, A.Z., Vincent, J.L. and Raichle, M.E., 2007. Intrinsic fluctuations within cortical systems account for intertrial variability in human behavior. *Neuron*, vol. 56, no. 1, pp. 171-184.
- Fox, P.T. and Raichle, M.E., 1986. Focal physiological uncoupling of cerebral blood flow and oxidative metabolism during somatosensory stimulation in human subjects. *Proceedings of the National Academy of Sciences*, vol. 83, no. 4, pp. 1140-1144.
- Fox, P., Raichle, M., Mintun, M. and Dence, C., 1988. Nonoxidative glucose consumption during focal physiologic neural activity. *Science*, vol. 241, no. 4864, pp. 462-464.

- Franceschini, M.A., Radhakrishnan, H., Thakur, K., Wu, W., Ruvinskaya, S., Carp, S. and Boas, D.A., 2010. The effect of different anesthetics on neurovascular coupling. *NeuroImage*, vol. 51, no. 4, pp. 1367-1377.
- Freeman, W.J., 1975. *Mass Action in the Nervous System*. New York: Academic Press.
- Freygang, W.H., Jr and Sokoloff, L., 1958. Quantitative measurement of regional circulation in the central nervous system by the use of radioactive inert gas. *Advances in Biological and Medical Physics*, vol. 6, pp. 263-279.
- Friston, K.J., Ashburner, J.T., Kiebel, S.J., Nichols, T.E. and Penny, W.D., eds., 2007. *Statistical Parametric Mapping: The Analysis of Functional Brain Images*. London: Academic Press.
- Friston, K.J., Jezzard, P. and Turner, R., 1994. Analysis of functional MRI time-series. *Human Brain Mapping*, vol. 1, no. 2, pp. 153-171.
- Fukuda, M., Vazquez, A.L., Zong, X. and Kim, S., 2013. Effects of the alpha2-adrenergic receptor agonist dexmedetomidine on neural, vascular and BOLD fMRI responses in the somatosensory cortex. *European Journal of Neuroscience*, vol. 37, no. 1, pp. 80-95.
- Gelman, N., Gorell, J.M., Barker, P.B., Savage, R.M., Spickler, E.M., Windham, J.P. and Knight, R.A., 1999. MR imaging of human brain at 3.0 T: Preliminary report on transverse relaxation rates and relation to estimated iron content. *Radiology*, vol. 210, no. 3, pp. 759-767.
- Gerrits, R.J., Stein, E.A. and Greene, A.S., 1998. Blood flow increases linearly in rat somatosensory cortex with increased whisker movement frequency. *Brain Research*, vol. 783, no. 1, pp. 151-157.
- Goense, J., Merkle, H. and Logothetis, N., 2012. High-resolution fMRI reveals laminar differences in neurovascular coupling between positive and negative BOLD responses. *Neuron*, vol. 76, no. 3, pp. 629-639.
- Goodman Gilman, A., Goodman, L.S. and Gilman, A., eds., 1980. *The Pharmacological Basis of Therapeutics*. 6th ed., New York: Macmillan Publishing.
- Gozzi, A., Schwarz, A., Reese, T., Bertani, S., Crestan, V. and Bifone, A., 2006. Region-specific effects of nicotine on brain activity: A pharmacological MRI study in the drug-naive rat. *Neuropsychopharmacology*, vol. 31, no. 8, pp. 1690-1703.
- Griffin, K.M., Blau, C.W., Kelly, M.E., O'Herlihy, C., O'Connell, P.R., Jones, J.F.X. and Kerskens, C.M., 2010. Propofol allows precise quantitative arterial spin labelling functional magnetic resonance imaging in the rat. *NeuroImage*, vol. 51, no. 4, pp. 1395-1404.
- Gröhn, O.H., Kettunen, M.I., Penttonen, M., Oja, J.M., van Zijl, P.C. and Kauppinen, R.A., 2000. Graded reduction of cerebral blood flow in rat as detected by the nuclear magnetic resonance relaxation time T2: A theoretical and experimental approach. *Journal of Cerebral Blood Flow and Metabolism*, vol. 20, no. 2, pp. 316-326.
- Gruetter, R., 1993. Automatic, localized in vivo adjustment of all first-and second-order shim coils. *Magnetic Resonance in Medicine*, vol. 29, no. 6, pp. 804-811.

- Gruetter, R. and Tkác, I., 2000. Field mapping without reference scan using asymmetric echo-planar techniques. *Magnetic Resonance in Medicine*, vol. 43, no. 2, pp. 319-323.
- Gsell, W., Burke, M., Wiedermann, D., Bonvento, G., Silva, A.C., Dauphin, F., Buhrle, C., Hoehn, M. and Schwindt, W., 2006. Differential effects of NMDA and AMPA glutamate receptors on functional magnetic resonance imaging signals and evoked neuronal activity during forepaw stimulation of the rat. *Journal of Neuroscience*, vol. 26, no. 33, pp. 8409-8416.
- Gyngell, M.L., Bock, C., Schmitz, B., Hoehn-Berlage, M. and Hossmann, K.A., 1996. Variation of functional MRI signal in response to frequency of somatosensory stimulation in alpha-chloralose anesthetized rats. *Magnetic Resonance in Medicine*, vol. 36, no. 1, pp. 13-15.
- Haase, A., Frahm, J., Matthaei, D., Hanicke, W. and Merboldt, K., 1986. FLASH imaging. rapid NMR imaging using low flip-angle pulses. *Journal of Magnetic Resonance*, vol. 67, no. 2, pp. 258-266.
- Hahn, E.L., 1950. Spin echoes. *Physical Review*, vol. 80, no. 4, pp. 580-594.
- Hämäläinen, M., Hari, R., Ilmoniemi, R.J., Knuutila, J. and Lounasmaa, O.V., 1993. Magnetoencephalography - theory, instrumentation, and applications to noninvasive studies of the working human brain. *Reviews of Modern Physics*, vol. 65, no. 2, pp. 413-497.
- Hara, K. and Harris, R.A., 2002. The anesthetic mechanism of urethane: The effects on neurotransmitter-gated ion channels. *Anesthesia & Analgesia*, vol. 94, no. 2, pp. 313-318.
- Harel, N., Lee, S., Nagaoka, T., Kim, D. and Kim, S., 2002. Origin of negative blood oxygenation level-dependent fMRI signals. *Journal of Cerebral Blood Flow and Metabolism*, vol. 22, no. 8, pp. 908-917.
- Haydon, P.G. and Carmignoto, G., July 2006. Astrocyte control of synaptic transmission and neurovascular coupling. *Physiological Reviews*, vol. 86, no. 3, pp. 1009-1031.
- Hayton, S.M., Kriss, A. and Muller, D.P., 1999. Comparison of the effects of four anaesthetic agents on somatosensory evoked potentials in the rat. *Laboratory Animals*, vol. 33, no. 3, pp. 243-251.
- Heeger, D.J., Huk, A.C., Geisler, W.S. and Albrecht, D.G., 2000. Spikes versus BOLD: What does neuroimaging tell us about neuronal activity?. *Nature Neuroscience*, vol. 3, no. 7, pp. 631-633.
- Herculano-Houzel, S., Mota, B. and Lent, R., 2006. Cellular scaling rules for rodent brains. *Proceedings of the National Academy of Sciences*, vol. 103, no. 32, pp. 12138-12143.
- Hewson-Stoate, N., Jones, M., Martindale, J., Berwick, J. and Mayhew, J., 2005. Further nonlinearities in neurovascular coupling in rodent barrel cortex. *NeuroImage*, vol. 24, no. 2, pp. 565-574.
- Hirano, Y., Stefanovic, B. and Silva, A.C., 2011. Spatiotemporal evolution of the functional magnetic resonance imaging response to ultrashort stimuli. *The Journal of Neuroscience*, vol. 31, no. 4, pp. 1440-1447.

- Hoffmann, A., Jäger, L., Werhahn, K.J., Jaschke, M., Noachtar, S. and Reiser, M., 2000. Electroencephalography during functional echo-planar imaging: Detection of epileptic spikes using post-processing methods. *Magnetic Resonance in Medicine*, vol. 44, no. 5, pp. 791-798.
- Huang, W., Plyka, I., Li, H., Eisenstein, E.M., Volkow, N.D. and Springer, C.S., 1996. Magnetic resonance imaging (MRI) detection of the murine brain response to light: Temporal differentiation and negative functional MRI changes. *Proceedings of the National Academy of Sciences*, vol. 93, no. 12, pp. 6037-6042.
- Hutchison, R.M., Mirsattari, S.M., Jones, C.K., Gati, J.S. and Leung, L.S., 2010. Functional networks in the anesthetized rat brain revealed by independent component analysis of resting-state fMRI. *Journal of Neurophysiology*, vol. 103, no. 6, pp. 3398-3406.
- Huttunen, J.K., Gröhn, O. and Penttonen, M., 2008. Coupling between simultaneously recorded BOLD response and neuronal activity in the rat somatosensory cortex. *NeuroImage*, vol. 39, no. 2, pp. 775-785.
- Huttunen, J.K., Niskanen, J.P., Lehto, L.J., Airaksinen, A.M., Niskanen, E.I., Penttonen, M. and Gröhn, O., 2011. Evoked local field potentials can explain temporal variation in blood oxygenation level-dependent responses in rat somatosensory cortex. *NMR in Biomedicine*, vol. 24, no. 2, pp. 209-215.
- Hyder, F., Behar, K.L., Martin, M.A., Blamire, A.M. and Shulman, R.G., 1994. Dynamic magnetic resonance imaging of the rat brain during forepaw stimulation. *Journal of Cerebral Blood Flow and Metabolism*, vol. 14, no. 4, pp. 649-655.
- Hyder, F., Kennan, R.P., Kida, I., Mason, G.F., Behar, K.L. and Rothman, D., 2000. Dependence of oxygen delivery on blood flow in rat brain: A 7 tesla nuclear magnetic resonance study. *Journal of Cerebral Blood Flow and Metabolism*, vol. 20, no. 3, pp. 485-498.
- Ingvar, D.H. and Lassen, N.A., 1962. Regional blood flow of the cerebral cortex determined by Krypton85. *Acta Physiologica Scandinavica*, vol. 54, no. 3-4, pp. 325-338.
- Ingvar, D.H. and Lassen, N.A., 1961. Quantitative determination of regional blood-flow in man. *The Lancet*, vol. 278, no. 7206, pp. 806-807.
- International Federation of Societies for Electroencephalography and Clinical Neurophysiology, 1974. *Electroencephalography and Clinical Neurophysiology*, vol. 37, no. 5, pp. 521-553.
- Ives, J.R., Warach, S., Schmitt, F., Edelman, R.R. and Schomer, D.L., 1993. Monitoring the patient's EEG during echo planar MRI. *Electroencephalography and Clinical Neurophysiology*, vol. 87, no. 6, pp. 417-420.
- Jenkins, B.G., 2012. Pharmacologic magnetic resonance imaging (phMRI): Imaging drug action in the brain. *NeuroImage*, vol. 62, no. 2, pp. 1072-1085.
- Jezzard, P., Duewell, S. and Balaban, R.S., 1996. MR relaxation times in human brain: Measurement at 4 T. *Radiology*, vol. 199, no. 3, pp. 773-779.
- Jezzard, P., Rauschecker, J.P. and Malonek, D., 1997. An in vivo model for functional MRI in cat visual cortex. *Magnetic Resonance in Medicine*, vol. 38, no. 5, pp. 699-705.

- Jones, M., Berwick, J., Hewson-Stoate, N., Gias, C. and Mayhew, J., 2005. The effect of hypercapnia on the neural and hemodynamic responses to somatosensory stimulation. *NeuroImage*, vol. 27, no. 3, pp. 609-623.
- Jones, M., Berwick, J. and Mayhew, J., 2002. Changes in blood flow, oxygenation, and volume following extended stimulation of rodent barrel cortex. *NeuroImage*, vol. 15, no. 3, pp. 474-487.
- Jones, M., Hewson-Stoate, N., Martindale, J., Redgrave, P. and Mayhew, J., 2004. Nonlinear coupling of neural activity and CBF in rodent barrel cortex. *NeuroImage*, vol. 22, no. 2, pp. 956-965.
- Jupp, B., Williams, J.P., Tesiram, Y.A., Vosmansky, M. and O'Brien, T.J., 2006. MRI compatible electrodes for the induction of amygdala kindling in rats. *Journal of Neuroscience Methods*, vol. 155, no. 1, pp. 72-76.
- Kalisch, R., Delfino, M., Murer, M.G. and Auer, D.P., 2005. The phenylephrine blood pressure clamp in pharmacologic magnetic resonance imaging: Reduction of systemic confounds and improved detectability of drug-induced BOLD signal changes. *Psychopharmacology*, vol. 180, no. 4, pp. 774-780.
- Kalisch, R., Elbel, G., Gössl, C., Czisch, M. and Auer, D.P., 2001. Blood pressure changes induced by arterial blood withdrawal influence bold signal in anesthetized rats at 7 tesla: Implications for pharmacologic MRI. *NeuroImage*, vol. 14, no. 4, pp. 891-898.
- Kamada, K., Pekar, J.J. and Kanwal, J.S., 1999. Anatomical and functional imaging of the auditory cortex in awake mustached bats using magnetic resonance technology. *Brain Research Protocols*, vol. 4, no. 3, pp. 351-359.
- Kannurpatti, S.S. and Biswal, B.B., 2004. Effect of anesthesia on CBF, MAP and fMRI-BOLD signal in response to apnea. *Brain Research*, vol. 1011, no. 2, pp. 141-147.
- Kannurpatti, S.S., Biswal, B.B. and Hudetz, A.G., 2003. Regional dynamics of the fMRI-BOLD signal response to hypoxia-hypercapnia in the rat brain. *Journal of Magnetic Resonance Imaging*, vol. 17, no. 6, pp. 641-647.
- Keilholz, S.D., Silva, A.C., Raman, M., Merkle, H. and Koretsky, A.P., 2004. Functional MRI of the rodent somatosensory pathway using multislice echo planar imaging. *Magnetic Resonance in Medicine*, vol. 52, no. 1, pp. 89-99.
- Keilholz, S.D., Silva, A.C., Raman, M., Merkle, H. and Koretsky, A.P., 2006. BOLD and CBV-weighted functional magnetic resonance imaging of the rat somatosensory system. *Magnetic Resonance in Medicine*, vol. 55, no. 2, pp. 316-324.
- Kety, S.S., 1957. The General Metabolism of the Brain in Vivo. pp. 221-237. Richter, D. ed., *Metabolism of the Nervous System*, London: Pergamon Press.
- Kety, S.S., 1948. Quantitative determination of cerebral blood flow in man. *Methods in Medical Research*, vol. 1, pp. 204-217.
- Kety, S.S. and Schmidt, C.F., 1945. The determination of cerebral blood flow in man by the use of nitrous oxide in low concentrations. *American Journal of Physiology*, vol. 143, no. 1, pp. 53-66.

- Kety, S.S. and Schmidt, C.F., 1948. The nitrous oxide method for the quantitative determination of cerebral blood flow in man: Theory, procedure and normal values. *The Journal of Clinical Investigation*, vol. 27, no. 4, pp. 476-483.
- Khubchandani, M., Mallick, H.N., Jagannathan, N.R. and Mohan Kumar, V., 2003. Stereotaxic assembly and procedures for simultaneous electrophysiological and MRI study of conscious rat. *Magnetic Resonance in Medicine*, vol. 49, no. 5, pp. 962-967.
- Kida, I. and Yamamoto, T., 2008. Stimulus frequency dependence of blood oxygenation level-dependent functional magnetic resonance imaging signals in the somatosensory cortex of rats. *Neuroscience Research*, vol. 62, no. 1, pp. 25-31.
- Kida, I., Yamamoto, T. and Tamura, M., 1996. Interpretation of BOLD MRI signals in rat brain using simultaneously measured near-infrared spectrophotometric information. *NMR in Biomedicine*, vol. 9, no. 8, pp. 333-338.
- Kim, S.G. and Bandettini, P., 2010. Principles of Functional MRI. pp. 3-22. Faro, S. and Mohamed, F. eds., *BOLD fMRI: A Guide to Functional Imaging for Neuroscientists*, New York: Springer.
- Kim, S. and Lee, S., 2004. Cortical layer-dependent CBF changes induced by neural activity. *International Congress Series*, vol. 1265, pp. 201-210.
- Kim, S. and Ogawa, S., 2012. Biophysical and physiological origins of blood oxygenation level-dependent fMRI signals. *Journal of Cerebral Blood Flow and Metabolism*, vol. 32, no. 7, pp. 1188-1206.
- Kim, T., Hendrich, K.S., Masamoto, K. and Kim, S.G., 2007. Arterial versus total blood volume changes during neural activity-induced cerebral blood flow change: Implication for BOLD fMRI. *Journal of Cerebral Blood Flow and Metabolism*, vol. 27, no. 6, pp. 1235-1247.
- Kim, T., Masamoto, K., Fukuda, M., Vazquez, A. and Kim, S., 2010. Frequency-dependent neural activity, CBF, and BOLD fMRI to somatosensory stimuli in isoflurane-anesthetized rats. *NeuroImage*, vol. 52, no. 1, pp. 224-233.
- Kleinschmidt, A., Obrig, H., Requardt, M., Merboldt, K., Dirnagl, U., Villringer, A. and Frahm, J., 1996. Simultaneous recording of cerebral blood oxygenation changes during human brain activation by magnetic resonance imaging and near-infrared spectroscopy. *Journal of Cerebral Blood Flow and Metabolism*, vol. 16, no. 5, pp. 817-826.
- Kwong, K.K., Belliveau, J.W., Chesler, D.A., Goldberg, I.E., Weisskoff, R.M., Poncelet, B.P., Kennedy, D.N., Hoppel, B.E., Cohen, M.S. and Turner, R., 1992. Dynamic magnetic resonance imaging of human brain activity during primary sensory stimulation. *Proceedings of the National Academy of Sciences*, vol. 89, no. 12, pp. 5675-5679.
- Lahti, K.M., Ferris, C.F., Li, F., Sotak, C.H. and King, J.A., 1998. Imaging brain activity in conscious animals using functional MRI. *Journal of Neuroscience Methods*, vol. 82, no. 1, pp. 75-83.
- Lahti, K.M., Ferris, C.F., Li, F., Sotak, C.H. and King, J.A., 1999. Comparison of evoked cortical activity in conscious and propofol-anesthetized rats using functional MRI. *Magnetic Resonance in Medicine*, vol. 41, no. 2, pp. 412-416.

- Landau, W.M., Freygang, W.H., Jr, Roland, L.P., Sokoloff, L. and Kety, S.S., 1955. The local circulation of the living brain; values in the unanesthetized and anesthetized cat. *Transactions of the American Neurological Association*, pp. 125-129.
- Lassen, N.A., Hoedt-Rasmussen, K., Sorensen, S.C., Skinhoje, J.E., Cronquist, S., Bodforss, B. and Ingvar, D.H., 1963. Regional cerebral blood flow in man determined by krypton. *Neurology*, vol. 13, pp. 719-727.
- Laufs, H., 2012. A personalized history of EEG-fMRI integration. *NeuroImage*, vol. 62, no. 2, pp. 1056-1067.
- Lauritzen, M., 2001. Cortical spreading depression in migraine. *Cephalalgia*, vol. 21, no. 7, pp. 757-760.
- Lauritzen, M., 2005. Reading vascular changes in brain imaging: Is dendritic calcium the key?. *Nature Reviews. Neuroscience*, vol. 6, no. 1, pp. 77-85.
- Lauritzen, M., 1984. Long-lasting reduction of cortical blood flow of the rat brain after spreading depression with preserved autoregulation and impaired CO₂ response. *Journal of Cerebral Blood Flow and Metabolism*, vol. 4, no. 4, pp. 546-554.
- Lauterbur, P.C., 1973. Image formation by induced local interactions: Examples employing nuclear magnetic resonance. *Nature*, vol. 242, no. 5394, pp. 190-191.
- Lee, S., Silva, A.C., Ugurbil, K. and Kim, S., 1999. Diffusion-weighted spin-echo fMRI at 9.4 T: Microvascular/tissue contribution to BOLD signal changes. *Magnetic Resonance in Medicine*, vol. 42, no. 5, pp. 919-928.
- Lees, P., 1972. Pharmacology and toxicology of alpha chloralose: A review. *The Veterinary Record*, vol. 91, no. 14, pp. 330-333.
- Leithner, C., Gertz, K., Schröck, H., Priller, J., Prass, K., Steinbrink, J., Villringer, A., Endres, M., Lindauer, U., Dirnagl, U. and Roys, G., 2008. A flow sensitive alternating inversion recovery (FAIR)-MRI protocol to measure hemispheric cerebral blood flow in a mouse stroke model. *Experimental Neurology*, vol. 210, no. 1, pp. 118-127.
- Leo, A.A.P., 1944. Spreading depression of activity in the cerebral cortex. *Journal of Neurophysiology*, vol. 7, no. 6, pp. 359-390.
- Leopold, D.A. and Logothetis, N.K., 2003. Spatial patterns of spontaneous local field activity in the monkey visual cortex. *Reviews in the Neurosciences*, vol. 14, no. 1-2, pp. 195-205.
- Leslie, R.A. and James, M.F., 2000. Pharmacological magnetic resonance imaging: A new application for functional MRI. *Trends in Pharmacological Sciences*, vol. 21, no. 8, pp. 314-318.
- Levin, E., McClernon, F. and Rezvani, A., 2006. Nicotinic effects on cognitive function: Behavioral characterization, pharmacological specification, and anatomic localization. *Psychopharmacology*, vol. 184, no. 3-4, pp. 523-539.
- Li, Z., DiFranza, J.R., Wellman, R.J., Kulkarni, P. and King, J.A., 2008. Imaging brain activation in nicotine-sensitized rats. *Brain Research*, vol. 1199, pp. 91-99.
- Liang, Z., King, J. and Zhang, N., 2012. Anticorrelated resting-state functional connectivity in awake rat brain. *NeuroImage*, vol. 59, no. 2, pp. 1190-1199.

- Lincoln, D.W., 1969. Correlation of unit activity in the hypothalamus with EEG patterns associated with the sleep cycle. *Experimental Neurology*, vol. 24, no. 1, pp. 1-18.
- Lindauer, U., Villringer, A. and Dirnagl, U., 1993. Characterization of CBF response to somatosensory stimulation: Model and influence of anesthetics. *The American Journal of Physiology*, vol. 264, no. 4 Pt 2, pp. H1223-8.
- Linville, D.G., Williams, S., Raszkiewicz, J.L. and Arneric, S.P., 1993. Nicotinic agonists modulate basal forebrain control of cortical cerebral blood flow in anesthetized rats. *Journal of Pharmacology and Experimental Therapeutics*, vol. 267, no. 1, pp. 440-448.
- Lippert, M.T., Steudel, T., Ohl, F., Logothetis, N.K. and Kayser, C., 2010. Coupling of neural activity and fMRI-BOLD in the motion area MT. *Magnetic Resonance Imaging*, vol. 28, no. 8, pp. 1087-1094.
- Liu, X., Li, R., Yang, Z., Hudetz, A.G. and Li, S., 2012. Differential effect of isoflurane, medetomidine, and urethane on BOLD responses to acute levo-tetrahydropalmatine in the rat. *Magnetic Resonance in Medicine*, vol. 68, no. 2, pp. 552-559.
- Liu, Z.M., Schmidt, K.F., Sicard, K.M. and Duong, T.Q., 2004. Imaging oxygen consumption in forepaw somatosensory stimulation in rats under isoflurane anesthesia. *Magnetic Resonance in Medicine*, vol. 52, no. 2, pp. 277-285.
- Logothetis, N.K., 2002. The neural basis of the blood-oxygen-level-dependent functional magnetic resonance imaging signal. *Philosophical Transactions of the Royal Society of London. Series B, Biological Sciences*, vol. 357, no. 1424, pp. 1003-1037.
- Logothetis, N.K., Guggenberger, H., Peled, S. and Pauls, J., 1999. Functional imaging of the monkey brain. *Nature Neuroscience*, vol. 2, no. 6, pp. 555-562.
- Logothetis, N.K., Pauls, J., Augath, M., Trinath, T. and Oeltermann, A., 2001. Neurophysiological investigation of the basis of the fMRI signal. *Nature*, vol. 412, no. 6843, pp. 150-157.
- Logothetis, N.K. and Wandell, B.A., 2004. Interpreting the BOLD signal. *Annual Review of Physiology*, vol. 66, pp. 735-769.
- Logothetis, N.K., 2012. Intracortical recordings and fMRI: An attempt to study operational modules and networks simultaneously. *NeuroImage*, vol. 62, no. 2, pp. 962-969.
- Lowe, A.S., Williams, S.C.R., Symms, M.R., Stoleran, I.P. and Shoaib, M., 2002. Functional magnetic resonance neuroimaging of drug dependence: Naloxone-precipitated morphine withdrawal. *NeuroImage*, vol. 17, no. 2, pp. 902-910.
- Maandag, N.J., Coman, D., Sanganahalli, B.G., Herman, P., Smith, A.J., Blumenfeld, H., Shulman, R.G. and Hyder, F., 2007. Energetics of neuronal signaling and fMRI activity. *Proceedings of the National Academy of Sciences*, vol. 104, no. 51, pp. 20546-20551.
- Maekawa, T., Tommasino, C., Shapiro, H.M., Keifer-Goodman, J. and Kohlenberger, R.W., 1986. Local cerebral blood flow and glucose utilization during isoflurane anesthesia in the rat. *Anesthesiology*, vol. 65, no. 2, pp. 144-151.

- Maggi, C.A. and Meli, A., 1986a. Suitability of urethane anesthesia for physiopharmacological investigations in various systems. part 1: General considerations. *Experientia*, vol. 42, no. 2, pp. 109-114.
- Maggi, C.A. and Meli, A., 1986b. Suitability of urethane anesthesia for physiopharmacological investigations. part 3: Other systems and conclusions. *Experientia*, vol. 42, no. 5, pp. 531-537.
- Maj, J., Grabowska, M. and Gajda, L., 1972. Effect of apomorphine on motility in rats. *European Journal of Pharmacology*, vol. 17, no. 2, pp. 208-214.
- Mäkiranta, M., Ruohonen, J., Suominen, K., Niinimäki, J., Sonkajärvi, E., Kiviniemi, V., Seppänen, T., Alahuhta, S., Jäntti, V. and Tervonen, O., 2005. BOLD signal increase precedes EEG spike activity - a dynamic penicillin induced focal epilepsy in deep anesthesia. *NeuroImage*, vol. 27, no. 4, pp. 715-724.
- Mansfield, P., 1977. Multi-planar image formation using NMR spin echoes. *Journal of Physics C: Solid State Physics*, vol. 10, no. 3, pp. L55-L58.
- Mansvelder, H.D., van Aerde, K.I., Couey, J.J. and Brussaard, A.B., 2006. Nicotinic modulation of neuronal networks: From receptors to cognition. *Psychopharmacology*, vol. 184, no. 3-4, pp. 292-305.
- Mantini, D., Perrucci, M.G., Cugini, S., Ferretti, A., Romani, G.L. and Del Gratta, C., 2007. Complete artifact removal for EEG recorded during continuous fMRI using independent component analysis. *NeuroImage*, vol. 34, no. 2, pp. 598-607.
- Marenco, T., Bernstein, S., Cumming, P. and Clarke, P.B.S., 2000. Effects of nicotine and chlorisondamine on cerebral glucose utilization in immobilized and freely-moving rats. *British Journal of Pharmacology*, vol. 129, no. 1, pp. 147-155.
- Marota, J.J., Ayata, C., Moskowitz, M.A., Weisskoff, R.M., Rosen, B.R. and Mandeville, J.B., 1999. Investigation of the early response to rat forepaw stimulation. *Magnetic Resonance in Medicine*, vol. 41, no. 2, pp. 247-252.
- Martin, C., Martindale, J., Berwick, J. and Mayhew, J., 2006. Investigating neural-hemodynamic coupling and the hemodynamic response function in the awake rat. *NeuroImage*, vol. 32, no. 1, pp. 33-48.
- Martin, C., Berwick, J., Johnston, D., Zheng, Y., Martindale, J., Port, M., Redgrave, P. and Mayhew, J., 2002. Optical imaging spectroscopy in the unanaesthetised rat. *Journal of Neuroscience Methods*, vol. 120, no. 1, pp. 25-34.
- Martindale, J., Mayhew, J., Berwick, J., Jones, M., Martin, C., Johnston, D., Redgrave, P. and Zheng, Y., 2003. The hemodynamic impulse response to a single neural event. *Journal of Cerebral Blood Flow and Metabolism*, vol. 23, no. 5, pp. 546-555.
- Masamoto, K., Fukuda, M., Vazquez, A. and Kim, S.G., 2009. Dose-dependent effect of isoflurane on neurovascular coupling in rat cerebral cortex. *The European Journal of Neuroscience*, vol. 30, no. 2, pp. 242-250.
- Masamoto, K., Kim, T., Fukuda, M., Wang, P. and Kim, S.G., 2007. Relationship between neural, vascular, and BOLD signals in isoflurane-anesthetized rat somatosensory cortex. *Cerebral Cortex*, vol. 17, no. 4, pp. 942-950.

- Masamoto, K. and Kanno, I., 2012. Anesthesia and the quantitative evaluation of neurovascular coupling. *Journal of Cerebral Blood Flow and Metabolism*, vol. 32, no. 7, pp. 1233-1247.
- Mathiesen, C., Caesar, K., Akgören, N. and Lauritzen, M., 1998. Modification of activity-dependent increases of cerebral blood flow by excitatory synaptic activity and spikes in rat cerebellar cortex. *The Journal of Physiology*, vol. 512, no. 2, pp. 555-566.
- Matsuura, T. and Kanno, I., 2001. Quantitative and temporal relationship between local cerebral blood flow and neuronal activation induced by somatosensory stimulation in rats. *Neuroscience Research*, vol. 40, no. 3, pp. 281-290.
- Matta, S.G., Balfour, D.J., Benowitz, N.L., Boyd, R.T., Buccafusco, J.J., Caggiula, A.R., Craig, C.R., Collins, A.C., Damaj, M.I., Donny, E.C., Gardiner, P.S., Grady, S.R., Heberlein, U., Leonard, S.S., Levin, E.D., Lukas, R.J., Markou, A., Marks, M.J., McCallum, S.E., Parameswaran, N., Perkins, K.A., Picciotto, M.R., Quik, M., Rose, J.E., Rothenfluh, A., Schafer, W.R., Stolerman, I.P., Tyndale, R.F., Wehner, J.M. and Zirger, J.M., 2007. Guidelines on nicotine dose selection for in vivo research. *Psychopharmacology*, vol. 190, no. 3, pp. 269-319.
- Mazziotta, J., Toga, A., Evans, A., Fox, P., Lancaster, J., Zilles, K., Woods, R., Paus, T., Simpson, G., Pike, B., Holmes, C., Collins, L., Thompson, P., MacDonald, D., Iacoboni, M., Schormann, T., Amunts, K., Palomero-Gallagher, N., Geyer, S., Parsons, L., Narr, K., Kabani, N., Goualher, G.L., Boomsma, D., Cannon, T., Kawashima, R. and Mazoyer, B., 2001. A probabilistic atlas and reference system for the human brain: International consortium for brain mapping (ICBM). *Philosophical Transactions of the Royal Society of London. Series B, Biological Sciences*, vol. 356, no. 1412, pp. 1293-1322.
- McCulloch, J., Kelly, P.A.T. and Ford, I., 1982. Effect of apomorphine on the relationship between local cerebral glucose utilization and local cerebral blood flow (with an appendix on its statistical analysis). *Journal of Cerebral Blood Flow and Metabolism*, vol. 2, no. 4, pp. 487-499.
- McNamara, D., Larson, D.M., Rapoport, S.I. and Soncrant, T.T., 1990. Preferential metabolic activation of subcortical brain areas by acute administration of nicotine to rats. *Journal of Cerebral Blood Flow and Metabolism*, vol. 10, no. 1, pp. 48-56.
- Mirsattari, S.M., Wang, Z., Ives, J.R., Bihari, F., Leung, L.S., Bartha, R. and Menon, R.S., 2006. Linear aspects of transformation from interictal epileptic discharges to BOLD fMRI signals in an animal model of occipital epilepsy. *NeuroImage*, vol. 30, no. 4, pp. 1133-1148.
- Mishra, A.M., Ellens, D.J., Schridde, U., Motelow, J.E., Purcaro, M.J., DeSalvo, M.N., Enev, M., Sanganahalli, B.G., Hyder, F. and Blumenfeld, H., 2011. Where fMRI and electrophysiology agree to disagree: Corticothalamic and striatal activity patterns in the WAG/rij rat. *The Journal of Neuroscience*, vol. 31, no. 42, pp. 15053-15064.
- Moruzzi, G., 1950. *Problems in Cerebellar Physiology*. Springfield: Charles C. Thomas.
- Mosso, A., 1881. *Ueber Den Kreislauf Des Blutes Im Menschlichen Gehirn*. Leipzig: Verlag von Veit & Comp.
- Mulert, C. and Lemieux, L., eds., 2010. *EEG-fMRI: Physiological Basis, Technique, and Applications*. Berlin: Springer.

- Nair, D.G., 2005. About being BOLD. *Brain Research Reviews*, vol. 50, no. 2, pp. 229-243.
- Nasrallah, F.A., Tan, J. and Chuang, K., 2012. Pharmacological modulation of functional connectivity: A2-adrenergic receptor agonist alters synchrony but not neural activation. *NeuroImage*, vol. 60, no. 1, pp. 436-446.
- Negishi, M., Abildgaard, M., Nixon, T. and Todd Constable, R., 2004. Removal of time-varying gradient artifacts from EEG data acquired during continuous fMRI. *Clinical Neurophysiology*, vol. 115, no. 9, pp. 2181-2192.
- Nersesyan, H., Hyder, F., Rothman, D.L. and Blumenfeld, H., 2004. Dynamic fMRI and EEG recordings during spike-wave seizures and generalized tonic-clonic seizures in WAG/rrij rats. *Journal of Cerebral Blood Flow and Metabolism*, vol. 24, no. 6, pp. 589-599.
- Ngai, A.C., Jolley, M.A., D'Ambrosio, R., Meno, J.R. and Winn, H.R., 1999. Frequency-dependent changes in cerebral blood flow and evoked potentials during somatosensory stimulation in the rat. *Brain Research*, vol. 837, no. 1-2, pp. 221-228.
- Nguyen, T.V., Brownell, A., Iris Chen, Y., Livni, E., Coyle, J.T., Rosen, B.R., Cavagna, F. and Jenkins, B.G., 2000. Detection of the effects of dopamine receptor supersensitivity using pharmacological MRI and correlations with PET. *Synapse*, vol. 36, no. 1, pp. 57-65.
- Nie, B., Chen, K., Zhao, S., Liu, J., Gu, X., Yao, Q., Hui, J., Zhang, Z., Teng, G., Zhao, C. and Shan, B., 2013. A rat brain MRI template with digital stereotaxic atlas of fine anatomical delineations in paxinos space and its automated application in voxel-wise analysis. *Human Brain Mapping*, vol. 34, no. 6, pp. 1306-1318.
- Norup Nielsen, A. and Lauritzen, M., 2001. Coupling and uncoupling of activity-dependent increases of neuronal activity and blood flow in rat somatosensory cortex. *The Journal of Physiology*, vol. 533, no. 3, pp. 773-785.
- Oeltermann, A., Augath, M.A. and Logothetis, N.K., 2007. Simultaneous recording of neuronal signals and functional NMR imaging. *Magnetic Resonance Imaging*, vol. 25, no. 6, pp. 760-774.
- Ogawa, S., Lee, T.M., Kay, A.R. and Tank, D.W., 1990a. Brain magnetic resonance imaging with contrast dependent on blood oxygenation. *Proceedings of the National Academy of Sciences*, vol. 87, no. 24, pp. 9868-9872.
- Ogawa, S., Lee, T.M., Nayak, A.S. and Glynn, P., 1990b. Oxygenation-sensitive contrast in magnetic resonance image of rodent brain at high magnetic fields. *Magnetic Resonance in Medicine*, vol. 14, no. 1, pp. 68-78.
- Ogawa, S., Tank, D.W., Menon, R., Ellermann, J.M., Kim, S.G., Merkle, H. and Ugurbil, K., 1992. Intrinsic signal changes accompanying sensory stimulation: Functional brain mapping with magnetic resonance imaging. *Proceedings of the National Academy of Sciences*, vol. 89, no. 13, pp. 5951-5955.
- Ogawa, S., Lee, T.M. and Barrere, B., 1993. The sensitivity of magnetic resonance image signals of a rat brain to changes in the cerebral venous blood oxygenation. *Magnetic Resonance in Medicine*, vol. 29, no. 2, pp. 205-210.
- Opdam, H.I., Federico, P., Jackson, G.D., Buchanan, J., Abbott, D.F., Fabinyi, G.C.A., Syngienotis, A., Vosmansky, M., Archer, J.S., Wellard, R.M. and Bellomo, R., 2002. A

sheep model for the study of focal epilepsy with concurrent intracranial EEG and functional MRI. *Epilepsia*, vol. 43, no. 8, pp. 779-787.

- Paasonen, J., Huttunen, J.K. and Gröhn, O., 2013. Comparison of six different anesthesia protocols for pHMRI. *Proceedings of the International Society of Magnetic Resonance in Medicine*, Salt Lake City, Utah, USA, pp. 2298.
- Pauling, L. and Coryell, C.D., 1936. The magnetic properties and structure of hemoglobin, oxyhemoglobin and carbonmonoxyhemoglobin. *Proceedings of the National Academy of Sciences*, vol. 22, no. 4, pp. 210-216.
- Pawela, C.P., Biswal, B.B., Hudetz, A.G., Schulte, M.L., Li, R., Jones, S.R., Cho, Y.R., Matloub, H.S. and Hyde, J.S., 2009. A protocol for use of medetomidine anesthesia in rats for extended studies using task-induced BOLD contrast and resting-state functional connectivity. *NeuroImage*, vol. 46, no. 4, pp. 1137-1147.
- Paxinos, G., ed., 2004. *The Rat Nervous System*. 3rd ed., Burlington: Academic Press.
- Paxinos, G. and Watson, C., 1998. *The Rat Brain in Stereotaxic Coordinates*. 4th ed., San Diego: Academic Press.
- Payne, B.R. and Peters, A., 2002. The Concept of Cat Primary Visual Cortex. pp. 1-129. Payne, B.R. and Peters, A. eds., *The Cat Primary Visual Cortex*, San Diego: Academic Press.
- Peeters, R.R., Tindemans, I., De Schutter, E. and Van der Linden, A., 2001. Comparing BOLD fMRI signal changes in the awake and anesthetized rat during electrical forepaw stimulation. *Magnetic Resonance Imaging*, vol. 19, no. 6, pp. 821-826.
- Peeters, R.R., Verhoye, M., Vos, B.P., Van Dyck, D., Van Der Linden, A. and De Schutter, E., 1999. A patchy horizontal organization of the somatosensory activation of the rat cerebellum demonstrated by functional MRI. *European Journal of Neuroscience*, vol. 11, no. 8, pp. 2720-2730.
- Pellerin, L. and Magistretti, P.J., 1994. Glutamate uptake into astrocytes stimulates aerobic glycolysis: A mechanism coupling neuronal activity to glucose utilization. *Proceedings of the National Academy of Sciences*, vol. 91, no. 22, pp. 10625-10629.
- Penttonen, M. and Buzsáki, G., 2003. Natural logarithmic relationship between brain oscillators. *Thalamus & Related Systems*, vol. 2, no. 2, pp. 145-152.
- Petzold, G. and Murthy, V., 2011. Role of astrocytes in neurovascular coupling. *Neuron*, vol. 71, no. 5, pp. 782-797.
- Pfeuffer, J., Merkle, H., Beyerlein, M., Steudel, T. and Logothetis, N.K., 2004. Anatomical and functional MR imaging in the macaque monkey using a vertical large-bore 7 tesla setup. *Magnetic Resonance Imaging*, vol. 22, no. 10, pp. 1343-1359.
- Poirier, C., Verhoye, M., Boumans, T. and Van der Linden, A., 2010. Implementation of spin-echo blood oxygen level-dependent (BOLD) functional MRI in birds. *NMR in Biomedicine*, vol. 23, no. 9, pp. 1027-1032.
- Posse, S., Wiese, S., Gembris, D., Mathiak, K., Kessler, C., Grosse-Ruyken, M., Elghahwagi, B., Richards, T., Dager, S.R. and Kiselev, V.G., 1999. Enhancement of BOLD-contrast

- sensitivity by single-shot multi-echo functional MR imaging. *Magnetic Resonance in Medicine*, vol. 42, no. 1, pp. 87-97.
- Purcell, E.M., Torrey, H.C. and Pound, R.V., 1946. Resonance absorption by nuclear magnetic moments in a solid. *Physical Review*, vol. 69, no. 1-2, pp. 37-38.
- Rauch, A., Rainer, G., Augath, M., Oeltermann, A. and Logothetis, N.K., 2008. Pharmacological MRI combined with electrophysiology in non-human primates: Effects of lidocaine on primary visual cortex. *NeuroImage*, vol. 40, no. 2, pp. 590-600.
- Rees, G., Friston, K. and Koch, C., 2000. A direct quantitative relationship between the functional properties of human and macaque V5. *Nature Neuroscience*, vol. 3, no. 7, pp. 716-723.
- Rioja, E., Kerr, C.L., McDonell, W.N., Dobson, H., Konyer, N.B., Poma, R. and Noseworthy, M.D., 2010. Effects of hypercapnia, hypocapnia, and hyperoxemia on blood oxygenation level-dependent signal intensity determined by use of susceptibility-weighted magnetic resonance imaging in isoflurane-anesthetized dogs. *American Journal of Veterinary Research*, vol. 71, no. 1, pp. 24-32.
- Rojas, M.J., Navas, J.A. and Rector, D.M., 2006. Evoked response potential markers for anesthetic and behavioral states. *American Journal of Physiology - Regulatory, Integrative and Comparative Physiology*, vol. 291, no. 1, pp. R189-R196.
- Rosen, B.R., Belliveau, J.W., Aronen, H.J., Kennedy, D., Buchbinder, B.R., Fischman, A., Gruber, M., Glas, J., Weisskoff, R.M., Cohen, M.S., Hochberg, F.H. and Brady, T.J., 1991. Susceptibility contrast imaging of cerebral blood volume: Human experience. *Magnetic Resonance in Medicine*, vol. 22, no. 2, pp. 293-299.
- Roy, C.S. and Sherrington, F.R.S., 1890. On the regulation of the blood-supply of the brain. *The Journal of Physiology*, vol. 11, pp. 85-108.
- Sachdev, R.N., Champney, G.C., Lee, H., Price, R.R., Pickens, D.R.3., Morgan, V.L., Stefansic, J.D., Melzer, P. and Ebner, F.F., 2003. Experimental model for functional magnetic resonance imaging of somatic sensory cortex in the unanesthetized rat. *NeuroImage*, vol. 19, no. 3, pp. 742-750.
- Sandstrom, D.J., 2004. Isoflurane depresses glutamate release by reducing neuronal excitability at the drosophila neuromuscular junction. *The Journal of Physiology*, vol. 558, no. 2, pp. 489-502.
- Sanganahalli, B.G., Herman, P. and Hyder, F., 2008. Frequency-dependent tactile responses in rat brain measured by functional MRI. *NMR in Biomedicine*, vol. 21, no. 4, pp. 410-416.
- Schäfer, K., Blankenburg, F., Kupers, R., Grüner, J.M., Law, I., Lauritzen, M. and Larsson, H.B.W., 2012. Negative BOLD signal changes in ipsilateral primary somatosensory cortex are associated with perfusion decreases and behavioral evidence for functional inhibition. *NeuroImage*, vol. 59, no. 4, pp. 3119-3127.
- Schmidt, C.F. and Kety, S.S., 1947. Recent studies of cerebral blood flow and cerebral metabolism in man. *Transactions of the Association of American Physicians*, vol. 60, no. 1, pp. 52-58.

- Schridde, U., Khubchandani, M., Motelow, J.E., Sangahalli, B.G., Hyder, F. and Blumenfeld, H., 2008. Negative BOLD with large increases in neuronal activity. *Cerebral Cortex*, vol. 18, no. 8, pp. 1814-1827.
- Schwarz, A.J., Danckaert, A., Reese, T., Gozzi, A., Paxinos, G., Watson, C., Merlo-Pich, E.V. and Bifone, A., 2006. A stereotaxic MRI template set for the rat brain with tissue class distribution maps and co-registered anatomical atlas: Application to pharmacological MRI. *NeuroImage*, vol. 32, no. 2, pp. 538-550.
- Schwarz, A.J., Gozzi, A. and Bifone, A., 2009. Community structure in networks of functional connectivity: Resolving functional organization in the rat brain with pharmacological MRI. *NeuroImage*, vol. 47, no. 1, pp. 302-311.
- Schweinhart, P., Fransson, P., Olson, L., Spenger, C. and Andersson, J.L., 2003. A template for spatial normalisation of MR images of the rat brain. *Journal of Neuroscience Methods*, vol. 129, no. 2, pp. 105-113.
- Shatillo, A., Huttunen, J., Airaksinen, A., Niskanen, J.P. and Gröhn, O., 2012. Spontaneous depolarization waves in medetomidine sedated sprague-dawley rats detected by fMRI. *Proceedings of the International Society of Magnetic Resonance in Medicine*, Melbourne, Australia, pp. 804.
- Sheth, S.A., Nemoto, M., Guio, M., Walker, M., Pouratian, N. and Toga, A.W., 2004. Linear and nonlinear relationships between neuronal activity, oxygen metabolism, and hemodynamic responses. *Neuron*, vol. 42, no. 2, pp. 347-355.
- Shih, Y.I., Chang, C., Chen, J. and Jaw, F., 2008. BOLD fMRI mapping of brain responses to nociceptive stimuli in rats under ketamine anesthesia. *Medical Engineering & Physics*, vol. 30, no. 8, pp. 953-958.
- Shmuel, A., Augath, M., Oeltermann, A. and Logothetis, N.K., 2006. Negative functional MRI response correlates with decreases in neuronal activity in monkey visual area V1. *Nature Neuroscience*, vol. 9, no. 4, pp. 569-577.
- Shmuel, A., Yacoub, E., Pfeuffer, J., Van, d.M., Adriany, G., Hu, X. and Ugurbil, K., 2002. Sustained negative BOLD, blood flow and oxygen consumption response and its coupling to the positive response in the human brain. *Neuron*, vol. 36, no. 6, pp. 1195-1210.
- Shoaib, M., Lowe, A.S. and Williams, S.C.R., 2004. Imaging localised dynamic changes in the nucleus accumbens following nicotine withdrawal in rats. *NeuroImage*, vol. 22, no. 2, pp. 847-854.
- Shyu, B.C., Lin, C.Y., Sun, J.J., Chen, S.L. and Chang, C., 2004. BOLD response to direct thalamic stimulation reveals a functional connection between the medial thalamus and the anterior cingulate cortex in the rat. *Magnetic Resonance in Medicine*, vol. 52, no. 1, pp. 47-55.
- Sicard, K., Shen, Q., Brevard, M.E., Sullivan, R., Ferris, C.F., King, J.A. and Duong, T.Q., 2003. Regional cerebral blood flow and BOLD responses in conscious and anesthetized rats under basal and hypercapnic conditions: Implications for functional MRI studies. *Journal of Cerebral Blood Flow and Metabolism*, vol. 23, no. 4, pp. 472-481.

- Sicard, K.M. and Duong, T.Q., 2005. Effects of hypoxia, hyperoxia, and hypercapnia on baseline and stimulus-evoked BOLD, CBF, and CMRO(2) in spontaneously breathing animals. *NeuroImage*, vol. 25, no. 3, pp. 850-858.
- Silva, A.C., Koretsky, A.P. and Duyn, J.H., 2007. Functional MRI impulse response for BOLD and CBV contrast in rat somatosensory cortex. *Magnetic Resonance in Medicine*, vol. 57, no. 6, pp. 1110-1118.
- Silva, A.C., Lee, S.P., Yang, G., Iadecola, C. and Kim, S.G., 1999. Simultaneous blood oxygenation level-dependent and cerebral blood flow functional magnetic resonance imaging during forepaw stimulation in the rat. *Journal of Cerebral Blood Flow and Metabolism*, vol. 19, no. 8, pp. 871-879.
- Silvennoinen, M.J., Clingman, C.S., Golay, X., Kauppinen, R.A. and van Zijl, P.C.M., 2003. Comparison of the dependence of blood R2 and R2* on oxygen saturation at 1.5 and 4.7 tesla. *Magnetic Resonance in Medicine*, vol. 49, no. 1, pp. 47-60.
- Silverman, J. and Muir, W.W., 3rd, 1993. A review of laboratory animal anesthesia with chloral hydrate and chloralose. *Laboratory Animal Science*, vol. 43, no. 3, pp. 210-216.
- Simon, L., Toth, J., Molnar, L. and Agoston, D.V., 2011. MRI analysis of mGluR5 and mGluR1 antagonists, MTEP and R214127 in the cerebral forebrain of awake, conscious rats. *Neuroscience Letters*, vol. 505, no. 2, pp. 155-159.
- Simons, D.J., Carvell, G.E., Hershey, A.E. and Bryant, D.P., 1992. Responses of barrel cortex neurons in awake rats and effects of urethane anesthesia. *Experimental Brain Research*, vol. 91, no. 2, pp. 259-272.
- Sinclair, M.D., 2003. A review of the physiological effects of alpha2-agonists related to the clinical use of medetomidine in small animal practice. *The Canadian Veterinary Journal*, vol. 44, no. 11, pp. 885-897.
- Singh, M., Kim, S. and Kim, T.S., 2003. Correlation between BOLD-fMRI and EEG signal changes in response to visual stimulus frequency in humans. *Magnetic Resonance in Medicine*, vol. 49, no. 1, pp. 108-114.
- Skoubis, P.D., Hradil, V., Chin, C.L., Luo, Y., Fox, G.B. and McGaraughty, S., 2006. Mapping brain activity following administration of a nicotinic acetylcholine receptor agonist, ABT-594, using functional magnetic resonance imaging in awake rats. *Neuroscience*, vol. 137, no. 2, pp. 583-591.
- Sloan, H.L., Austin, V.C., Blamire, A.M., Schnupp, J.W.H., Lowe, A.S., Allers, K.A., Matthews, P.M. and Sibson, N.R., 2010. Regional differences in neurovascular coupling in rat brain as determined by fMRI and electrophysiology. *NeuroImage*, vol. 53, no. 2, pp. 399-411.
- Sokoloff, L., 1960. The Metabolism of the Central Nervous System in Vivo. pp. 1843-1864. Field, J., Magoun, H.W. and Hall, V.E. eds., *Handbook of Physiology, Section I, Neurophysiology, Vol 3*, Washington: American Physiological Society.
- Sokoloff, L., Reivich, M., Kennedy, C., Rosiers, M.H.D., Patlak, C.S., Pettigrew, K.D., Sakurada, O. and Shinohara, M., 1977. The [14C]deoxyglucose method for the measurement of local cerebral glucose utilization: Theory, procedure, and normal values in the conscious and anesthetized albino rat. *Journal of Neurochemistry*, vol. 28, no. 5, pp. 897-916.

- Sokoloff, L., Mangold, R., Wechsler, R.L., Kennedy, C. and Kety, S.S., 1955. The effect of mental arithmetic on cerebral circulation and metabolism. *The Journal of Clinical Investigation*, vol. 34, no. 7, pp. 1101-1108.
- Sommers, M.G., van Egmond, J., Booij, L.H. and Heerschap, A., 2009. Isoflurane anesthesia is a valuable alternative for alpha-chloralose anesthesia in the forepaw stimulation model in rats. *NMR in Biomedicine*, vol. 22, no. 4, pp. 414-418.
- Staewen, R.S., Johnson, A.J., Ross, B.D., Parrish, T., Merkle, H. and Garwood, M., 1990. 3-D FLASH imaging using a single surface coil and a new adiabatic pulse, BIR-4. *Investigative Radiology*, vol. 25, no. 5, pp. 559-567.
- Stefanacci, L., Reber, P., Costanza, J., Wong, E., Buxton, R., Zola, S., Squire, L. and Albright, T., 1998. fMRI of monkey visual cortex. *Neuron*, vol. 20, no. 6, pp. 1051-1057.
- Stefanovic, B., Warnking, J.M. and Pike, G.B., 2004. Hemodynamic and metabolic responses to neuronal inhibition. *NeuroImage*, vol. 22, no. 2, pp. 771-778.
- Steriade, M., Gloor, P., Llinas, R.R., Lopes de Silva, F.H. and Mesulam, M.M., 1990. Report of IFCN committee on basic mechanisms. basic mechanisms of cerebral rhythmic activities. *Electroencephalography and Clinical Neurophysiology*, vol. 76, no. 6, pp. 481-508.
- Sumiyoshi, A., Riera, J.J., Ogawa, T. and Kawashima, R., 2011. A mini-cap for simultaneous EEG and fMRI recording in rodents. *NeuroImage*, vol. 54, no. 3, pp. 1951-1965.
- Sumiyoshi, A., Suzuki, H., Ogawa, T., Riera, J.J., Shimokawa, H. and Kawashima, R., 2012. Coupling between gamma oscillation and fMRI signal in the rat somatosensory cortex: Its dependence on systemic physiological parameters. *NeuroImage*, vol. 60, no. 1, pp. 738-746.
- Takano, T., Tian, G., Peng, W., Lou, N., Libionka, W., Han, X. and Nedergaard, M., 2006. Astrocyte-mediated control of cerebral blood flow. *Nature Neuroscience*, vol. 9, no. 2, pp. 260-267.
- Talairach, J. and Tournoux, P., 1988. *Co-Planar Stereotaxic Atlas of the Human Brain: 3-D Proportional System: An Approach to Cerebral Imaging*. New York: Thieme Medical Publishers.
- Thulborn, K.R., Waterton, J.C., Matthews, P.M. and Radda, G.K., 1982. Oxygenation dependence of the transverse relaxation time of water protons in whole blood at high field. *Biochimica Et Biophysica Acta (BBA) - General Subjects*, vol. 714, no. 2, pp. 265-270.
- Tsai, P.S., Kaufhold, J.P., Blinder, P., Friedman, B., Drew, P.J., Karten, H.J., Lyden, P.D. and Kleinfeld, D., 2009. Correlations of neuronal and microvascular densities in murine cortex revealed by direct counting and colocalization of nuclei and vessels. *The Journal of Neuroscience*, vol. 29, no. 46, pp. 14553-14570.
- Uchida, S., Kagitani, F., Nakayama, H. and Sato, A., 1997. Effect of stimulation of nicotinic cholinergic receptors on cortical cerebral blood flow and changes in the effect during aging in anesthetized rats. *Neuroscience Letters*, vol. 228, no. 3, pp. 203-206.
- Uchida, S., Kawashima, K. and Lee, T.J.F., 2002. Nicotine-induced NO-mediated increase in cortical cerebral blood flow is blocked by alpha2-adrenoceptor antagonists in the anesthetized rats. *Autonomic Neuroscience: Basic & Clinical*, vol. 96, no. 2, pp. 126-130.

- Ueki, M., Mies, G. and Hossmann, K.A., 1992. Effect of alpha-chloralose, halothane, pentobarbital and nitrous oxide anesthesia on metabolic coupling in somatosensory cortex of rat. *Acta Anaesthesiologica Scandinavica*, vol. 36, no. 4, pp. 318-322.
- Ureshi, M., Kershaw, J. and Kanno, I., 2005. Nonlinear correlation between field potential and local cerebral blood flow in rat somatosensory cortex evoked by changing the stimulus current. *Neuroscience Research*, vol. 51, no. 2, pp. 139-145.
- Ureshi, M., Matsuura, T. and Kanno, I., 2004. Stimulus frequency dependence of the linear relationship between local cerebral blood flow and field potential evoked by activation of rat somatosensory cortex. *Neuroscience Research*, vol. 48, no. 2, pp. 147-153.
- Vafaee, M.S. and Gjedde, A., 2004. Spatially dissociated flow-metabolism coupling in brain activation. *NeuroImage*, vol. 21, no. 2, pp. 507-515.
- Valdes Hernandez, P.A., Sumiyoshi, A., Nonaka, H., Haga, R., Aubert Vasquez, E., Ogawa, T., Iturria Medina, Y., Riera, J.J. and Kawashima, R., 2011. An in vivo MRI template set for morphometry, tissue segmentation and fMRI localization in rats. *Frontiers in Neuroinformatics*, vol. 5, no. 26, pp. 1-19.
- Van Audekerke, J., Peeters, R., Verhoye, M., Sijbers, J. and Van der Linden, A., 2000. Special designed RF-antenna with integrated non-invasive carbon electrodes for simultaneous magnetic resonance imaging and electroencephalography acquisition at 7T. *Magnetic Resonance Imaging*, vol. 18, no. 7, pp. 887-891.
- Van Camp, N., D'Hooge, R., Verhoye, M., Peeters, R.R., De Deyn, P.P. and Van der Linden, A., 2003. Simultaneous electroencephalographic recording and functional magnetic resonance imaging during pentylenetetrazol-induced seizures in rat. *NeuroImage*, vol. 19, no. 3, pp. 627-636.
- Van Camp, N., Peeters, R.R. and Van der Linden, A., 2005. A comparison between blood oxygenation level-dependent and cerebral blood volume contrast in the rat cerebral and cerebellar somatosensory cortex during electrical paw stimulation. *Journal of Magnetic Resonance Imaging*, vol. 22, no. 4, pp. 483-491.
- Van Camp, N., Verhoye, M., De Zeeuw, C.I. and Van der Linden, A., 2006a. Light stimulus frequency dependence of activity in the rat visual system as studied with high-resolution BOLD fMRI. *Journal of Neurophysiology*, vol. 95, no. 5, pp. 3164-3170.
- Van Camp, N., Verhoye, M. and Van der Linden, A., 2006b. Stimulation of the rat somatosensory cortex at different frequencies and pulse widths. *NMR in Biomedicine*, vol. 19, no. 1, pp. 10-17.
- van den Burg, E.H., Peeters, R.R., Verhoye, M., Meek, J., Flik, G. and Van der Linden, A., 2005. Brain responses to ambient temperature fluctuations in fish: Reduction of blood volume and initiation of a whole-body stress response. *Journal of Neurophysiology*, vol. 93, no. 5, pp. 2849-2855.
- Van der Linden, A., Van Camp, N., Ramos-Cabrera, P. and Hoehn, M., 2007. Current status of functional MRI on small animals: Application to physiology, pathophysiology, and cognition. *NMR in Biomedicine*, vol. 20, no. 5, pp. 522-545.
- van Zijl, P.C., Eleff, S.M., Ulatowski, J.A., Oja, J.M., Ulug, A.M., Traystman, R.J. and Kauppinen, R.A., 1998. Quantitative assessment of blood flow, blood volume and

- blood oxygenation effects in functional magnetic resonance imaging. *Nature Medicine*, vol. 4, no. 2, pp. 159-167.
- Wang, L., Saalmann, Y., Pinsk, M., Arcaro, M. and Kastner, S., 2012. Electrophysiological low-frequency coherence and cross-frequency coupling contribute to BOLD connectivity. *Neuron*, vol. 76, no. 5, pp. 1010-1020.
- Weber, B., Keller, A.L., Reichold, J. and Logothetis, N.K., 2008. The microvascular system of the striate and extrastriate visual cortex of the macaque. *Cerebral Cortex*, vol. 18, no. 10, pp. 2318-2330.
- Weber, R., Ramos-Cabrera, P., Wiedermann, D., van Camp, N. and Hoehn, M., 2006. A fully noninvasive and robust experimental protocol for longitudinal fMRI studies in the rat. *NeuroImage*, vol. 29, no. 4, pp. 1303-1310.
- Willis, C.K., Quinn, R.P., McDonnell, W.M., Gati, J., Partlow, G. and Vilis, T., 2001. Functional MRI activity in the thalamus and occipital cortex of anesthetized dogs induced by monocular and binocular stimulation. *Canadian Journal of Veterinary Research*, vol. 65, no. 3, pp. 188-195.
- Woolrich, M.W., Ripley, B.D., Brady, M. and Smith, S.M., 2001. Temporal autocorrelation in univariate linear modeling of FMRI data. *NeuroImage*, vol. 14, no. 6, pp. 1370-1386.
- Worsley, K.J., Evans, A.C., Marrett, S. and Neelin, P., 1992. A three-dimensional statistical analysis for CBF activation studies in human brain. *Journal of Cerebral Blood Flow and Metabolism*, vol. 12, no. 6, pp. 900-918.
- Worsley, K.J. and Friston, K.J., 1995. Analysis of fMRI time-series revisited--again. *NeuroImage*, vol. 2, no. 3, pp. 173-181.
- Wright, G.A., Hu, B.S. and Macovski, A., 1991. Estimating oxygen saturation of blood in vivo with MR imaging at 1.5 T. *Journal of Magnetic Resonance Imaging*, vol. 1, no. 3, pp. 275-283.
- Wu, G., Luo, F., Li, Z., Zhao, X. and Li, S.J., 2002. Transient relationships among BOLD, CBV, and CBF changes in rat brain as detected by functional MRI. *Magnetic Resonance in Medicine*, vol. 48, no. 6, pp. 987-993.
- Wyrwicz, A.M., Chen, N., Li, L., Weiss, C. and Disterhoft, J.F., 2000. fMRI of visual system activation in the conscious rabbit. *Magnetic Resonance in Medicine*, vol. 44, no. 3, pp. 474-478.
- Yacoub, E., Duong, T.Q., Van De Moortele, P.F., Lindquist, M., Adriany, G., Kim, S.G., Ugurbil, K. and Hu, X., 2003. Spin-echo fMRI in humans using high spatial resolutions and high magnetic fields. *Magnetic Resonance in Medicine*, vol. 49, no. 4, pp. 655-664.
- Yacoub, E., Shmuel, A., Pfeuffer, J., Van De Moortele, P., Adriany, G., Andersen, P., Vaughan, J.T., Merkle, H., Ugurbil, K. and Hu, X., 2001. Imaging brain function in humans at 7 tesla. *Magnetic Resonance in Medicine*, vol. 45, no. 4, pp. 588-594.
- Yamada, K.A., Moerschbaecher, J.M., Hamosh, P. and Gillis, R.A., 1983. Pentobarbital causes cardiorespiratory depression by interacting with a GABAergic system at the ventral surface of the medulla. *Journal of Pharmacology and Experimental Therapeutics*, vol. 226, no. 2, pp. 349-355.

- Yang, X., Renken, R., Hyder, F., Siddeek, M., Greer, C.A., Shepherd, G.M. and Shulman, R.G., 1998. Dynamic mapping at the laminar level of odor-elicited responses in rat olfactory bulb by functional MRI. *Proceedings of the National Academy of Sciences*, vol. 95, no. 13, pp. 7715-7720.
- Young, W.L., Barkai, A.I., Prohovnik, I., Nelson, H. and Durkin, M., 1991. Effect of PaCO₂ on cerebral blood flow distribution during halothane compared with isoflurane anaesthesia in the rat. *British Journal of Anaesthesia*, vol. 67, no. 4, pp. 440-446.
- Zago, S., Lorusso, L., Ferrucci, R. and Priori, A., 2012. Functional Neuroimaging: A Historical Perspective. pp. 1-29. Bright, P. ed., *Neuroimaging - Methods*, InTech.
- Zhang, Z., Andersen, A.H., Avison, M.J., Gerhardt, G.A. and Gash, D.M., 2000. Functional MRI of apomorphine activation of the basal ganglia in awake rhesus monkeys. *Brain Research*, vol. 852, no. 2, pp. 290-296.
- Zhao, F., Zhao, T., Zhou, L., Wu, Q. and Hu, X., 2008. BOLD study of stimulation-induced neural activity and resting-state connectivity in medetomidine-sedated rat. *NeuroImage*, vol. 39, no. 1, pp. 248-260.
- Zhao, J.M., Clingman, C.S., Närviäinen, M.J., Kauppinen, R.A. and van Zijl, P.C.M., 2007. Oxygenation and hematocrit dependence of transverse relaxation rates of blood at 3T. *Magnetic Resonance in Medicine*, vol. 58, no. 3, pp. 592-597.
- Zotev, V.S., Matlashov, A.N., Volegov, P.L., Savukov, I.M., Espy, M.A., Mosher, J.C., Gomez, J.J. and Kraus Jr., R.H., 2008. Microtesla MRI of the human brain combined with MEG. *Journal of Magnetic Resonance*, vol. 194, no. 1, pp. 115-120.

JOANNA HUTTUNEN
*A Study of
Rodent Brain Function
with Functional and
Pharmacological Magnetic
Resonance Imaging*

Preclinical functional and pharmacological magnetic resonance imaging offers an extensive array of possibilities with which to measure brain activity. In this thesis, neurovascular coupling in the somatosensory cortex of the rat brain was investigated and a protocol for pharmacological activation that would account for baseline fluctuations was developed. These studies have implications for both understanding brain function and for designing functional imaging paradigms in anesthetized animals.



UNIVERSITY OF
EASTERN FINLAND

PUBLICATIONS OF THE UNIVERSITY OF EASTERN FINLAND
Dissertations in Health Sciences

ISBN 978-952-61-1177-3